UNIVERSITY OF OKLAHOMA

GRADUATE COLLEGE

DEVELOPMENT OF BENCHTOP CAPILLARY-BASED ANALYTICAL INSTRUMENTS FOR CHROMATOGRAPHIC SEPARATION AND DETECTION

A DISSERTATION

SUBMITTED TO THE GRADUATE FACULTY

in partial fulfillment of the requirements for the

Degree of

DOCTOR OF PHILOSOPHY

By

KYLE BRIAN LYNCH
Norman, Oklahoma
2018

DEVELOPMENT OF BENCHTOP CHEMISTRY-BASED ANALYTICAL INSTRUMENTS FOR CHROMATOGRAPHIC SEPARATION AND DETECTION

A DISSERTATION APPROVED FOR THE
DEPARTMENT OF CHEMISTRY AND BIOCHEMISTRY

BY

_____
Dr. Shaorong Liu, Chair

_____
Dr. Roger Harrison

_____
Dr. Si Wu

_____
Dr. Robert White

_____
Dr. Zhibo Yang

This doctoral thesis is dedicated to my grandparents Hugh Lynch and Alice Federlick and my parents Hugh and Maria Lynch. Without their help and support, none of this would have been possible.

Acknowledgements

Without the advice and constant encouragement of my mentor and PI Dr. Shaorong Liu, this doctoral thesis would not have been possible. I would like to gratefully and sincerely acknowledge Prof. Shaorong Liu along with his wife, Joann Lu, for their constant support and reinforcement in the past six years. Through Dr. Liu's supervision and Joann's help, my work was efficient and successful.

I would like to thank my committee members, Dr. Robert White, Dr. Robert Thomson, Dr. Zhibo Yang, and Dr. Roger Harrison. Their kind and help throughout the years was very appreciated.

I would like to thank all the lab members in the past and present. They are Dr. Congying Gu, Dr. Qiangshen Pu, Dr. Wei Wang, Dr. Ruibo Li, Dr. Lei Zhou, Dr. Haiqing Yu, Dr, Xiaochun Wang, Dr. Min Zhang, Dr. Jiangtao Ren, Dr. Zaifang Zhu, Dr. Apeng Chen, Dr. Huang Chen, Mitchell Weaver, Yu Yang, Piliang Xiang, and Matthew A. Beckner. Their help and suggestions contributed a lot to the completion of my doctoral thesis.

Finally, I would like to thank the publisher ELSEVIER, including journals Talanta and Journal of Separation Science, for publishing my work and permitting me to reuse it in this doctoral thesis. Thanks to all other the publishers for giving me the permission to reuse some figures in this dissertation.

Table of Contents

List of Tables

List of Figures

Abstract

Point-of-Care (POC) analysis in recent years has driven the need for the miniaturization of chemistry instruments in the analytical field. One such instrument class involves chromatographic systems for the separation and detection of complex samples. From this need, micro Total Analytical Systems (microTAS) as well as Lab-on-Chip (LOC) systems have been developed. These systems allow for the potential of cost reduction in manufacturing as well as on-site analysis. One method to obtain a significant size reduction in the instruments is to transition all liquid flow to a capillary-based system. Within this dissertation we show that through the minimization of the liquid channels, new portable separation and detection systems can be developed.

In the second chapter, we describe the development of a high- performance liquid chromatography (HPLC) capillary-based cartridge for complex separations. HPLC has traditionally required the need for high-pressure piston pumps that are inherently large in size. In order to mitigate this issue, we have developed and reported monolithic capillary-based electroosmotic pumps (EOPs) capable of producing an output pressure greater than 1200 bar. EOPs are proving to be a promising alternative to traditional piston pumps and can be applied to either capillary or chip-based systems. Within our HPLC cartridge, we develop a novel valve system capable of providing gradient elution and nanovolume injection (Figure 2-1). A two-loop system allowed dual EOP units to drive a gradient separation while refilling the second loop for subsequent column reconditioning. When the valve is switched and reconditioning begins, the gradient profile can be regenerated for the next separation.

In the third chapter, a narrow capillary benchtop laser induced fluorescence detector is developed. Currently, low- and sub-micrometer capillary systems capable of on-column detection are not commercially available. Through the development of this confocal LIF detector prototype, we were able to characterize its limitations including the limit of detection (LOD), linear dynamic range (LDR), and background drift through a flow injection analysis (FIA) system within a 2-um-i.d. capillary. We obtained a very low LOD of around ~70 fluorescein molecules (equating to a 12 yoctomole fluorescein LOD). A wide LDR was reported at three orders of magnitude while a 1.2-fold root-mean-square (rms) noise was obtained. Following the characterization, a DNA ladder sample was separated by bare narrow capillary-hydrodynamic chromatography (BaNC-HDC). Through this testing, we were able to further demonstrate the feasibility of the system by obtaining both well-resolved peaks as well as quantitative information for the DNA fragments.

In the fourth chapter, we describe the development of a multiple channel UV/Vis optical fiber-based absorbance detector for high throughput screening of chromatographic separations. There has been increasing interest in online comprehensive two-dimensional liquid chromatography (2D-LC) systems. These systems allow for a high peak resolution of complex samples that traditional one-dimensional liquid chromatography could not provide. However, current configurations of commercial 2D-LC systems involve two or more columns with two detectors and provide separation times in the tens of hours. In order to shorten the total separation time, a novel configuration for 2D-LC was developed and the detector for said system is presented here. The detector consists of four major components: a deuterium lighthouse;

an optical fiber module assembly; a 13-channel flow cell fitted with a 13-photodiode detection system; and a data acquisition and monitoring terminal. When characterizing the detector, we were able to obtain background noise level in the tens of μAU and a linear range of ~2.5 AU.

Chapter 1: Introduction

Background

Point-of-Care (POC) analysis is becoming an ever-popular necessity in the fields of medicine [1], forensics [2], homeland security [3], and biomedical analysis [4] to name a few. However, due to traditional drawbacks of LC including size, weight, cost, and instrument complexity, HPLC has not been widely implemented in the field. With continued improvements to the various LC components including the pumping systems, injectors, columns, and detectors through the use of new machining techniques, development of smaller electronics and breakthroughs in material science, truly miniaturized HPLC systems are a reality in the 21st century leading to an ever-increasing possibility of applications. In this dissertation we present three benchtop capillary-based analytical instruments for chromatographic separation (HPLC cartridge) and detection (LIF detector and multiple channel absorbance detector) of peptides and proteins.

Miniaturized capillary-based systems

Miniaturized liquid chromatography systems lend themselves towards increased portability. In order to successfully construct a miniaturized and/or portable device, one must take into consideration the overall weight of the system, ability to provide both isocratic and gradient elution, a stable flow rate, and ease of operation. Advancements in pumping systems, columns, and detectors have driven the development of micro Total Analytical Systems (microTAS).

Electroosmotic pumps (EOP)

The growing trend in micro analytical systems, including miniaturized HPLC systems, has allowed the prospect for electroosmotic pumps (EOPs) to be popularized in recent decades [5-7]. EOPs utilize electroosmosis through charged porous media (pumping elements) to generate pressure and flow. This porous media may either be positively or negatively charged based on the polarity of the high voltage power supply (HVPS) and the direction of the flow desired. Electroosmotic pumps offer a cost-effective and simplistic method for producing the necessary flow rates and pressures required for liquid chromatographic systems while having several other inherent benefits. For example, this style of pump naturally creates pulse-free flows, unlike most traditional pump systems. The liquid profile of EOPs more resemble a plug rather than parabolic in shape with pressure driven systems. The rate and direction of flow is easily manipulated through a change in the voltage magnitude and polarity [8]. These pumps are readily miniaturized and integrated in both lab-on-chip and traditional systems, all the while reducing complexity due to no moving parts.

Our group has developed different electroosmotic pump configurations for use in portable LC systems. With the advent of monolithic polymerized columns for electroosmotic pumping systems, step [9, 10], linear [11, 12] and programmable [13] gradients were all obtained. Pumps capable of generating 1200 bar [14] have been reported, however lower pressures (~120 bar) are more routinely used to drive separations at a flow rate of ~200 nL/min. Depending on the specifications of the pump required, one may choose to either put several of the same charged monolith in parallel to achieve additive flow and averaged pressure or combine positive and negatively

charged monoliths in series to create a Pressure Power Supply (PPS), which allows for additive pressure with averaged flow. This technique is often compared to how batteries work and sample configurations may be seen in Figure 1-1. Within the proposed HPLC cartridge presented within this dissertation, we utilize the first technique (parallel negatively charged EOPs) to generate a miniaturized high-pressure pump capable of pressures ~2500 psi and flow rates ~1 μL/min. Scanning electron microscope (SEM) images of the negatively charged monolithic EOPs utilized within this research can be seen in Figure 1-2.

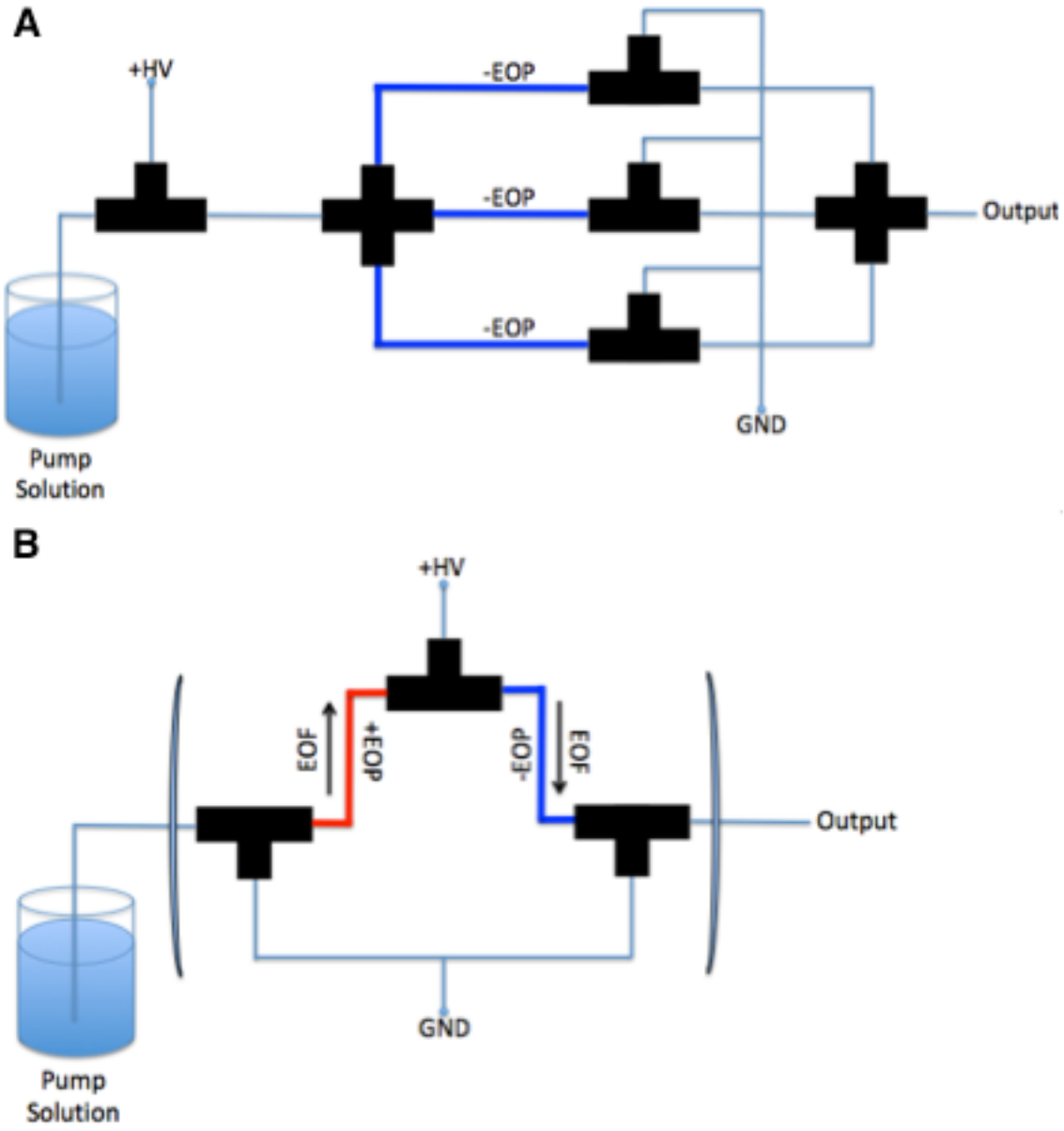

Figure 1-1 Monolithic pump setup

+HV – positive high voltage; GND – ground; EOP – electroosmotic pump; EOF – electroosmotic flow

A: parallel EOP configuration; B: pressure pump system (PPS) (series EOP configuration)

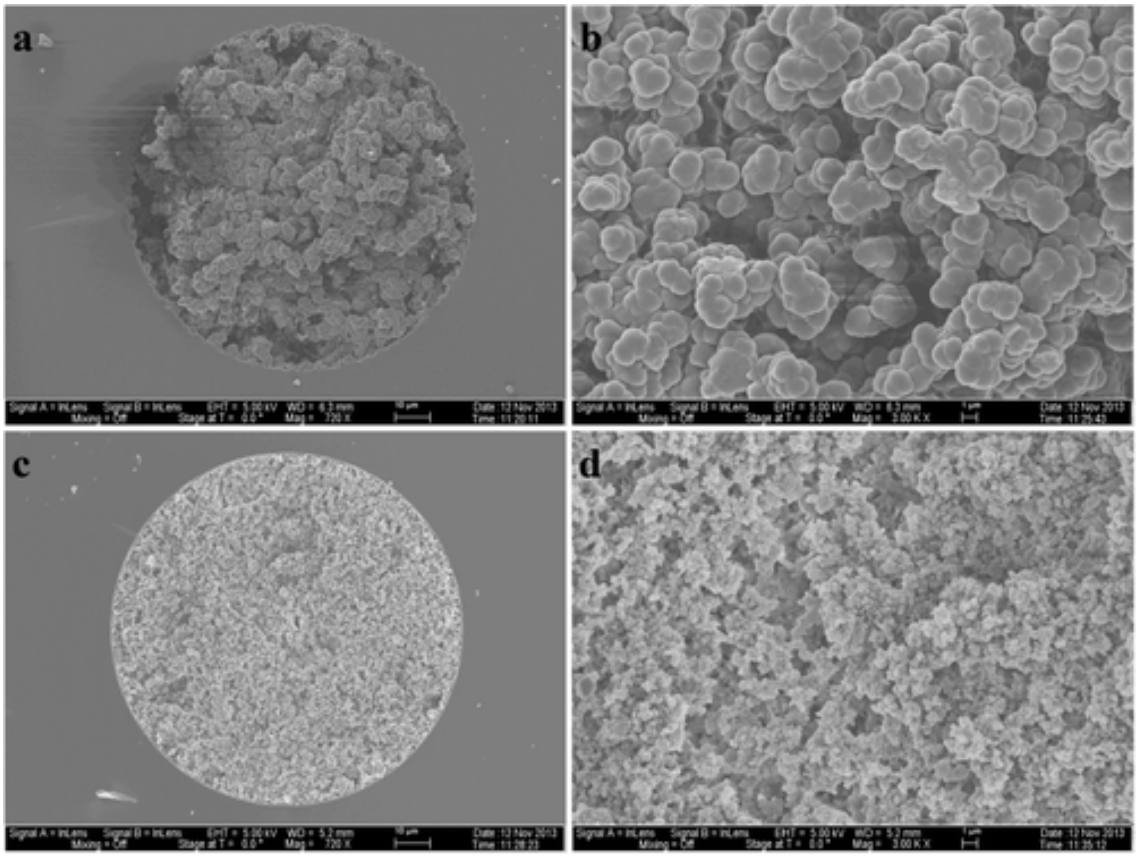

Figure 1-2 SEM images of typical negative monoliths

[Reprinted with permission from Zhou et al., Analytical Chemistry 86(24) 12214-12219. Copyright (2014) American Chemical Society.]

Although electroosmotic pumping systems are small in size and have low dwell volume compared to conventional pumping systems, limitations to EOP do exist. These may include pump-solution incompatibility with high organic contents, flow rate fluctuations due to condition variations at the pumping element surfaces, unstable voltage sources, and/or chemical breakdown within the pumping element itself. Each of these limitations lend to the fact that EOPs have never been commercialized in the 20 years of their existence. Although EOP pressures and flow rates are approaching the workable range for LC separations and its size lends itself to a miniaturized HPLC system, further research is needed to provide stable flow rates and a reproducible and programmable gradient before they will ever reach the market.

Capillary columns

Since the early HPLC systems, it has been known that in order to increase resolution and decrease separation times, packing particle sizes and column dimensions need to be minimized. The advent of microcolumns (0.5-1.5-mm-i.d.) lead to the development of capillary-based columns (0.1-0.05-mm-i.d.) and then to microcapillary columns (50-200-μm-i.d.) [15] in the late 1970s. Tsuda et al. [16] as well as Jorgenson's groups [17, 18] continued to pioneer columns with the further reduction of column diameter to 5-500-μm-i.d. . During this development of microcapillary columns, much research went into the slurry packing of fused silica particles in order to increase the columns homogeneity and thus improve its efficiency and reproducibility [17, 19-25]. Jorgenson, in one of these developments, decreased the particle diameter to 1.5 and 1-μm-i.d. showing that extremely high efficiency columns (<200,000 plates/m) could be developed [26]. Through this decreased column size and particle diameter a new type of

liquid chromatography, ultrahigh-pressure liquid chromatography (UHPLC) where pressures may reach levels higher than 1100 bar [27], has been developed.

Researchers soon realized that although decreasing the packing particles size can lead to more than one million plates/m [28], very high pressure pumps were required to drive these separations. This requirement thus limited the application of these columns to miniaturized liquid chromatography systems. Monolithic capillary columns, conceived in the early 1990s, addressed this backpressure issue by replacing a packed slurry with polymerized monomers within the column [29-31]. To date, separation efficiencies with monolithic columns between 100,000 and 250,000 plate/m have been obtained [32-34] and with added functionalization including organic polymers [35, 36] and zwitterionic functionalization as well as incorporation of metallic nanoparticles, metal organic frameworks, and carbon-based nanomaterials, monolithic capillary-based columns continue being on the forefront of column research.

Filled columns, whether they are packed or contain a monolith, represent one subclass of capillary-based columns. Open tubular capillary columns, in turn, represent the other. Open tubular capillary columns have only recently (last two decades) begun to make an impact on chromatographic separations compared to that of filled columns. Open tubular columns can exist as porous layer open tubular (PLOT) [37-41] or wall coated open tubular (WCOT) columns [42-44]. Improvements in coatings of open tubular capillary columns have allowed for an increase in column efficiency while taking advantage of a smaller inner diameter that minimizes the effect of dispersion compared to that of packed columns. However, generally speaking, the overall length of the open tubular column must be increased in order to create an equivalent separation to

that of a filled column.

The projects presented within this dissertation incorporate a number of different capillary columns. Within Chapter 2, commercially available packed C18 reversed-phase (RP) columns are used for trypsic digests of bovine serum albumin (BSA) and myoglobin. In Chapter 3, open tubular columns for bare narrow capillary-hydrodynamic chromatography (BaNC-HDC) are used to separate a 1 kb plus DNA ladder. Lastly, in Chapter 4, monolithic columns of both strong anion exchange (SCX) and RP modes are used for an E. Coli lysate separation.

Detectors

As the size of chromatographic systems continue to decrease, the stress is placed for the detection systems to complement the separations. Extensive amounts of research and review articles have gone into various detection methods including Raman Spectroscopy [2, 3, 45, 46], UV, Visible and NIR Spectroscopy [47-52], Laser and LED Induced Fluorescence [53-58], electrochemical detectors [59-64], X-ray fluorescence [65-67]. The majorities of these miniaturized detectors are designed around the detection of a specific class of compounds but may be adapted to supply the needs of others. The simplest class of detectors to miniaturize and thus integrate into an μHPLC system is absorbance detectors. Although absorbance can give a great detail of information, the researcher is limited to a specific subset of substances based on what wavelength of light he/she chooses. Mass spectrometry on the other hand can provide the researcher with a great deal of information both qualitatively and quantitatively. Miniature mass spectrometer development and commercialization are progressing rapidly [68] and many applications are anticipated as μHPLC and miniaturized mass

spectrometer are integrated with one another.

Laser Induced Fluorescent (LIF) detection is a highly sensitive technique for analyzing native fluorescent and fluorescently tagged molecules. LIF detectors are highly suitable for miniaturized LC systems due to their low sample consumption, short testing time, high sensitivity, a relative low complexity of their components and are easily integrated into microfluidic chip-based systems. Compact LIF detectors continue to be developed throughout the academic community. Fang et al. [53] developed a handheld LIF detector with a 450 nm laser diode and tested the prototype with CE, flow cytometry, and droplet analysis. Novak et al. [69] developed a low-cost miniaturized LIF detector for lab-on-chip applications with sensitivities in the nanomolar region and incorporated lock-in amplification for measurements under ambient light. Although LIF detectors lend themselves to miniaturized LC systems with their high sensitivities and small size, the researcher is limited to applications based not only on the laser wavelength chosen but also the inherent need for a fluoraphore, whether that be native or labeled, to exist in the first place.

Absorbance detectors have existed since the beginning of liquid chromatography. The first commercialized fixed wavelength detector was announced in 1978 for use with HPLC [70]. Since then, advancements in electronics, light sources, and optics have lead to the decrease in detector sizes. One of the greatest breakthroughs in technology enabling the advancement in microsized detectors is the use of light emitting diodes (LEDs) as the light source. Within the last decade, numerous absorbance detectors have been developed, most integrating LEDs both in the visible and UV region, as their light sources [71-77].

Here two novel miniaturized detectors are presented for various real world applications. A benchtop laser induced fluorescence (LIF) with yoctomole limits of detection is presented in Chapter 3. In the following chapter, Chapter 4, a multiple-channel ultraviolet (UV) absorbance detector is presented for its use in two-dimensional liquid chromatographic (2D-LC) separations.

Techniques and instrumental development for microHPLC

High Performance Liquid Chromatography (HPLC) has its roots back into the early 20th century. Martin and Synge [78] conducted initial studies in the early 1940s but advancement within the field did not take place until the 1960s when scientists realized that reducing the packing-particle diameter of the column while subsequently increasing the mobile phase velocity through an increased pressure could lead to dramatically improved separations [79-83]. It was during this time period that separation times decreased while resolutions increased showing that high performance liquid chromatography was here to stay.

Leading chromatographers in the 1980s, Baram et al., constructed the first 'portable liquid chromatograph' utilizing a multi-wavelength photometric detector and it weighed in at approximately 45 kg [84]. A few years later, Otagawa et al. published a paper documenting the use of another miniaturized HPLC for the analysis of primary aromatic amines in coal-derived materials [85]. Although no specific weight was given for the system, it was considerably smaller in size than the earlier model by Baram et al. In the late 1990s, Baram et al. [86], Tulchinsky [87], and a company by the name of ICON Scientific, Inc. [88] all released new miniaturized HPLCs with continued improvements to size, power, and overall separations.

The practicalities of miniaturized LC systems arise from the inherent benefits they provide. These may include but are not limited to a lower overall system solvent volume, smaller sample and mobile phase consumption, and the possible increased portability of the system. By reducing total system volume, a decrease in dwell and dead volume as well as extra-column volume is expected. The dwell volume, otherwise known as the volume difference between the systems delivery method and the front of the column, is impacted by the tubing (both internal diameter (I.D.) and length) as well as any valves/mixers that make up the total fluid path [89].

Extra-column volume, or the volume from the injector to the detector, may consist of tubing connections, detector flow cells, preheaters, injection volume, as well as the column volume. Both dwell volume and extra-column volume effect the overall separation but in very different capacities. Dwell volume may impact the time as well as the gradient while extra-column volume impacts the peak width, efficiency, and resolution of the separation. Along the same lines but often confused, dead-volume, or the volume of they system that is unmoving or unswept through the chromatographic system, can be a serious problem for chromatographers leading to the tailing and broadening of peaks thus compromising peak separation and quantification and in turn resulting in an overall lower peak resolution [90]. By minimizing these unwanted volumes through the overall decrease in the systems size, one hopes to improve their overall separation. Several groups have coupled these microTAS/point-of-care systems with liquid chromatography to create portable devices as summarized in Table 1-1 below.

Pump Type	Weight (kg)	Dimensions (cm)	Injector	Column	Detector
Electroosmotic					
Lynch 2017 [11]	3	20 x 20 x 17.5	Stop-flow (60 nL)	Silica RP	fixed-λ UV*
Ishida 2015 [91]	2	26 x 18 x 21	Continuous-flow (20 nL)	Micro-chip RP	Micro EDC
Syringe Piston					
Sharma 2015 [92]	4.5	31 x 18x 14	Stop-flow (60 nL)	Monolith	fixed-λ UV
Sharma 2014 [93]	1.75	-	Stop-flow (60 nL)	Monolith	fixed-λ UV
Boringa 1998 [94]	10	28 x 43 x 15	Stop-flow (100 nL)	AEX	EDC
Baram 1996 [86]	14	53 x 20 x 30	Auto-stop-flow (1-100 uL)	Silica RP	multi-λ UV
Dual-Piston					
Commercial [88]	3.5	12 x 19	Continuous-flow (20 nL)	-	fixed-λ UV
Commercial [95]	-	-	Continuous-flow (20 nL)	-	fixed-λ UV
Tulchinsky [87]	9.5	41 x 25 x 23	Continuous-flow (20 nL)	Silica RP	fixed-λ UV
Otagawa [85]	-	-	Continuous-flow (20 nL)	Silica RP	EDC

Table 1-1 Miniaturized HPLC Systems

Prototype and commercial based miniature HPLC systems

Two groups have recently developed portable total HPLC systems. Sharma et al. characterized and reported two functioning portable LC systems in 2014 [93] and 2015. The first, an isocratic nanoflow pumping system was integrated with a fixed wavelength (254 nm) UV detector. The system was demonstrated through the isocratic separation of 6 different benzene compounds over the course of 19 minutes. It showed promising results; however, the limitation of isocratic gradient does not allow for complex sample analysis. Shortly after the publication of the first system, a modification to the pumping system from a single syringe pump to a dual syringe pump system allowed for programmable gradient elution shown in Figure 1-3 [92]. A total weight of ~4.5 kg for the system was realized. It was capable of generating up to 550 bar pumping pressure, a 60 nL injection volume, and a maximum gradient loop capacity of 74 uL with a typical flow rate at 350 nL/min. Sharma et al. characterized the system using a three-component pesticide mixture as well as a five phenol mixture.

The last notable portable liquid chromatograph system within recent years was one developed by Ishida et al. [91] in 2015 and is shown in Figure 1-4. It consisted of a battery-operated system integrated with an electroosmotic pump and a microfluidic device containing an integrated column and electrochemical detector. The flow rate ranged from 0 to 10 μL/min with a high degree of precision due to the use of flow sensors. The overall weight of the system was 2 kg, proving to be one of the more lightweight systems ever developed and had an operating time of 24 h with dry batteries. The chip itself was designed to minimize the dead volume between the column end and the detector; limiting it to only 10 nL. The column was a packed ODS particle reverse-phase column and the system performance was tested using standards

of alkylphenols, catecholamine, catechin, and amino acids [91]. This is the first complete system integrating a microfluidic chip and shows a promising future for microfluidic HPLC systems.

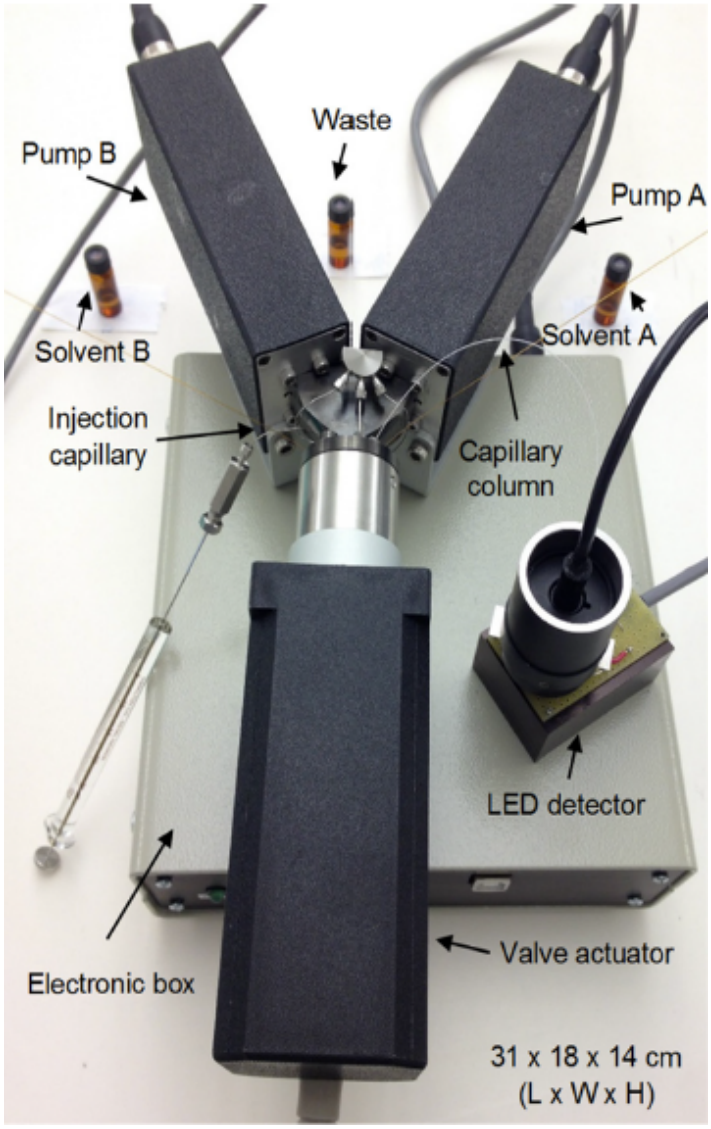

Figure 1-3 Photograph of hand-portable gradient nanoflow pumping system

Hand-portable HPLC system developed by Sharma et al.. It utilizes custom pumps developed by Vici to deliver a consistent flow rate and reproducible gradient. They utilize a miniaturized LED detector built in-house as their detector.

[Reprinted with permission from Sharma et al., Analytical Chemistry 87(20) 10457-10461. Copyright (2015) American Chemical Society.]

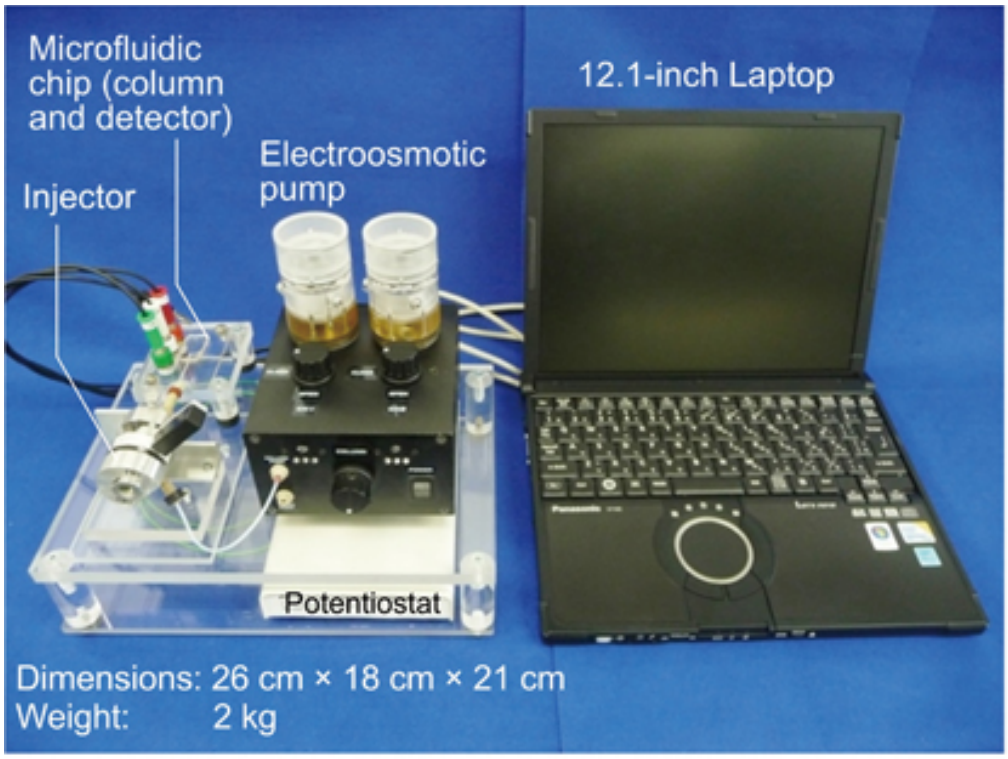

Figure 1-4 Photograph of fully integrated microchip HPLC system

Fully integrated microchip HPLC systems developed by Ishida et al.. Through the use of an electroosmotic pump and on-chip column and detector, this functional miniaturized HPLC system capable of flow rates into the uL/min range while utilizing an electrochemical detector to identify their analytes of interest.

Laser-induced fluorescent (LIF) detectors for sub-pM detection

The high specificity and sensitivity associated with LIF detectors make this a powerful technique for the detection of chromatographic separations. The speed at which these separations may occur as well as the wide assortment of applications including detection of pollutants, combustion products, proteins and DNA for cell analysis, food contaminants, and plasmas continue to make LIF detection a widely used analytical tool in research laboratories. Fluorescence may occur naturally from natively fluorescent compounds or can be induced through the labeling of analytes of interest.

The basic principle of fluorescence (Figure 1-5) occurs when a fluorophore absorbs energy in the form of light or other electromagnetic radiation causing a photon to reach a higher energy state (excited state). This unstable excited state is then allowed to vibrationally relax to the lowest excited singlet state (S1) and eventually relax down to the ground state (S0) with the simultaneous emission of light. This light produced is know as the fluorescence and has a lifetime of approximately 10^{-5}s to 10^{-10}s [96]. Due to the vibrational relaxation of the excited state, the energy of the fluorescence is generally less than the energy of the absorbed photon. This difference causes a longer wavelength for the fluorescence than the excitation creating what is known as the Stokes shift. It is this fundamental characteristic of fluorescence that allows the emission light to be separated from that of the excitation light.

The common setup for fluorescence allows the signal to be collected against a dark background, lowering the overall noise of the signal and thus lending itself to the overall high sensitivity of the system. The utilization of a longer excitation wavelength and the removal of impurities through chemical (i.e. oxidation), adsorption (i.e. charcoal) [97], or photobleaching [98] are several additional approaches for reducing the background signal. Several factors such as pH, dissolved oxygen, concentration, solvent choice, and temperature may affect the fluorescence intensity [99] since the environment and electronic structure of the fluorophore determines the Stokes shift and overall intensity. By successfully optimizing these conditions and carefully choosing the correct laser/fluorophore combination, concentration detection limits of 10^{-13} to 10^{-17} M and mass detection limits of 10^{-19} to 10^{-23} are possible [100-103].

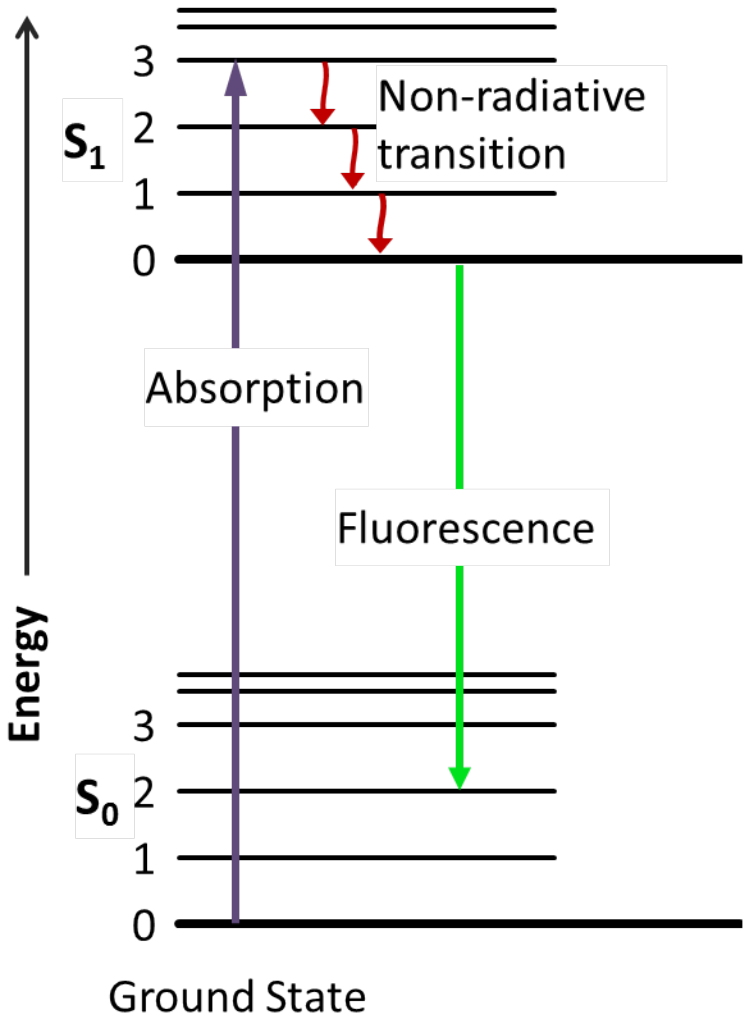

Figure 1-5 Jablonski diagrapm of a fluorescence molecule

Parallel HPLC instrumentation for high-throughput screening

In order to increase the throughput of conventional sample separations, research into parallel HPLC systems arose in the late 1990s [104-106]. Early systems for analytical/preparative analysis offered automated parallel detection of just two columns and were later increased to eight. During the time of increasing drug discovery, these systems allowed for a much-needed increase in sample throughput. The fluidics associated with parallel HPLC systems was mitigated through novel valve design; however, the limitations of these systems arose in the form of the detectors. Early systems just dedicated a single UV absorbance detector to each column.

The first commercial system developed by Waters was developed to address the need for a dedicated stand-alone absorbance detector that allowed for parallel column analysis [107]. This system known as MUX (multiplexed) Technology enabled either four or eight channels to be ran in parallel and was able to purify almost 4000 samples in 10 days. The detector, Waters 2488 Multi-channel UV/Vis Detector (Fig. 1-6) utilized a furcated fiber optic cable to split the light to each of the dedicated column channel flow cells. They also developed a multiple electrospray input for one of their quadruple mass spectrometers (Micromass' Quattro Ultima). Other companies soon followed with parallel screening HPLC systems including Sepiatec's 8x Screening HPLC system [108] and Dionex's UltiMate x2 Dual HPLC system with UV detection [109].

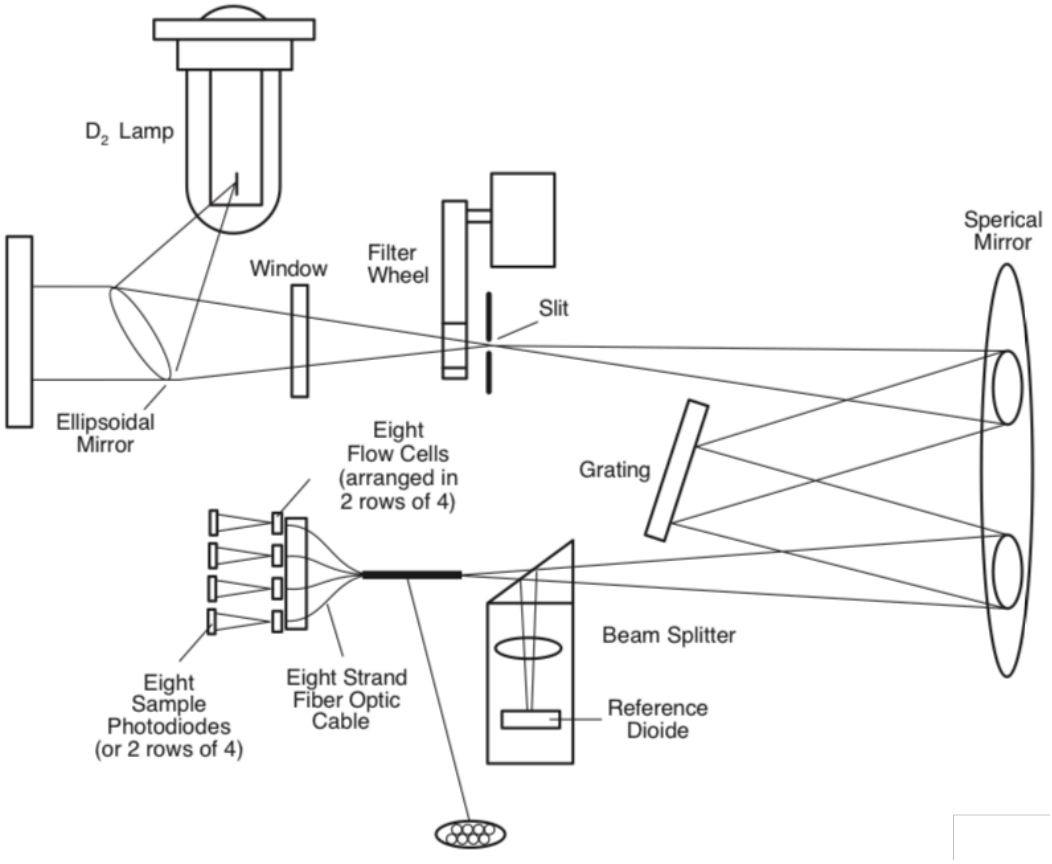

Figure 1-6 Schematic of Waters 2488 multi-channel UV/Vis detector

[Adapted with permission from Waters Corporation]

Currently with the advent of two-dimensional HPLC (2D-LC), the need beyond just drug screening for such parallel systems exists. With only three commercial systems, each with their own limitations, 2D-LC systems have been designed around only utilizing one or two separation columns in the second dimension. These leads to increasingly lengthy separations as all of the fractions from the first dimension must be stored in collection loops until they can be ran using the detector. Agilent currently has two configuration modes for 2D-LC. The first and most widely used technique utilizes an eight-position valve with two storage units (Figure 1-7A). The second method, known as multiple heart-cutting LC (mLC-LC) allows for twelve fractions to be taken from the first dimension, stored, and subsequently analyzed using the second dimension column (Figure 1-7B). However, each of these systems utilize only a single UV detector and thus are either limited in the fraction size based on the overall 2^{nd}-D separation time or can have smaller fraction sizes but the overall time to sequentially run each fraction is immense. In order to mitigate the downsides of each of these configurations, a multiple-channel detector could be used to run fractions concurrently.

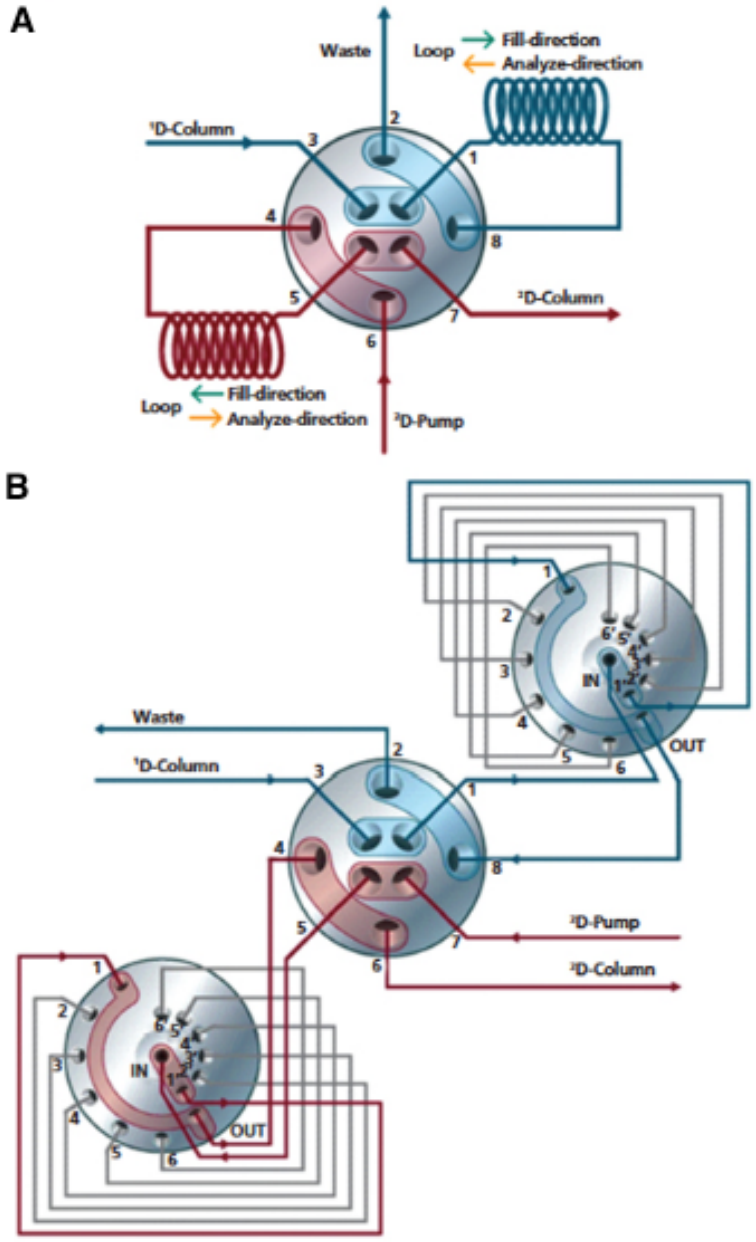

Figure 1-7 Agilent's commercialized 2D-LC valve setup

(A) comprehensive LC (LCxLC) and (B) multiple heart-cutting LC (mLC-LC)

[Adapted with permission from Agilent Technologies]

The materials in Chapter 1 are adapted from Talanta, (2018). **177**:94-103. The copyright was obtained from Elsevier and the license number is 4315050158423. For more details, please see Appendix A.

Chapter 2: High-performance liquid chromatographic cartridge with gradient elution capability coupled with an ultraviolet absorbance detector and mass spectrometer for protein and peptide analysis

Abstract

This work discusses the construction and performance of a HPLC cartridge we have developed that resulted from a culmination of previous research. We have recently developed an innovative approach to creating gradient elution's through the use of dual electroosmotic pump units and a series of three valves. This approach proved to be the most reproducible and robust in producing gradients compared to our previously tested methods. Through the use of this approach, we have assembled an HPLC cartridge powered and controlled through a computer capable of separating complex protein samples. The prototype cartridge is 20 cm × 20 cm × 17.5 cm (L × W × H respectively) and weighs approximately 3 kilograms. We have successfully coupled the cartridge with a UV absorbance detector and a mass spectrometer for protein/peptide analyses. It is readily coupled with other detectors such as electrochemical detector and laser-induced fluorescence detector.

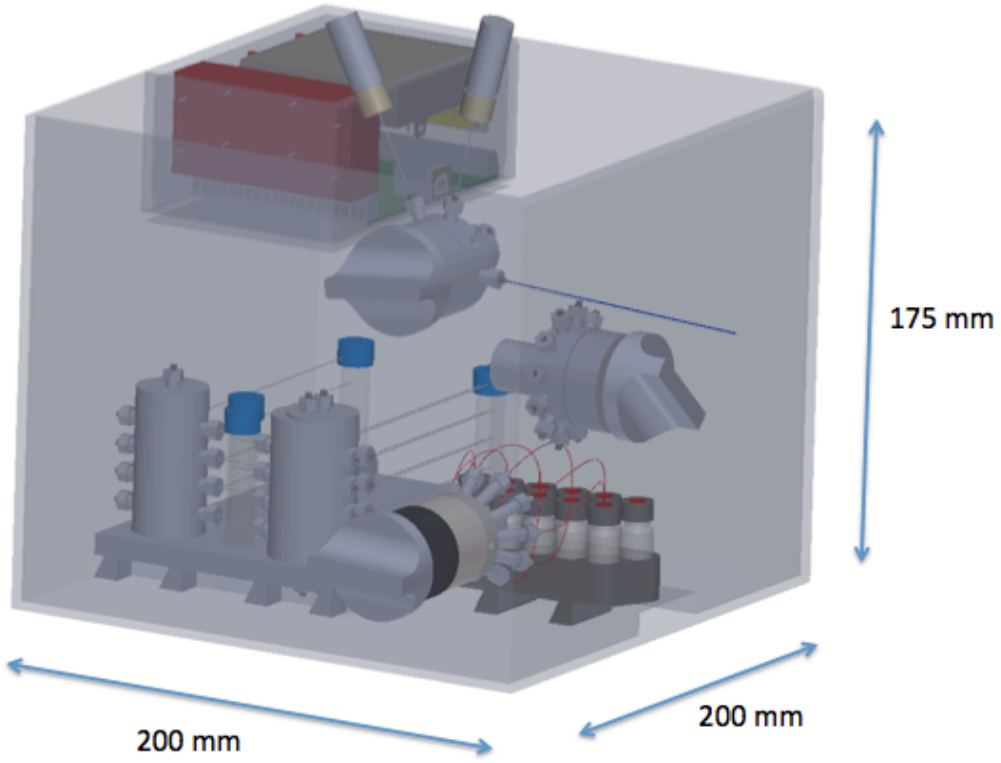

Figure 2-1 Three-dimensional rendering of the HPLC cartridge

Introduction

Miniaturizing high performance liquid chromatography (HPLC) has attracted increasing attention because it can reduce the instrument manufacturing costs and perform onsite analysis. In the late 1980s, the first portable, low-pressure LC system was developed by Otagawa et al., but problems existed with the system. The main problem was the flow rate irreproducibility leading to irreproducible separations. The other problem was that it produced only an isocratic gradient. Isocratic elution was not suitable for separating complex samples and it usually took too long for all analytes to be eluted out [110]. Since this early work, many other portable systems have been developed, but each lacking key features making its commercialization difficult [111]. In order to develop a miniaturized HPLC with little sample preparation, it needs to be able to separate a complex sample efficiently and quickly; thus a gradient elution is highly desired.

Capillary and on-chip columns have allowed for nanoflow and low-volume separations. This leads to the elimination of large amounts of organic waste as well as low volumes of sample and solvents needed to perform the separation [34, 111, 112]. Electroosmotic pumps (EOPs) allow one to reduce pump size while still permitting for high-pressure separations. EOPs couple well with capillary system and have been widely studied throughout our lab. In recent years, breakthroughs in electrochemistry, lab-on-chip, as well as valve and pump design have allowed for miniaturized gradient systems to be developed at a faster rate. Sharma et al. is one group that has published "hand-portable" LC systems (gradient and isocratic) that utilizes cutting edge pump and valve design [92, 93, 113]. Their system is battery operated, but it is limited to a

gradient of 60 μL and its robustness and versatility are not yet fully tested.

In this work, a novel approach to a low-cost HPLC cartridge is presented. This capillary-based cartridge incorporates the use of EOPs to drive its separation. Through stacking of pumps we have been able to generate pressures upwards of 1200 bar and flow rates in the microliter range [114, 115]; enabling packed column separation to take place. This cartridge utilizes a series of valves, a custom-built high-voltage power supply (HVPS), two EOP units with a custom built manifold, and a packed capillary column. The cartridge was controlled and powered by a computer via a USB port and data acquisition card (DAQ), while data was also collected and processed via the same DAQ and computer. The total weight of the cartridge is around 3 kg making it one of the lightest systems capable of gradient elution developed to date.

The cartridge can be coupled with a variety of detectors such as absorbance and fluorescence detectors [77, 116-118]. For small inorganic and organic ionic compounds, a conductivity detector would also be an appropriate choice due to its compact size. Here we demonstrate the feasibility of coupling the cartridge with two of the most common utilized detectors (an UV absorbance detector and a mass spectrometer) for protein/peptide analyses.

Experimental section

Chemicals and materials

Ethylene glycol dimethacrylate (EDMA, 98% w/w, hereinafter "%" indicates "% w/w" unless otherwise stated) and butyl methacrylate (BMA) were purchased from Alfa Aesar (Ward Hill, MA). 1-propanol and 2,2'-azobisiso-butyronitrile (AIBN, 98%) was bought from Aldrich (Steinheim, Germany).

Methacryloyloxypropyltrimethoxysilane (g-MAPS, 98%) was obtained from Acros (Fairlawn, NJ). Acrylamide, N,N'-Methylene bisacrylamide (bis), N,N,N',N'-Tetramethylethylenediamine (TEMED) and ammonium persulfate (APS) were purchased from Bio-Rad Laboratories (Hercules, CA). 1,4-Butanediol (99%) was purchased from Emerald BioSystems (Bainbridge Island, WA). Proteomics grade modified trypsin was obtained from Promega (Madison, WI). LC-MS grade acetonitrile (ACN) was bought from Fisher Scientific (Fair Lawn, NJ). 2-Acrylamido-2-methylpropane sulfonic acid (AMPS, 99%), BSA, myoglobin, sodium hydroxide, ammonium bicarbonate, and sodium acetate were purchased from Sigma-Aldrich (St. Louis, MO). Fused silica capillaries were obtained from Polymicro Technologies (Phoenix, AZ). Hydrochloric acid was obtained from EMD Millipore (Darmstadt, Germany). All solutions were prepared with ultra-pure water purified by a NANO pure infinity ultrapure water system (Barnstead, Newton, WA).

Cartridge configuration

Fig. 2-2 presents the configuration of the HPLC prototype cartridge. It consisted of two EOP units powered with a dual polarity high voltage power supply (HVPS), a 12-port switching valve (V1, Valco Instruments, Houston, TX), a 10-port stream selector (V2, Valco Instruments), a 60-nL injection valve (V3, Valco Instruments), and a packed capillary column (100 Å, 3 mm, 75 mm _ 100 mm, Waters, Atlantis dc18 NanoEase Column). Each EOP unit was composed of four parallel monolithic columns; these columns were connected in parallel via an in-house fabricated PEEK manifold. The prototype (Fig. 2-3) was 20 cm × 20 cm × 17.5 cm (l×w×h respectively) and weighed approximately three kilograms; most of the weight came from the clear lexan

material used to create the box for initial visual assistance. This weight will further be reduced with a different and lighter box material.

Fig. 2-4 presents the construction of an EOP unit. It was comprised of an in-house custom manifold that allowed for the connection of up to eight monolith capillaries to be connected in parallel; in this work only four monolith capillaries were utilized due to the flow rates required. When connected this way individual monolith pressures were averaged while flow rates were additive. High voltage was applied to the vial attached to the monolith capillaries whereas ground was applied to the vial connected to the bubbleless electrodes attached to the manifold 90 degrees to the monolithic columns. A common outlet out the top of the manifold allowed for the pump to either pull or push the downstream liquid depending on the polarity of the high voltage. One EOP unit (EOP-1 in Fig. 2-2) was employed to draw liquid in order to fill eluent loops and the other (EOP-2) to push and drive the liquid for sample separation. The protocols for preparing the bubbleless electrode and assembling the EOP were reported previously [119]. Each pump unit was capable of producing an unrestricted flow rate of approximately 800 nL/min with a pressure of 2000 psi at 5 kV.

Fig. 2-5 presents the HVPS assembly. It consisted of a positive and negative polarity EMCO C80 8 kV power supply (EMCO High Voltage Corp. Sutter Creek, CA). A printed circuit board was designed in-house to control the HVPS and a custom LabView program regulated the two power supplies separately through the use of a data acquisition board 1408LS DAQ-USB (Measurement Computing Corporation, Norton, MA). This board powered the pump units of the HPLC as well as allowed the data acquisition via the detector to take place through a USB port of a computer. A Linear

UVIS 200 absorbance detector (Linear Instruments, Reno, NV) was used as the primary detector in this work for cartridge characterization and testing. The detector was set at 214 nm for peptide and protein separations.

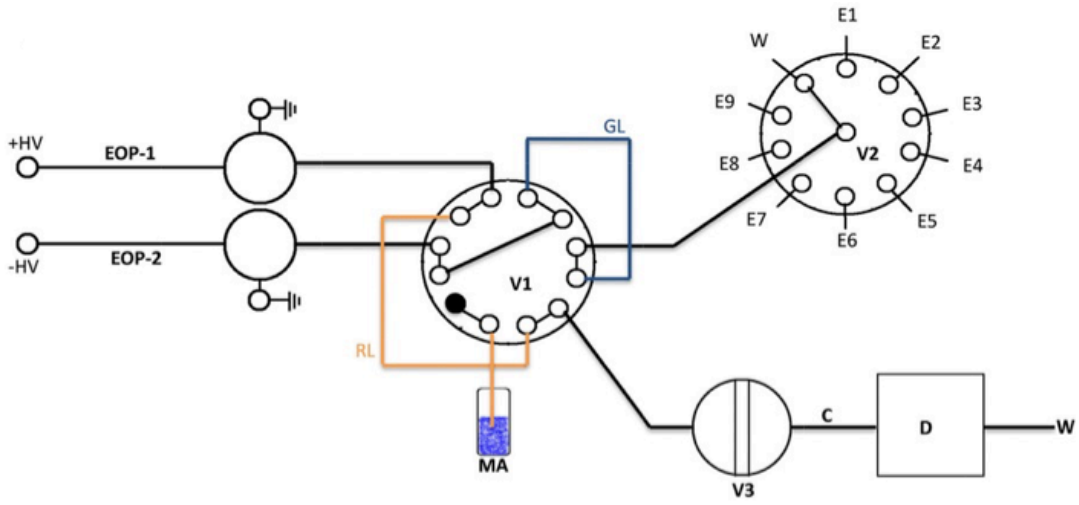

Figure 2-2 Schematic diagram of capillary-based HPLC cartridge

Overall system diagram. V1, two-position switching valve; GL, gradient loop (250 µm id × 50 cm length); RL, recondition loop (250 µm id × 50 cm length); MA, mobile phase A; V2, ten-port selection valve; E1–E9, nine eluent solutions; V3, 60-nL injection valve; D, linear UV-VIS absorbance detector set at 214 nm; C, packed capillary column (100 Å, 3 µm, 75 µm × 100 mm, Waters, Atlantis dc18 NanoEase Column); and W: waste. The black dot in V1 indicates that port was blocked.

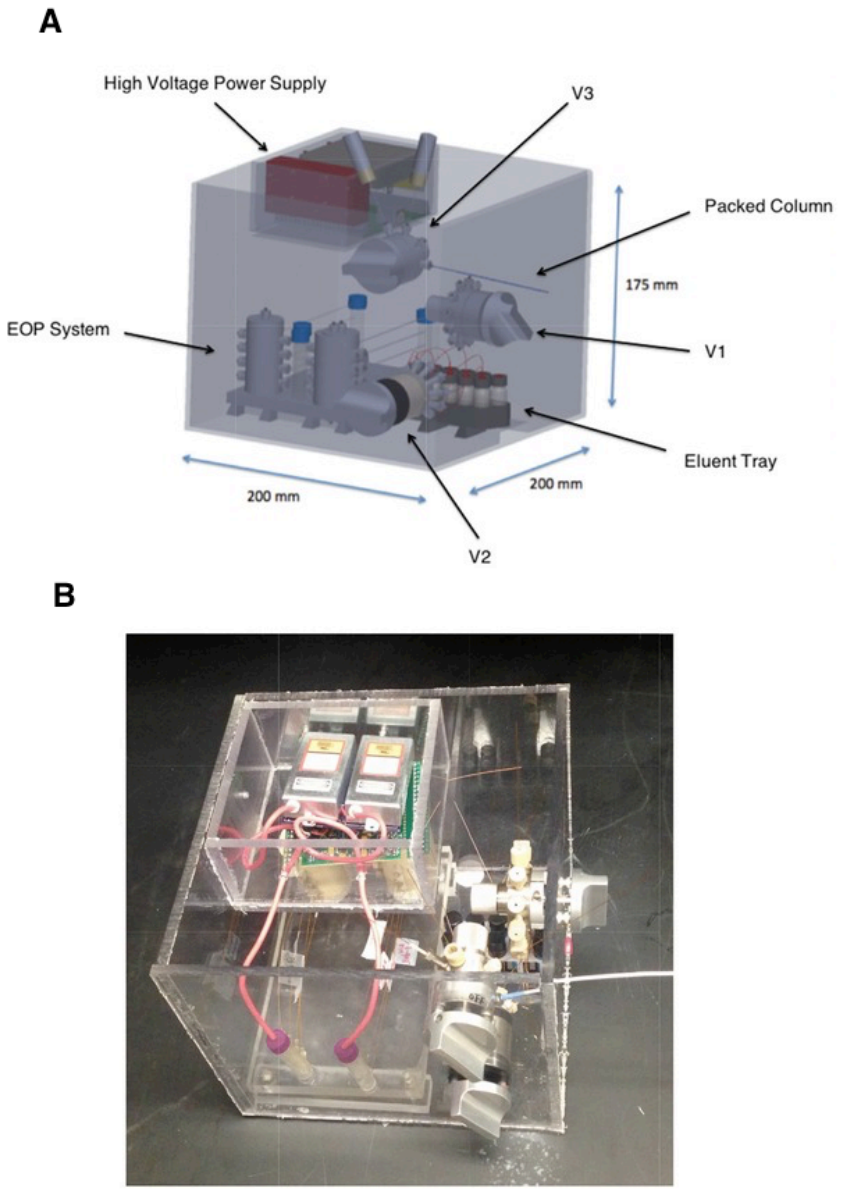

Figure 2-3 Overall integrated cartridge system

(A) Three‑dimensional rendering of the μHPLC system made within the laboratory. (C) Comprising an EOP system, high‑voltage power supply, a 12‑port two‑position valve, a ten‑port stream selector valve, a 60‑nL injector, capillary column, and a UV detector.

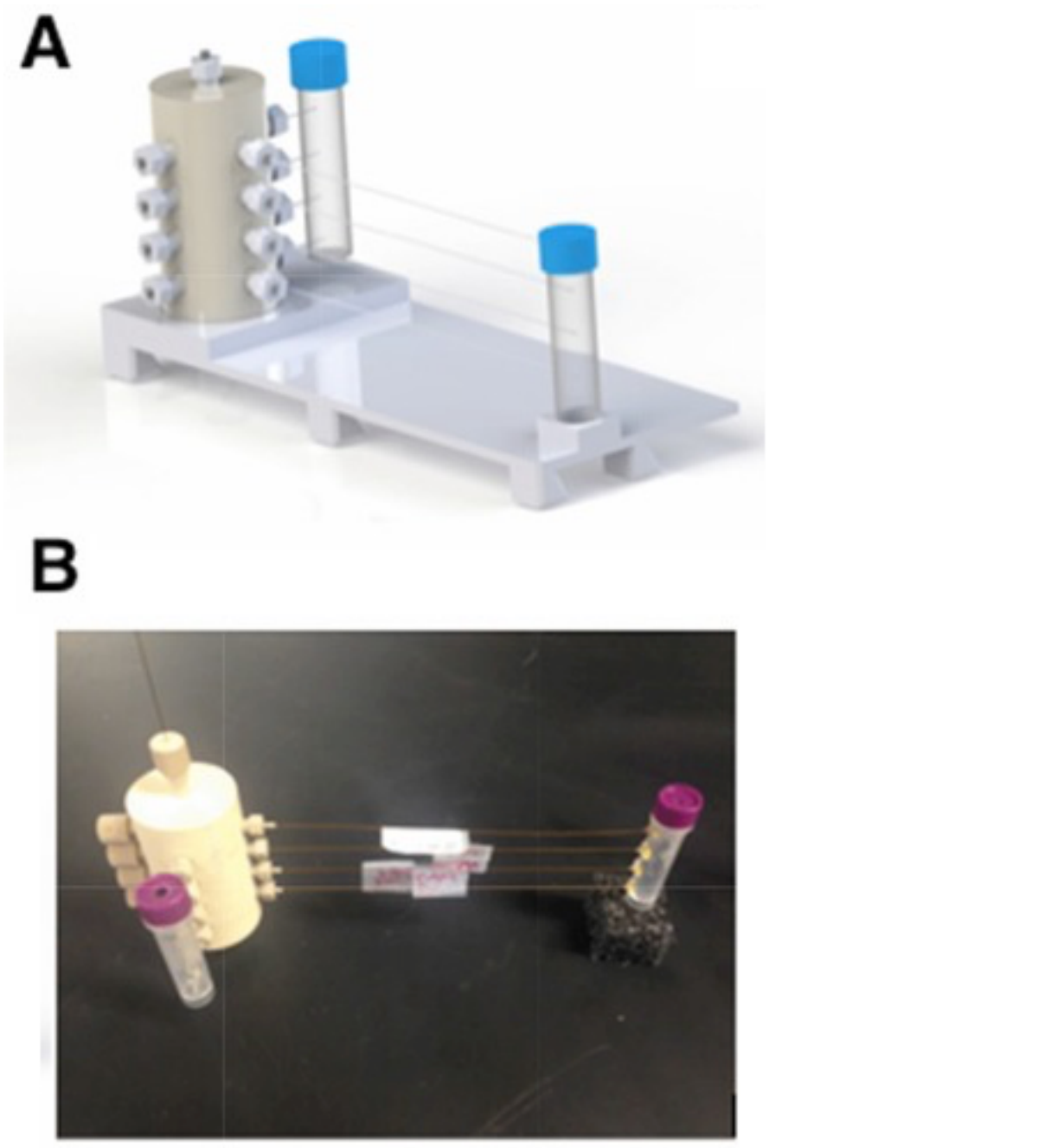

Figure 2-4 EOP pump system

(A) Three-dimensional rendering and (B) actual image of the EOP pump system made within the laboratory. Comprising of four –EOP, four bubbleless electrodes, a pump manifold, and two buffer reservoirs.

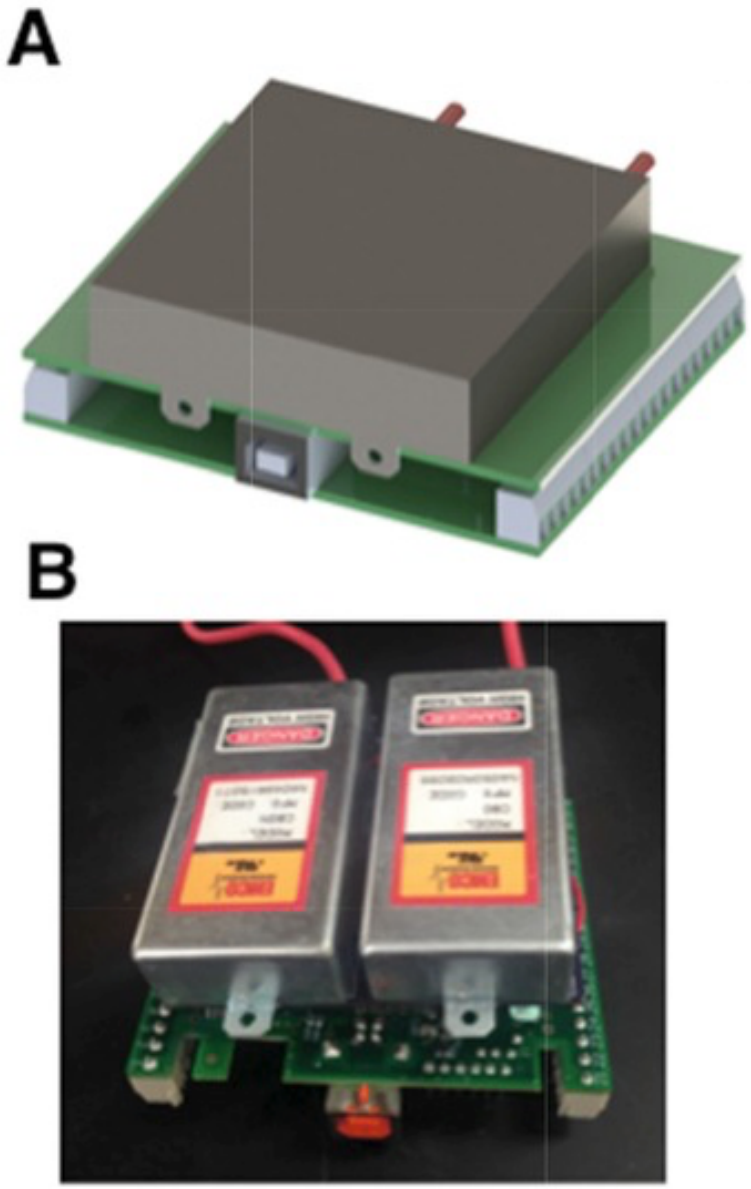

Figure 2-5 HVPS system

Three-dimensional rendering of the HVPS system made within the laboratory. Comprising a custom enclosure, a custom printed circuit board (PCB), a National Instruments 1408LS DAQ, and two EMCO C80 HVPS. (A) The initial 3D design. (B) The finalized HVPS system used within the HPLC cartridge.

Monolith capillary preparation-EOP and bubbleless electrode

The preparation protocol was similar to what we had described previously and can be viewed in depth in our previous literature [119]. An abridged version of the vinylization process was as followed. A capillary of approximately 150 cm (100-mm-i.d. x 360-mm-o.d.) was first flushed with acetone and 1.0 M NaOH, each for 10 min and then filled and sealed with 1.0 M NaOH where it was allowed to back in an oven at 100°C for 2 h. Once the capillary was removed from the oven, it was flushed with water, 0.1 M HCl, and acetone in that order; each for 20 min. After the capillary was sufficiently dried with N_2, the capillary was filled with 30% (v/v) g-MAPS in acetone, sealed, and placed back in the oven at 50°C for 14 h. The capillary at this point was rinsed with acetone and dried with N_2 at 60 psi for 2 h where it was now successfully vinylized and ready for the monolith preparation. The vinylized capillary was then cut to 16-cm-long segments. After degassing with helium, a solution containing 10.0 mg AMPS, 230.0 mg BMA, 160.0 mg EDMA, 4.0 mg AIBN, 424.0 mg 1-propanol, 116.0 mg 1,4-butanediol and 60.0 uL water was loaded into a capillary segment. A pressure supplied by a nitrogen cylinder was applied at a rate of 600 psi to the ends of the capillary and the capillary was placed in a water bath at 60°C for 20 h to allow complete polymerization to take place. After polymerization, approximately 2 cm of the capillary ends was trimmed and the monolithic column was flushed first with acetonitrile at 1500-2000 psi overnight and then with a 3.0 mM sodium acetate solution (pH 5.0) using an HPLC pump to remove unreacted monomers and other chemicals. Characterization of monoliths based on their voltage, flow rate, and output pressure can be seen in Fig. 2-6.

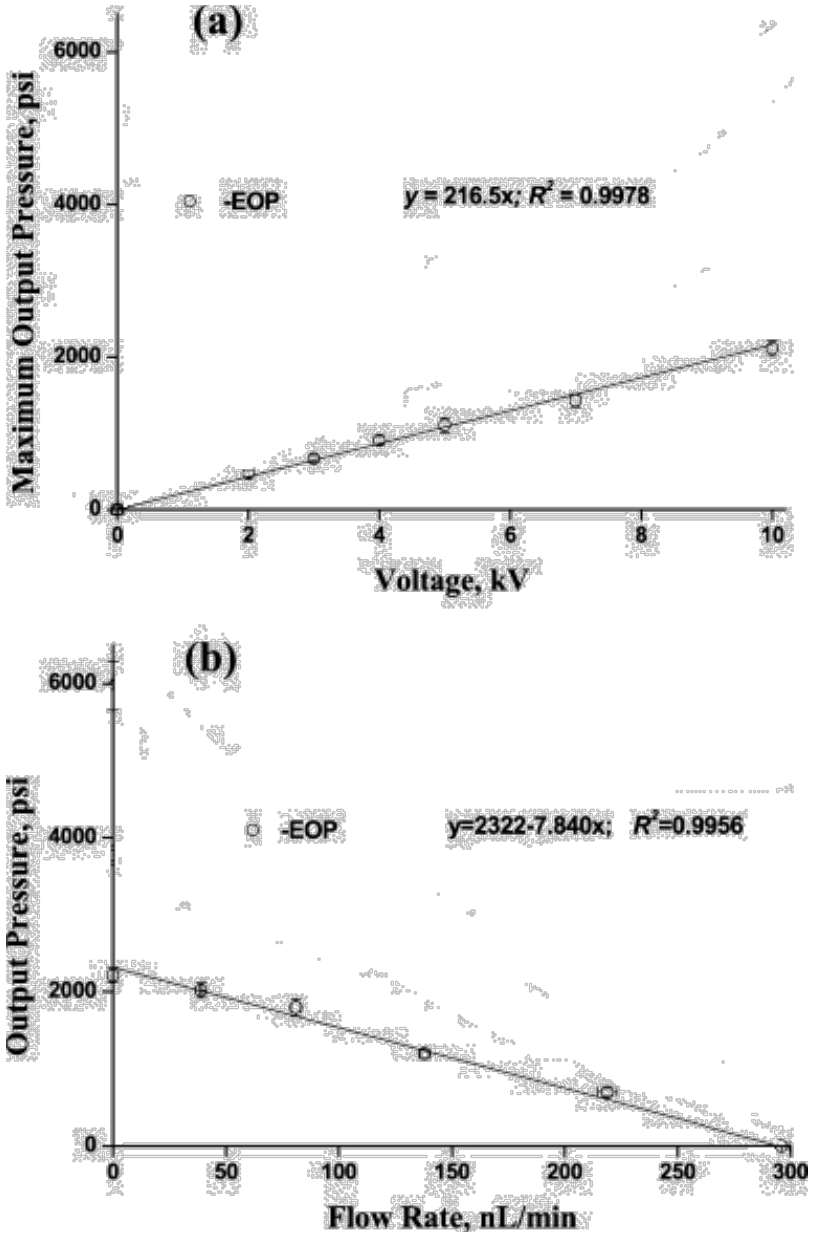

Figure 2-6 Characterization of -EOP

(A) Maximum pressure output vs. applied voltage and (B) output pressure vs. flow rate. -EOP – 75-µm-i.d. ×15 cm, and pump solution – 3 mM sodium acetate at pH 5.0. [Modified from Chen et al., Analytica Chimica Acta 844 (2014) 90-98.. Copyright (2014) American Chemical Society.

To prepare the bubbleless electrode, a capillary with the dimensions of 150-µm-i.d. (360 µm o.d.) and 20-cm long was cut and the inner wall was cleaned with NaOH (1.0 M) through the flushing of the capillary for 45 min, DI water for 15 min, and lastly acetonitrile for 15 min. Once the capillary was then sufficiently dried with nitrogen gas, the inner wall allowed to react with a solution containing 30% (v/v) g-MAPS in acetone at 50 ºC for 14 h. Then, the capillary was flushed again with acetonitrile and dried once more with nitrogen gas. Next, a degassed solution containing 9.0 %T (%T: the total weight concentration of acrylamide and bis in the solution), 3.0 %C (% C: bis concentration relative to acrylamide), 0.2% (v/v) TEMED, and 0.1% APS was pressurized into the capillary at 0 ºC overnight and then 4 ºC for another 24 h. After polymerization, 1-cm of the capillaries at both ends was trimmed off followed by a 50 mM sodium tetraborate solution being electrophoretically driven through the polyacrylamide within the capillary until a stable current was obtained. Finally, the resulting capillary was cut into 2-cm pieces and thus creating a bubbleless electrode.

Preparation of samples: peptide and protein

Tryptic digests of BSA and myoglobin were used to evaluate the performance of the µHPLC cartridge. One milligram protein (BSA or myoglobin) was dissolved in 100 µL of 25 mM ammonium bicarbonate (pH 8.25) to a concentration of 10 mg/mL, and 0.2 µL of 1 M dithiothreitol was added into the solution. Trypsin at 1 µg/µl (Sequencing Grade Modified Trypsin, Frozen; Promega Cat# V5113) was then added into the solution at a ratio of 100:1 (protein:trypsin, w/w). After incubating in a water bath at 37 °C for 8 hours, the solution was centrifuged at 8000 rpm/min for 5 min. The supernatant was passed through an ULTRAFREE-MC 5000 NMWL Filter Unit (Merck-Millipore,

Germany) to get rid of any undigested proteins. The tryptic digests were ready for use or for storage at -20 °C.

Wild type and mutant myoglobin samples were obtained from Dr. Jun Yi [120]. In brief, a horse heart myoglobin gene with a single base mutation (hhMb, H64V) was engineered and expressed in E. *coli*. The lysed proteins from E. *coli* were concentrated by ammonium sulfate precipitation and the mutant myoglobin was purified by a DEAE-Sepharose column. The wild type and mutant myoglobins were then mixed and diluted to a concentration of 10 mg/mL as a stock solution and stored at -20 °C.

Gradient profile monitoring using C^4D

In order to monitor the profile of the generated gradient, the use of a capacitively coupled contactless conductivity detector (C^4D), TraceDec, Innovative Sensor Technologies, Strasshof, Austria) was employed. The C^4D allowed the impedance to be measured through the variation in conductivity from the changing acetonitrile concentration of the eluent solution (Figure 2-7). The actual profile of the gradient was obtained by converting the signal acquired with a calibration curve (Figure 2-8).

An Agilent 1200 HPLC system also utilized in order to produce performance comparisons for the linear gradient profiles. To produce low flow rates comparable to that of the μHPLC system, a micro-Tee (Upchurch Scientific) and a fused silica capillary (50-μm-i.d. × 360-μm-o.d. × 50 cm length) were used as a restrictor to generate desired backpressures for the separations.

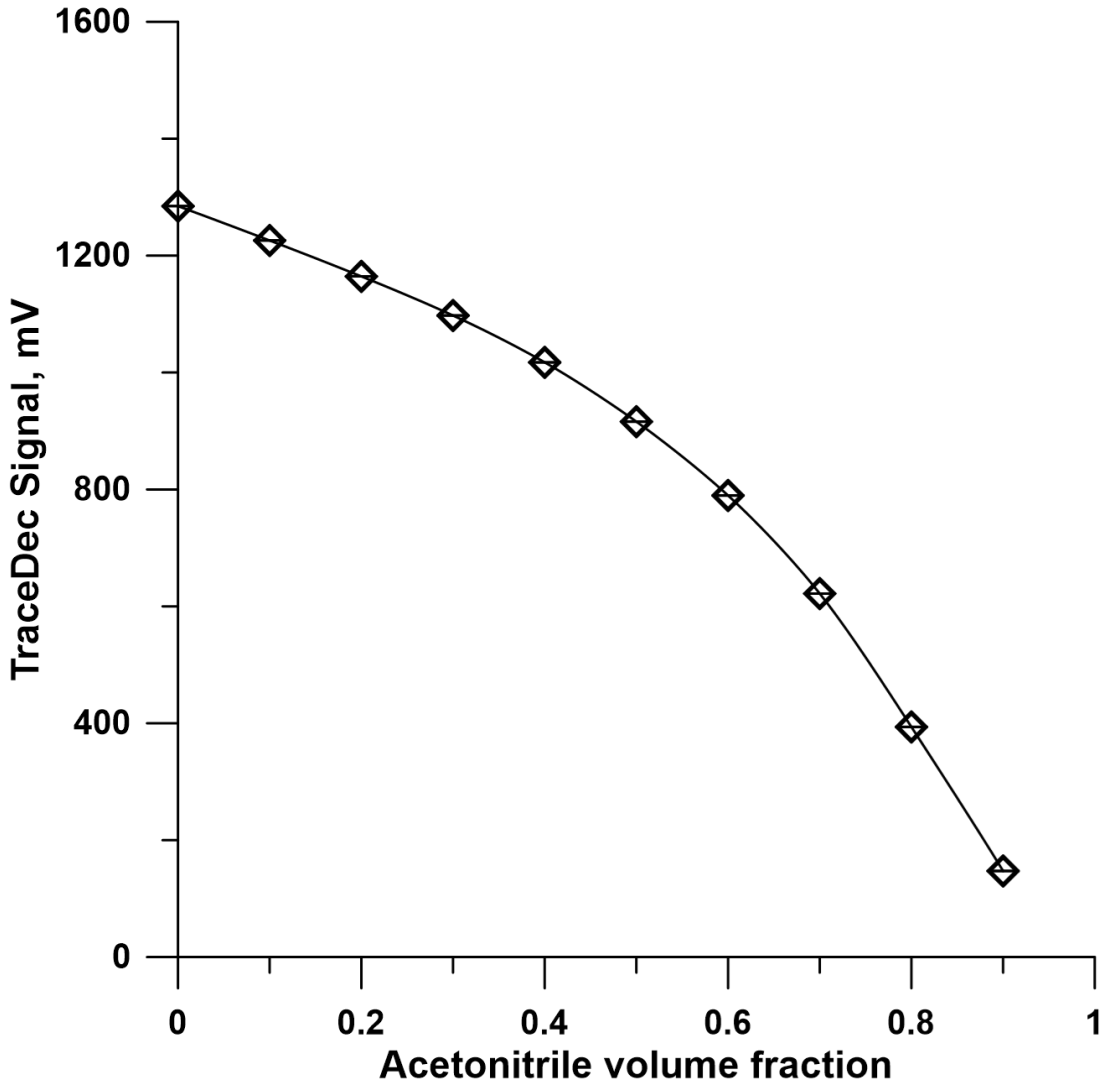

Figure 2-7 C^{4}D signal for acetonitrile volume fraction

Solution: 0.1% (v/v) TFA + water + acetonitrile. TraceDec condition: frequency, high; voltage, -18 dB; gain, 50%; offset, 0. Capillary, 75 μm ID X 360 μm OD. [Reprinted with permission from Gu et al., Analytical Chemistry (2012). 84(21):9609-9614. Copyright (2012) American Chemical Society]

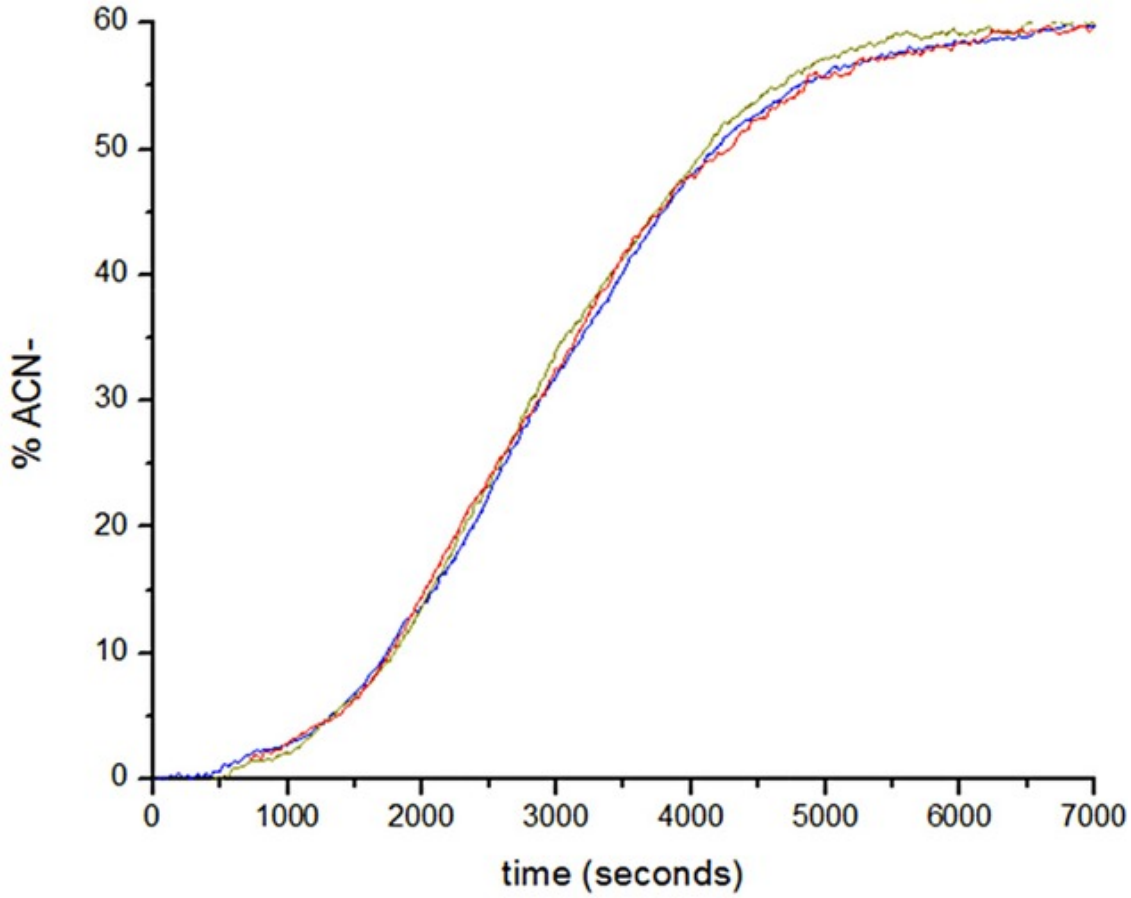

Figure 2-8 Reproducible gradient profiles

Reproducible gradient profiles E1–E9 had compositions, respectively, of 60, 50, 40, 30, 20, 15, 9, 6, and 3% acetonitrile in 0.1% TFA. This was to achieve a gradient from 0 to 60%. A contactless conductivity detector was used to monitor the gradient change.

Results and discussion

Nano-flow gradient profile

Referring to Fig. 2-2, one of the 10 ports of the selection valve (V2) was connected to waste (W), and the other nine eluents were connected 1 through 9 (E1 through E9). A linear gradient was achieved using V2 and nine different eluent concentrations. As V2 was switched from E1 to E2, E2 to E3, … and E8 to E9 for 3 minutes each while a voltage of -4kV was applied to EOP-2, E1 – E9 would be aspirated into the gradient loop (GL). In this work, the compositions of E1, E2, E3, E4, E5, E6, E7, E8 and E9 were respectively 60%, 50%, 40%, 30%, 20%, 15%, 9%, 6%, and 3% acetonitrile in 0.1% TFA. This was to achieve a gradient from 0-60%, which was the optimal range for separating both myoglobin and BSA digest as shown in our previous studies [119, 121, 122]. As stated above, the gradient consists of 3 minutes of each eluent leading to a gradient volume of ~15 uL. [Apparently, there were no constraints with regard to the volume of GL.] This volume gives a separation time of 80 minutes using a column flow rate of 200 nL/min. Fig. 2-8 presents typical reproducibility results of a gradient profile.

Operation consideration and recommendation

From t = 0 to t = 10 min, a voltage of +4 kV was applied to EOP-2 to rinse the GL while V2 was connected to W. The pump rate under this condition was ~500 nL/min. This ensured the GL was filled with buffer solution so as not to contaminate the pump monoliths when the eluents were drawn up. Higher voltage could be applied to increase flow rate but it was not necessary and also good for avoiding excessive Joule heating. Then the high voltage was switched to -4 kV and V2 was switched from E1 to

E2, E2 to E3, … and E8 to E9 for 3 minutes each. Once the -4 kV was turned off, nine eluent solutions resided inside GL. The total time for these operations was 25 min.

At the same time, a voltage of +3 kV was applied to EOP-1; the pump rate at this voltage was ~150 nL/min. The EOP drove mobile phase A (composition 0% ACN in 0.1% TFA) in the recondition loop (RL) to equilibrate the column for sample injection. After t = 25 min, the sample injection valve (V3) was switched from "load" to "injection" to inject a sample into the column; proteins were stacked at the column head under mobile phase A conditions. [Note: A 60-nL injection valve was used at this time through a time-controlled injection scheme (8 s at a flow rate of ~150 nL/min) to inject ~20 nL of a sample into the column for separation.] After sample injection, V3 was switched back to "load" position, V1 was switched to its second position and EOP-1 drove the gradient eluent through the injector and column for chromatographic separation.

During the separation, -4 kV was applied to EOP-2 for 20 min to refill RL with mobile phase A, and the high voltage was turned off. After the separation was complete, V1 was switched back to initiate a new run.

Peptide separation

We coupled the HPLC cartridge with a UV absorbance detector and performed separations of peptides (tryptic digests of bovine serum albumin and myoglobin). We compared the performance of our HPLC cartridge to an Agilent 1200 HPLC system. The tryptic digest separation results are presented in Fig. 2-9 for BSA and Fig. 2-10 for myoglobin. Comparable resolutions were obtained for the two systems. Although the chromatograms are visually different, these differences were attributed primarily to the

differences in gradient profiles for the two systems. It is also important to note that the delay time associated with our HPLC cartridge was roughly half of that of the Agilent 1200 system due to the reduced connection capillary volumes.

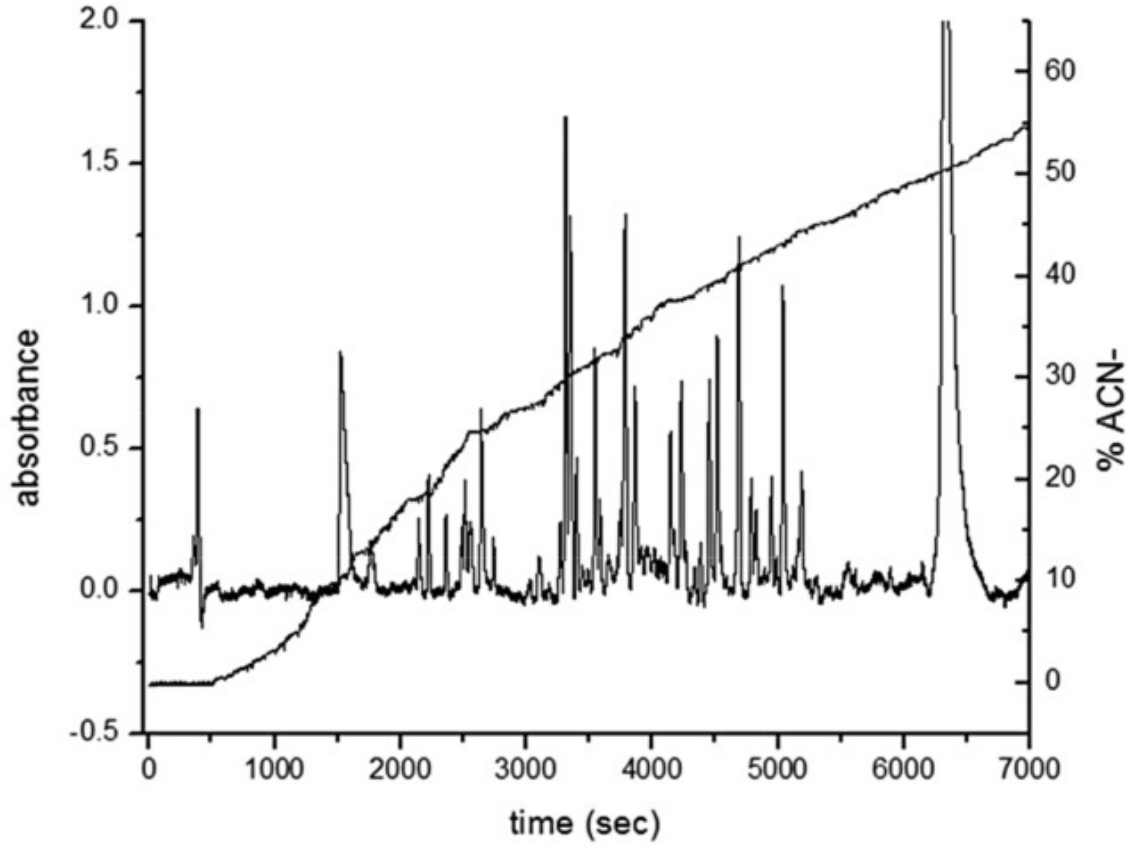

Figure 2-9 Separation chromatogram. Sample-trypsin digest of BSA

Chromatogram is for separation of BSA digests. Each separation contained a 20-nL sample injection volume and was performed at a column flow rate of 150 nL/min. The gradient profile was measured at a position between V1 and V3. Sample concentration of 10 mg/mL. The absorbance signal was monitored at 214 nm.

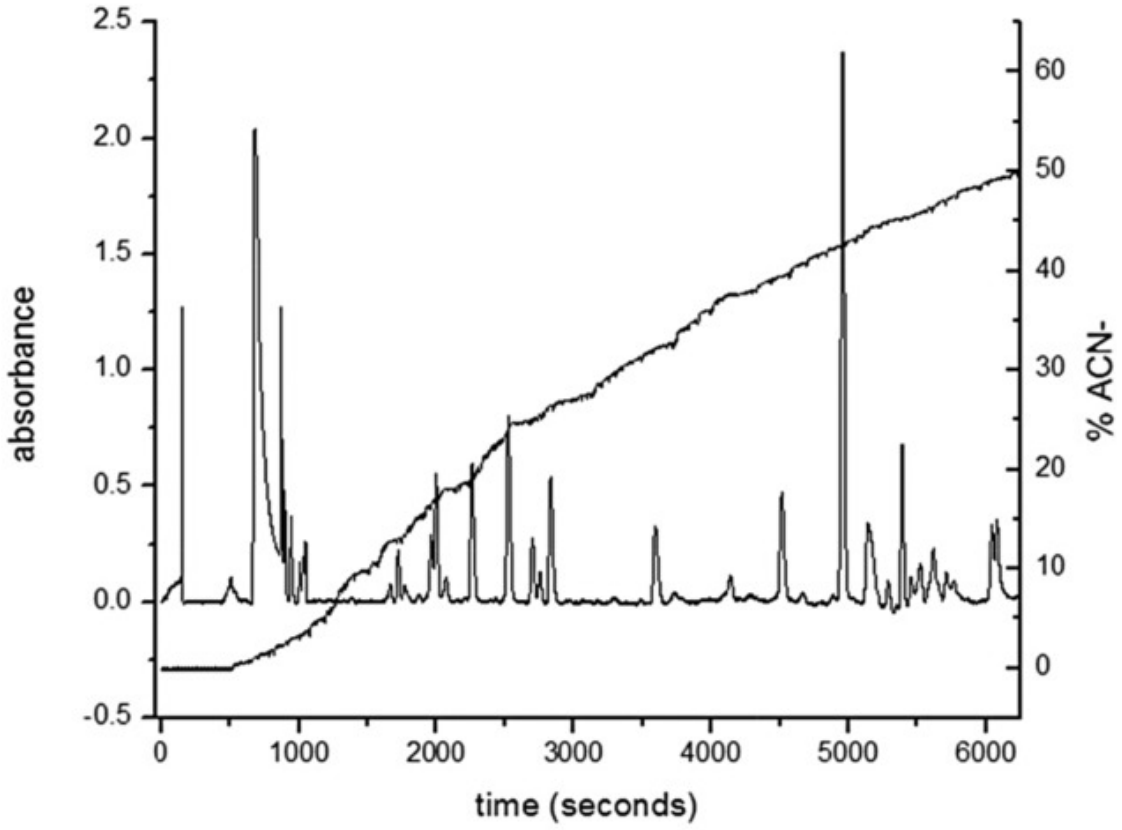

Figure 2-10 Separation chromatogram. Sample-trypsin digest of myoglobin

Chromatogram is for myoglobin digests separation contained a 20-nL sample injection volume and was performed at a column flow rate of 150 nL/min. The gradient profile was measured at a position between V1 and V3. Sample concentration of 10 mg/mL. The absorbance signal was monitored at 214 nm.

We incorporated the HPLC cartridge with a mass spectrometer and performed separations of a real-world protein sample. Fig. 2-11 presents the results. The goal was to distinguish normal proteins ("health status") from abnormal ones ("disease status'). A single amino acid substitution in a protein may result in the loss of the protein functions and subsequently cause a disease [123]. It has been shown that myoglobin, as an oxygen carrier, plays a vital role in preventing the heart from injury [124, 125]. A single mutation of myoglobin, a histidine converted to valine at position 64 (hh Mb, H64V), increases the possibility of heart injury [120]. Peak A in Fig. 2-11 represents the wild type, whereas peak C represents the H64V myoglobin mutant and peak B is the mutant with an extra methionine at the N-terminus end. Addition of methionine to the mutant occurs only when the protein is expressed in the bioengineered E. coli [126]. The measured molecular weights for peaks A, B and C were 16951.36, 16912.79, and 17045.73 Da, compared to the theoretical values of 16951.49, 16913.48, and 17044.67 Da respectively.

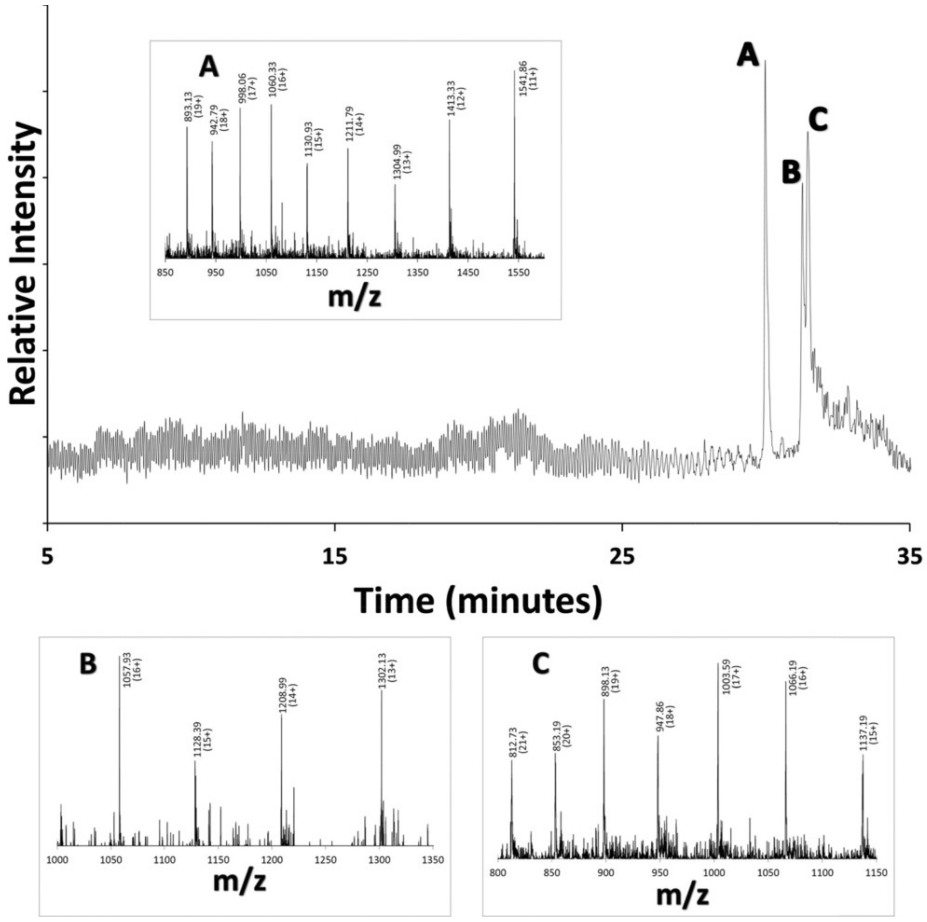

Figure 2-11 ESI-MS data for coupled HPLC cartridge. Sample-mutated myoglobin (H64V)

HPLC cartridge coupled with MS for protein analysis. Sample: a mixture of mutated myoglobin (H64V) and wild‑type myoglobin (20 ng/mL each). Injection volume: ~20 nL with an injection time of 8 s. A linear gradient from 0– to 60% acetonitrile was applied to the separation column as described within the text. Column flow rate was ~150 nL/min, ESI voltage was set at 3.0 kV, and the MS was set as a full scanning mode with *m*/*z* range of 700–2000. Insets A–C are mass spectra of peaks A–C from the overall separation, respectively, with *m*/*z*.

Concluding remarks

In this work, a HPLC cartridge capable of producing reproducible linear gradients was constructed. Through the use of electroosmotic pumps, high-pressure separations of complex protein samples were obtained. The creation of an innovative miniaturized dual polarity high voltage power supply as well as a specialized manifold for each eletroosmotic pump system allowed for the overall size to be small while still having comparable performances of that of a commercial system. This was the first prototype designed allowing for further optimization to decrease size and weight of the system. This work showed the capability of the cartridge when coupled with a UV absorption detector and a mass spectrometer. It is our hope to create an HPLC cartridge with interchangeable detectors depending on the analyte being identified. Work is currently being completed in our lab to provide miniaturized detectors for this cartridge.

The materials in Chapter 2 are adapted from. Lynch et al., Journal of Separation Science, 2017. 40(13):2752-2758. The copyright was obtained from John Wiley and Sons, and the license number is 4315041474845. For more details, please see Appendix B.

One figure in Chapter 2 is adapted from Zhang et al., Journal of Chromatography A.1460: 68-73 (2016). The copyright was obtained from Elsevier and the license number is 4316591286765. For more details, please see Appendix C.

One figure in Chapter 2 is adapted from Chen et al., Analytica Chimica Acta 887 (2015) 230-236. The copyright was obtained from Elsevier and the license number is 4316600057156. For more details, please see Appendix D.

Chapter 3: Confocal laser-induced fluorescence detector for narrow capillary systems with yoctomole limit of detection

Abstract

Laser-induced fluorescence (LIF) detectors for low-micrometer and sub-micrometer capillary on-column detection are not commercially available. In this work, we describe in details how to construct a confocal LIF detector to address this issue. We characterize the detector by determining its limit of detection (LOD), linear dynamic range (LDR) and background signal drift; a very low LOD (~70 fluorescein molecules or 12 yoctomole fluorescein), a wide LDR (greater than 3 orders of magnitude) and a small background signal drift (~1.2-fold of the root mean square noise) are obtained. For detecting analytes inside a low-micrometer and sub-micrometer capillary, proper alignment is essential. We present a simple protocol to align the capillary with the optical system and use the position-lock capability of a translation stage to fix the capillary in position during the experiment. To demonstrate the feasibility of using this detector for narrow capillary systems, we build a 2-μm-i.d. capillary flow injection analysis (FIA) system using the newly developed LIF prototype as a detector and obtain an FIA LOD of 14 zeptomole fluorescein. We also separate a DNA ladder sample by bare narrow capillary – hydrodynamic chromatography and use the LIF prototype to monitor the resolved DNA fragments. We obtain not only well-resolved peaks but also the quantitative information of all DNA fragments.

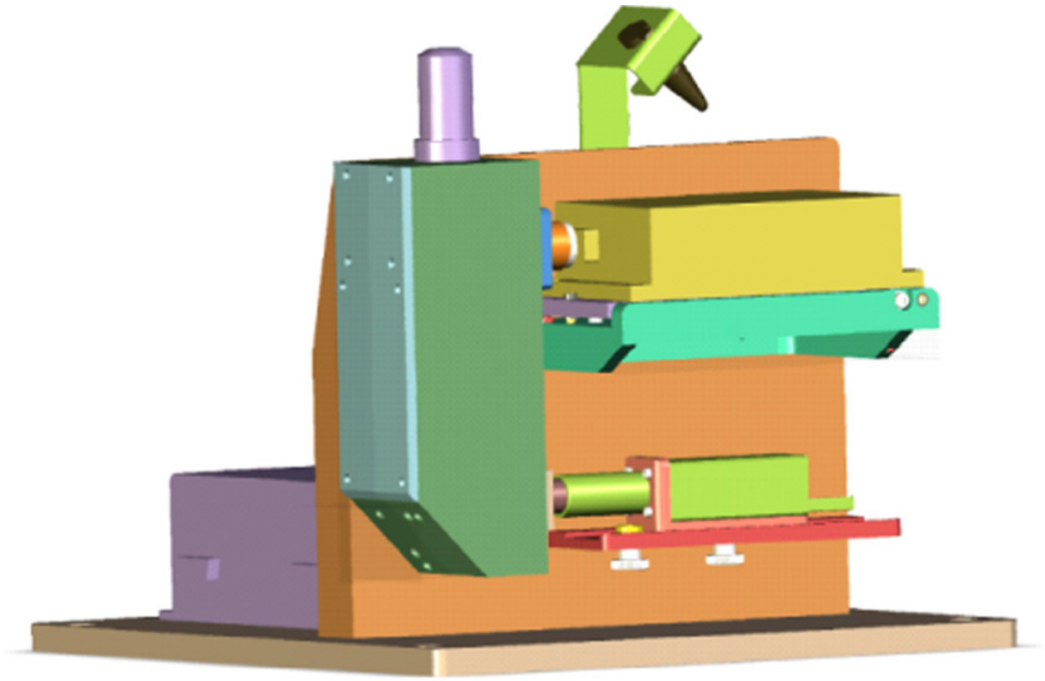

Figure 3-1 Three-dimensional rendering of the LIF detector

Introduction

Laser-induce fluorescence (LIF) is one of the most sensitive techniques for molecular detection. It is widely used for monitoring compounds resolved by chromatography [1,2] and capillary electrophoresis (CE) [3,4] (including microfluidic chip-based analysis [5]). However, most of these instruments are either customer-made or specialized for particular utilizations. Only a few stand-alone LIF detectors are developed [6–10] and none is manufactured for low micrometer to sub-micrometer inner diameter (i.d.) capillary systems.

Genes are pieces of DNA that carry the genetic instructions used in developing all living organisms. Separating and analyzing DNA fragments is usually the first step toward understanding and manipulating how DNA works. DNA separations are commonly performed suing slab-gel electrophoresis. To enhance the resolving power, reduce the separation time, and increase the throughput, researchers are now frequently using capillary gel electrophoresis or capillary array electrophoresis. All the above techniques utilize viscous gel sieving matrices (either cross-linked or linear polymers). As these matrices in capillaries need to be loaded and replenished after each run, loading/reloading viscous matrices into micrometer-bore capillaries is tedious and time-consuming.

We have recently developed an innovative separation technique for separating and sizing DNA without using sieving matrices [11–15]. Because the separation is preceded inside a Bare Narrow Capillary (BaNC) and the separation mechanism is based primarily on hydrodynamic chromatography (HDC) [16,17], we term this technique BaNC-HDC. DNA fragments from a few base pairs (bp) to more than one

hundred kilobase pairs (kbp) have been nicely resolved [15]. Similar work has also been performed in other labs [18,19]. Owing to the small diameter (a few hundreds of nanometers to a few micrometers) of the separation capillary, no detectors are commercially available for BaNC-HDC. Since narrow capillaries are commercially produced by Polymicro Technologies - a subsidiary of Molex, the lack of suitable LIF detectors has been a major barrier for other researchers to investigate and/or use BaNC-HDC. In order to address this issue, here we describe how to construct a confocal LIF detector and how to use it for BaNC-HDC. With this detector we also build the first 2-μm-tubing flow injection analysis (FIA) system. To our knowledge, this is the smallest tubing FIA system reported so far. Reduced tubing size will lead to decreased reagent consumptions and sample quantity requirements. Characterizations of the instrument are also discussed.

Experimental section

Chemicals and materials

Fused-silica capillaries were products of Polymicro Technologies (Phoenix, AZ). GeneRuler™ 1-kb plus DNA ladder (SM1331) was obtained from Fermentas Life Sciences Inc. (Glen Burnie, MD), and YOYO-1 was from Molecular Probes (Eugene, OR). Concentrated hydrochloric acid, ethylenediaminetetraacetic acid (EDTA), fluorescein, sodium hydroxide, and tris(hydroxymethyl)aminomethane (Tris) were purchased from Fisher Scientific (Fisher, PA).

Preparation of DNA sample and solutions

The stock solution of 100 ng/μL 1-kb plus DNA ladder was prepared by mixing 39 μL of 10 mM TE buffer, 10 μL 500 ng/μL DNA, and 1 μL YOYO-1. Working standard DNA solutions were made by diluting the stock solution with DDI water at the ratio as needed. Eluent and DNA samples were stored at 4 °C.

Running buffer, 10 mM TE buffer, was composed of 10 mM Tris–HCl and 1.0 mM Na_2EDTA at pH 8.0. It was prepared using DDI water from a NANO pure infinity ultrapure water system (Barnstead, Newton, WA). Before use, the running buffer was filtered through a 0.22-μm filter (VWR, TX) and vacuum-degassed. 1 mM fluorescein stock solution was prepared by dissolving the desired amount in 10 mM TE buffer and, when in use, diluted to the required concentration with additional 10 mM TE buffer. The stock solution of 100 ng/μL 1-kb plus DNA ladder was prepared by mixing 39 μL 10 mM TE buffer, 10 μL 500 ng/μL DNA, and 1 μL YOYO-1. Working standard DNA solutions were made by diluting the stock solution with 10 mM TE buffer at the ratio as needed. Running buffer and samples were stored at 4 °C.

LIF Detector Construction

Fig. 3-2 presents a schematic diagram of a BaNC-HDC system in which major components of the LIF detector are shown. A 488 nm solid-state laser module (Melles Griot, Rochester, NY) was used as the excitation light source. After passing through a 488 nm laser cleanup filter (Melles Griot), the laser beam was reflected by a dichroic mirror (Semrock, Rochester, NY) with high reflectance below 491 nm and focused to the narrow capillary by an objective lens (0.32 NA, 16× magnification, Melles Griot). The same objective lens collected and collimated the emitted fluorescent light. After the collimated fluorescence passed through the same dichroic mirror, it was reflected by a mirror (Melles Griot), filtered by a 510 nm long-pass filter (Semrock, Rochester, NY), and focused by a lens (Melles Griot) through a 800 μm pinhole onto a photomultiplier tube (H5784-01, Hamamatsu, Shizuoka, Japan). The output signals was acquired by a USB data acquisition card (Measurement Computing, Norton, MA) and displayed on a computer running an in-lab LabView program. Fig. 3-3A presents a picture of the assembled LIF detector (note: the pressure chamber and the narrow capillary were not considered as part of the LIF detector), and Fig. 3-3 B-D presents the details of how all components are arranged and packed together.

The backbone of the detector was a vertical support that was firmly attached to a base plate (see Fig. 1B). A laser holder and a PMT holder were bolted onto the vertical support. There was a leveling plate on the laser holder and it was used to perform some fine adjustments of the laser height and direction. An optical tube was also bolted onto the vertical support and aligned with the laser and PMT (see Fig. 3-3C). In order to show how optical components were arranged inside the optical tube, we made the tube

wall transparent (see Fig. 3-4). The objective was fixed to the top of the tube via threads. The dichroic mirror was fixed to backside of the tube. The reflector was fixed at the bottom of the tube and it could be adjusted via an Allen wrench to direct the fluorescence light properly to the pinhole in front of the PMT. Fig. 3-3D presents a view from the other side of the vertical support to which a waste reservoir holder was attached. A laser power supply was fixed to the base plate. An X-Z translation stage was bolted onto the back of the optical tube and a capillary holder was fixed to the translation stage.

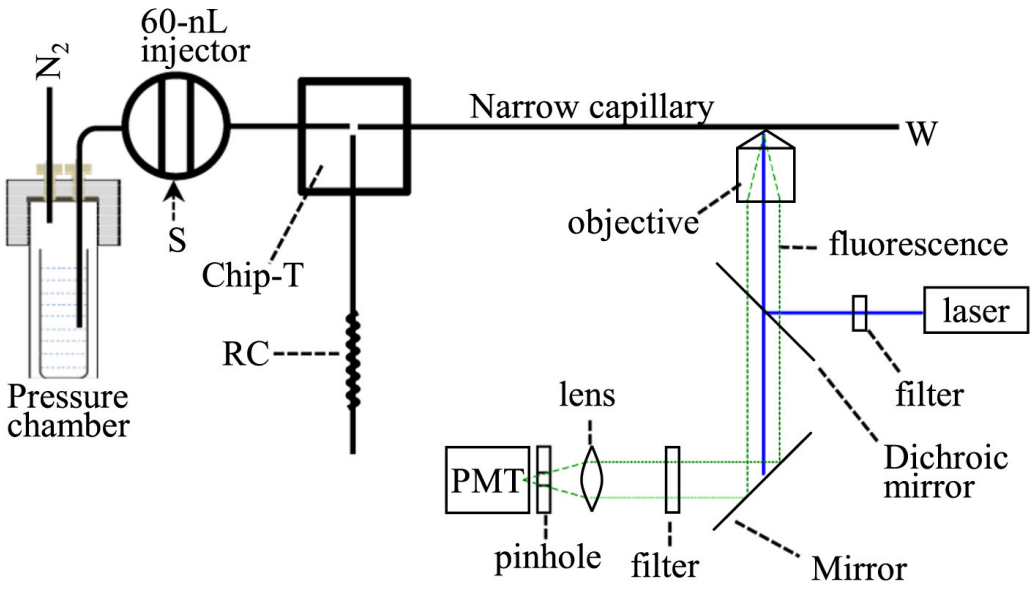

Figure 3-2 Schematic for BaNC-HDC system and LIF detector

Schematic configuration of BaNC-HDC system. The narrow capillary had a total length of 47 cm (41 cm effective), an i.d. of 2 μm and o.d. of 150 μm. RC had a length of 6.5 cm an i.d. of 20 μm and an o.d. of 150 μm.

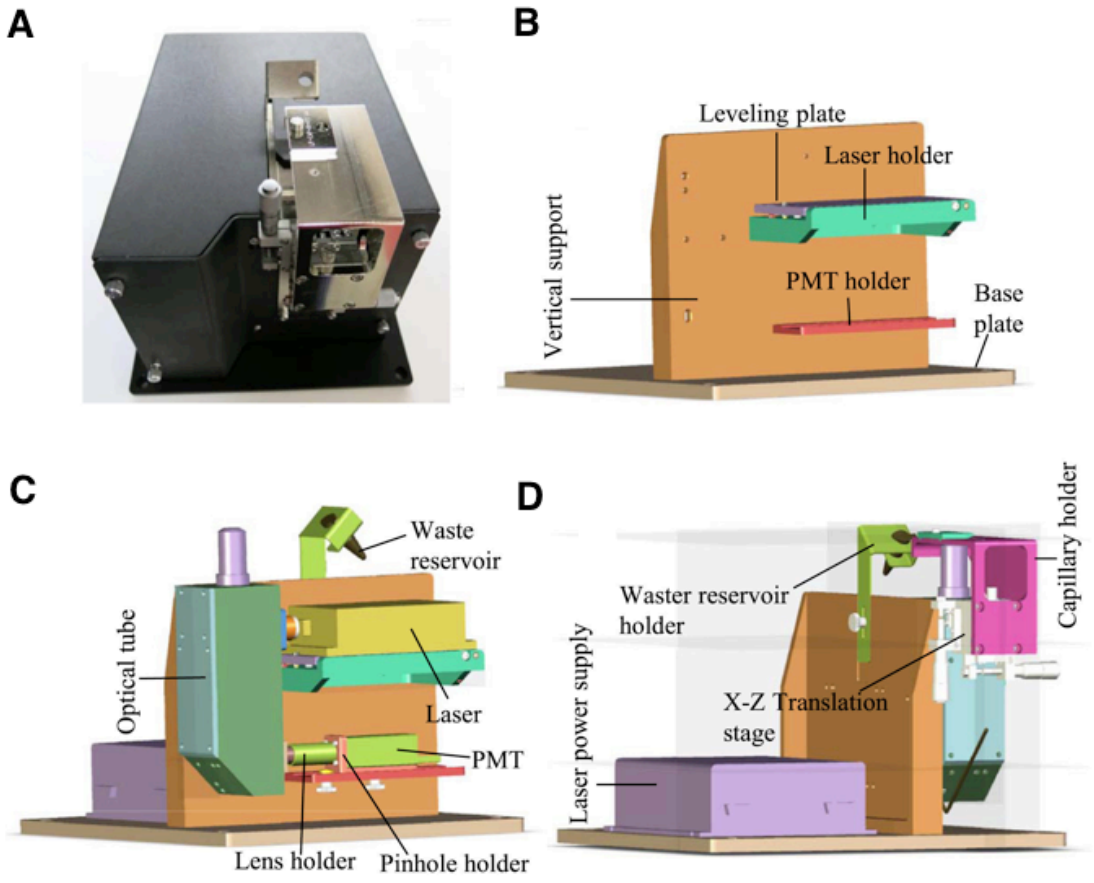

Figure 3-3 Assembled LIF detector and internal components

(A) Picture of assembled LIF detector. (B) Detector backbone. (C) Arrangement of parts inside detector. (D) View from other side of vertical support.

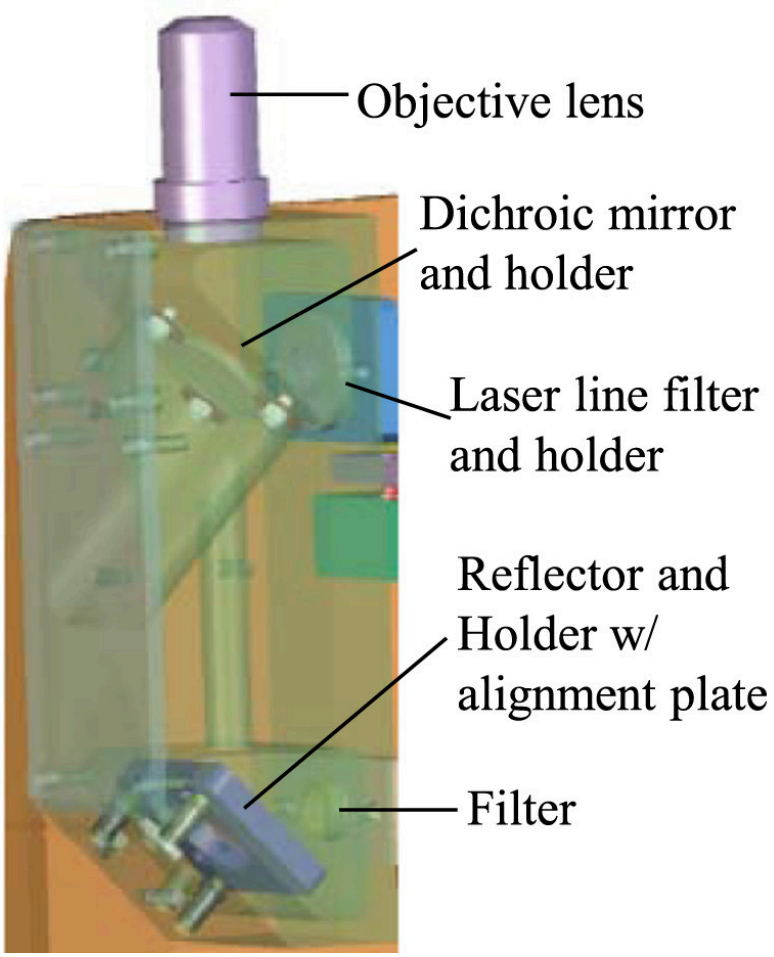

Figure 3-4 Optical components of LIF system

Optical component arrangement inside optical tube.

Alignment of the capillary with LIF detector

A detection window was opened at ~41 cm from the sampling end of a narrow capillary (47-cm-long×2-μm-i.d.×150-μm-o.d.) by removing the polyimide coating with flame. The detection window was then fixed onto the capillary holder coarsely aligned with the objective lens using the X-Z translation stage. Then, a fluorescein solution (1 μM fluorescein in 10 mM TE buffer at pH ~8.0) was flow through the capillary at a constant flow rate and the fluorescence signal was monitored. The position of the detection window was adjusted via the X-Z translation stage until the maximum signal output was reached. At this time, the detection window was considered to be aligned with the LIF detector and the X and Z positions of the translation stage were locked.

Flow injection analysis of fluorescein

To prepare for flow injection analysis right after capillary alignment, the capillary was thoroughly washed with a carrier solution (10 mM TE buffer) until the fluorescence signal reached the background level. Referring to Fig. 3-2, as the carrier solution was driven through the 60-nL injection valve to the microfabricated Chip-T, it was split into two steams; one stream went to the narrow capillary while the other went through a restriction capillary (RC). When a sample was injected by the injection valve, only a small portion of the sample was injected into the narrow capillary. Under the indicated conditions and a chamber pressure of ~500 psi, the splitting ratio was about 70,000:1; leading to an injection volume of ~0.85 pL. Five fluorescein solutions were injected from low concentration to high concentrations and each solution was injected five times at one-minute intervals.

BaNC-HDC separation of DNA ladder

Referring to Fig. 3-2, 10 mM TE buffer at pH 8.0 was loaded in the reservoir inside the pressure chamber as eluent. During the separation, the eluent was constantly driven through the 60-nL injection valve to the microfabricated Chip-T; one small portion of eluent went to the narrow capillary. When a sample was injected by the 60-nL injection valve, ~0.85 pL sample was injected into the narrow capillary. Fluorescence signal was continuously monitored by the LIF detector. After all the DNA fragments were eluted out, the next sample was injected for analysis. No column reconditioning was needed!

Results and discussion

Linear dynamic range and limit of detection

Fig. 3-5A presents the fluorescence signal obtained when fluorescein solutions (0 nM, 5.3 nM, 10 nM, 53 nM, 0.1 μM, 0.53 μM, 1.0 μM and 5.3 μM in 10 mM TE buffer) were flushed through the narrow capillary. The inset presents a Y-axis-expanded version of the same results from 0 to 53 nM. Excluding the data point for 5.3 μM, good linear relationship existed between fluorescence intensity and fluorescein concentration (see Fig. 3-5B, R^2=0.9993). Using the criterion for signal-to-noise ratio of 3, we determined the limit of detection (LOD) to be 0.8 nM. Therefore, the linear dynamic range of the detector was greater than 3 orders of magnitude. If we assume the laser spot on the narrow capillary had a diameter of ~50 μm, the volume of the solution that was illuminated was $\pi\times(1\ \mu m)^2\times 50\ \mu m=1.6\times10^{-22}$ L. That is to say, the LOD of the LIF detector was ~70 fluorescein molecules or 12 yoctomoles (10^{-21}).

Fig. 3-6 presents the results of a drift test as 10 mM TE buffer was flushed through the capillary for an hour. As can be seen, the background signal was pretty stable; signal drift was 1.2 standard deviation of the background signal over an hour. To check whether the LIF detector worked properly, we injected a fluorescein sample (10 nM in 10 mM TE buffer) to see how it responded to it. The signal between ~100–150 s was obtained when 10 nM fluorescein was flushed through the capillary. The signal was comparable to what we got in Fig. 3-5.

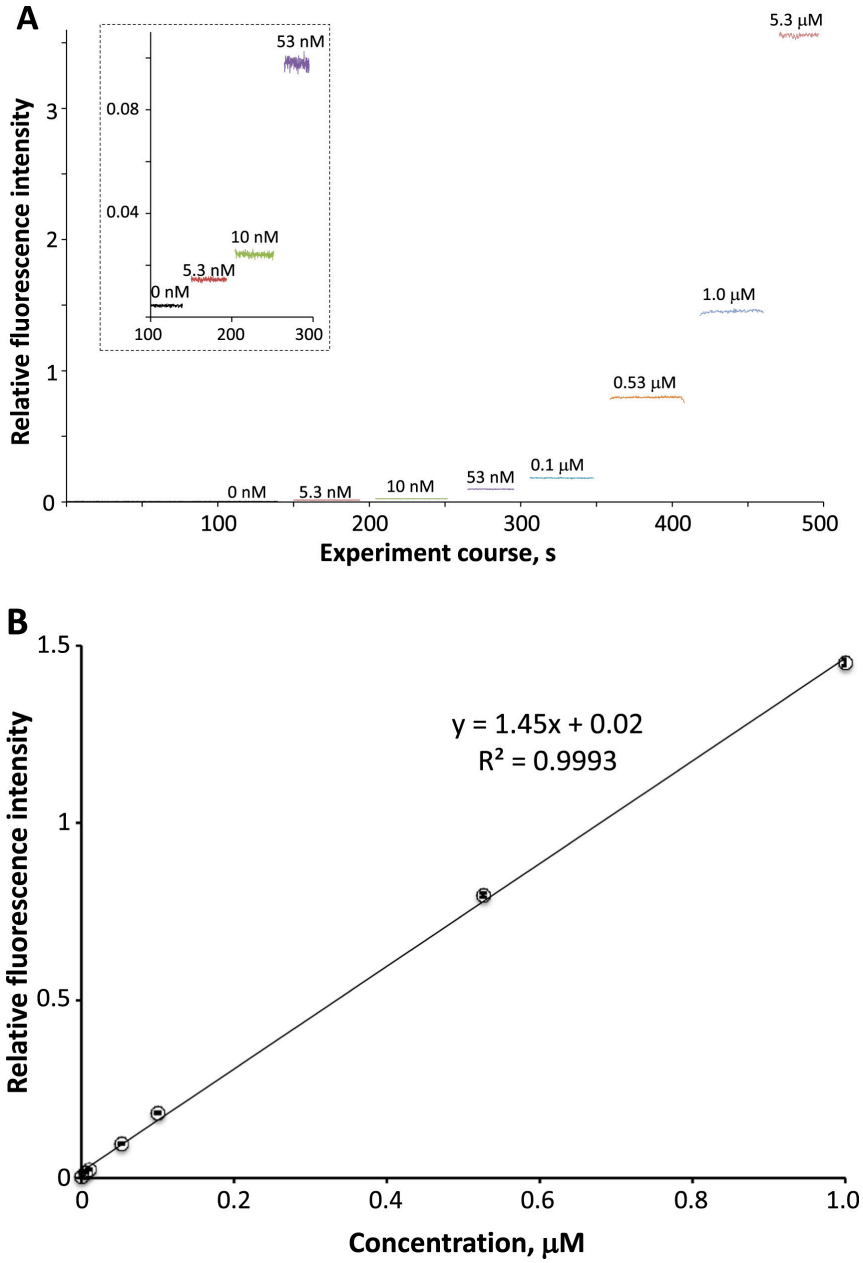

Figure 3-5 Fluorescence intensity as function of fluorescein concentration

Fluorescence signals obtained as different fluorescein solutions were flushed through the narrow capillary (total length of 47 cm (41 cm effective), i.d. of 2 µm and o.d. of 150 µm) under a pressure of 500 psi. (B) Calibration curve of fluorescein from 5.3 nM to 1.0 µM.

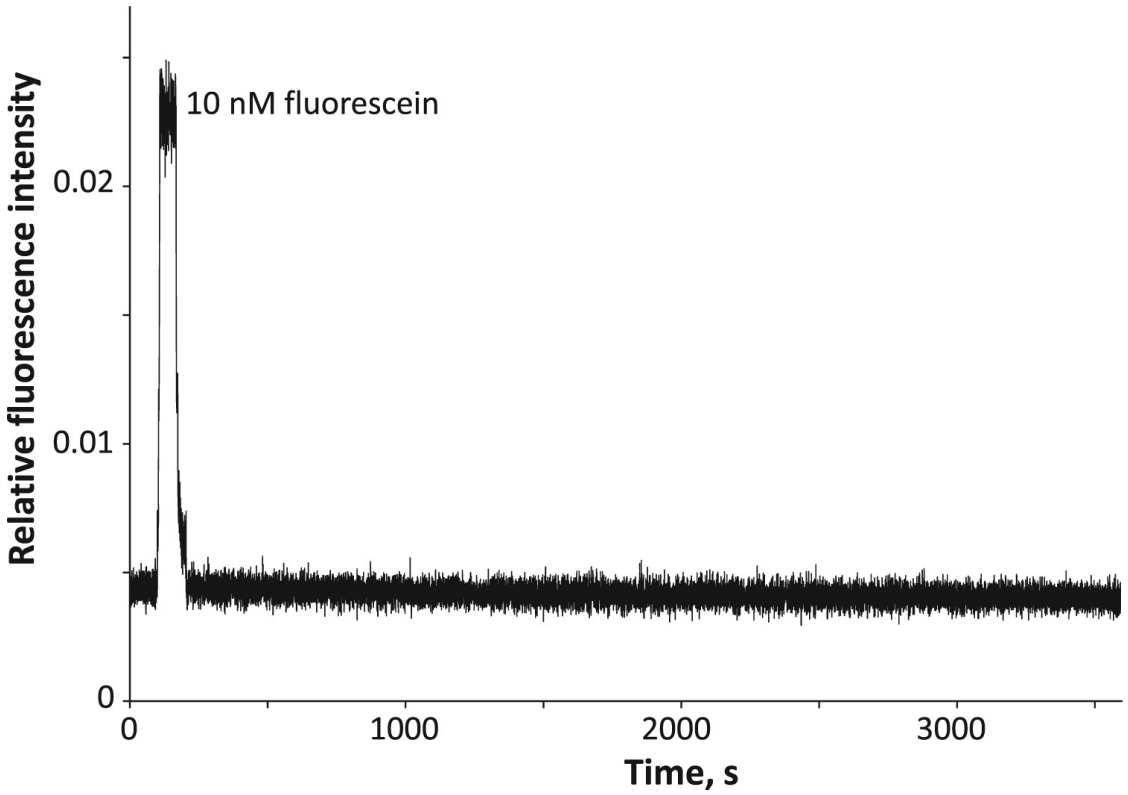

Figure 3-6 Drift and noise characterization

Drift and noise characterization over 1 h. The experiment was performed by flushing 10 mM TE buffer (pH=8.0) through the narrow capillary under 500 psi. The peak signal was obtained by flushing 10 nM fluorescein in 10 mM TE buffer through the narrow capillary under the same conditions. Dynamic drift of the background signal (relative fluorescence intensity) was calculated to be 4.0×10^{-4} per hour, while noise was calculated to be 3.4×10^{-4}.

Flow injection analysis of fluorescein

To demonstrate the performance of the newly developed LIF prototype, we performed a flow injection analysis of fluorescein using the system as presented in Fig. 3-2. This is probably the smallest tubing flow injection system ever reported. Samples were injected via the injection valve at a rate of one injection per minute. Fig. 3-7 presents the results; there were five fluorescein solutions, each was analyzed five times. A linear regression equation was established in the concentration range of 50 nM–1 μM. The linear regression coefficient (R^2) was 0.996. When we used the criteria of S/N=3, an LOD of ~17 nM fluorescein or 14 zeptomole (10^{-21}) of fluorescein (17 nM×0.85 pL) was obtained. This also revealed the dispersion factor of this flow injection system was ~21.

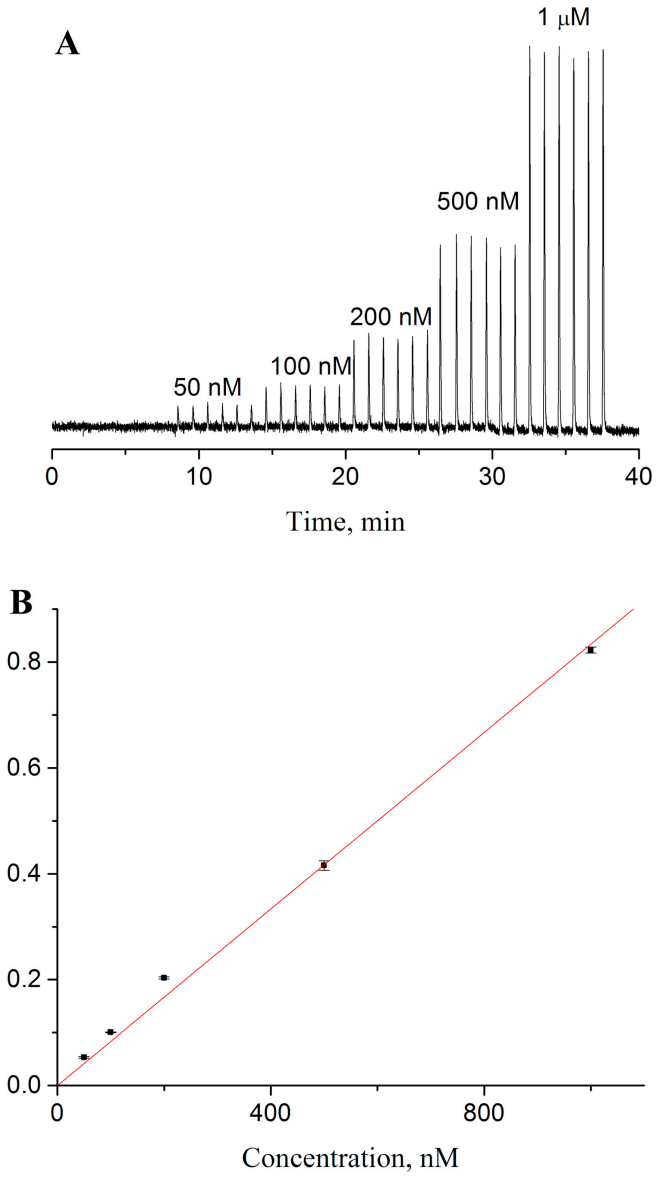

Figure 3-7 Flow injection analysis of fluorescein

Flow injection analysis of fluorescein. The capillary had a total length of 47 cm (41 cm effective), an i.d. of 2 μm, and an o.d. of 150 μm. The carrier solution was 10 mM TE buffer at pH ~8.0, and the fluorescein solutions were prepared with the carrier solution. The injection volume was estimated to be 0.85 pL. (A) FIA chromatogram. (B) Linear regression results.

Analysis of DNA ladder

We coupled the developed LIF prototype to BaNC-HDC. Fig. 3-8 presents the chromatograms of separating a standard sample of 1 kb plus DNA ladder at five different concentrations, and Fig. 3-9 presents the calibration curves of all fifteen DNA fragments in the range of 0.075–20 kbp. The linear regression coefficients were in the range of 0.985–0.991. For large DNA fragments we could detect them at the zeptomole level. It should be noted that each DNA molecule was intercalated with many YOYO dye molecules.

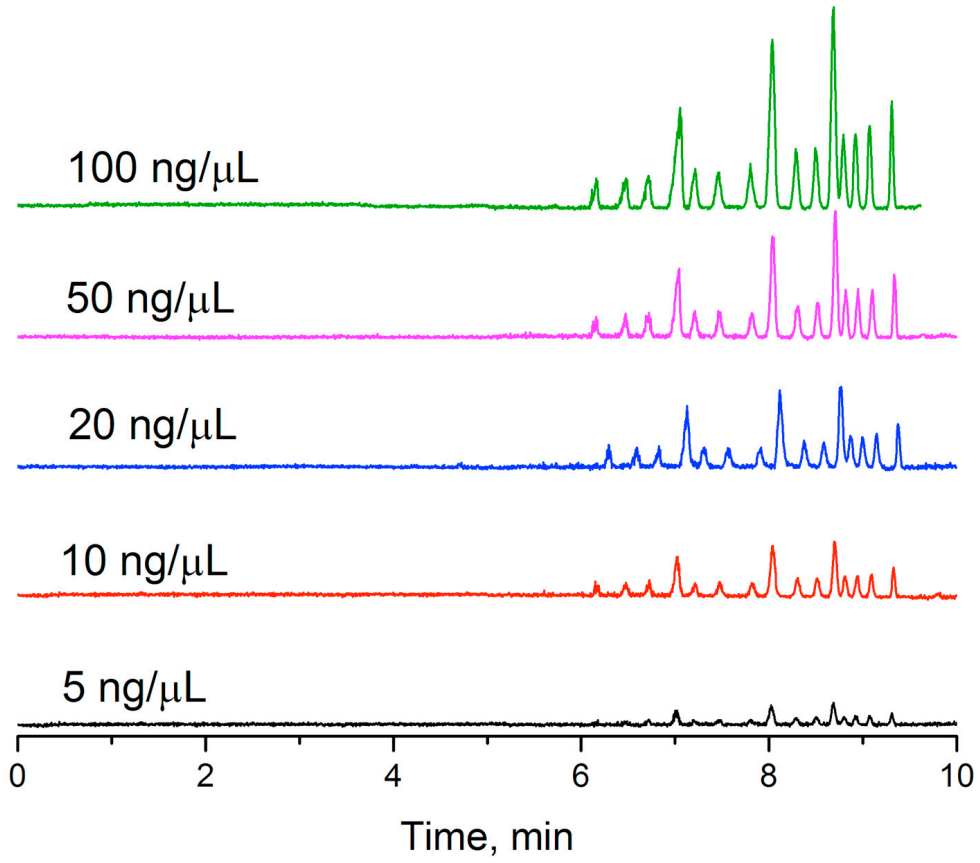

Figure 3-8 Separation Cchromatogram. Sample-DNA ladder

Using developed LIF detector for monitoring BaNC-HDC separation. Chromatograms. The total concentrations of 1-kbp plus DNA marker were indicated in the figure. Conditions: the capillary had a total length of 47 cm (41 cm effective), an i.d. of 2 μm, and an o.d. of 150 μm, the injection volume was estimated to be 0.85 pL, the eluent was 10 mM TE buffer at pH 8.0, and the elution pressure was 500 psi.

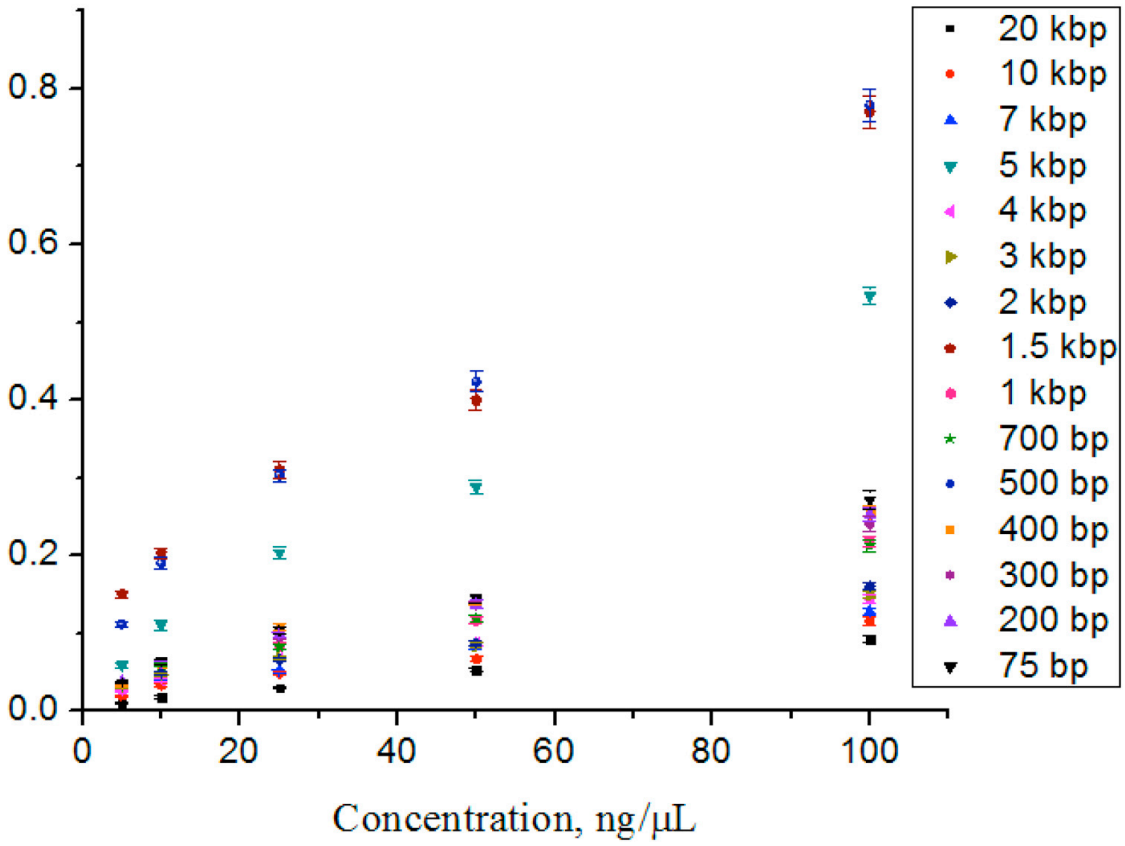

Figure 3-9 Calibration curves for different DNA fragments

The calibration curves for different DNA fragments. Relative peak areas at different concentrations were obtained from A. The trend-lines had linear regression coefficients of 0.985–0.991.

Concluding remarks

We have built a prototype LIF detector for monitoring fluorescence signal within a narrow capillary. The component arrangement has been described in detail, which should be helpful if one wants to construct similar detector on his/her own. We have also characterized the detector. Using a 2-μm-i.d. capillary as a separation column, we have determined the limit of detection of the detector to be 0.8 nM fluorescein, which is corresponding to ~70 fluorescein molecules in the detection volume. We have also determined the linear dynamic range of the detector to be more than 3 orders of magnitude. To demonstrate the feasibility of using the prototype for monitoring resolved analytes in a narrow capillary, we used a 2-μm-i.d. capillary to separate a 1 kb plus DNA ladder by BaNC-HDC. The detector not only can monitor all the fifteen resolved DNA fragments but also can quantitate each fragment with good precision and accuracy.

The materials in Chapter 3 are adapted from Lynch et al., Talanta (2017) 165:240-244. The copyright was obtained from Elsevier, and the license number is 4315041314106. For more details, please see Appendix E.

Chapter 4: Multiple-channel ultraviolet absorbance detector for two-dimensional chromatographic separations

Abstract

In recent years, much research has gone into developing online comprehensive two-dimensional liquid chromatographic systems allowing for high peak capacities in comparable separation times to that of one-dimensional liquid chromatographic systems. However, the speed requirements in the second dimension (2^{nd}-D) still remain one challenge for complex biological samples due to the current configuration of two column/two detector systems. Utilization of multiple 2^{nd}-D columns can mitigate this challenge. To adapt this approach, we need a multiple channel detector. Here we develop a versatile multichannel ultraviolet (UV) light absorbance detector that is capable of simultaneously monitoring separations in 12 columns. The detector consists of a deuterium lighthouse, a flow cell assembly (a 13-channel flow cell fitted with a 13-photodiode-detection system), and a data acquisition and monitoring terminal. Through the use of a custom high optical quality furcated fiber and precise machining of a flow cell, the background noise level is measured in the tens of μAU. We obtain a linear dynamic range of three orders of magnitude (150 μAU to 150 mAU). Compared to a commercialized multichannel UV light absorbance detector like the Waters 2488 UV/Vis, our device provides up to an increase in channel detection while residing within the same noise region and linear range.

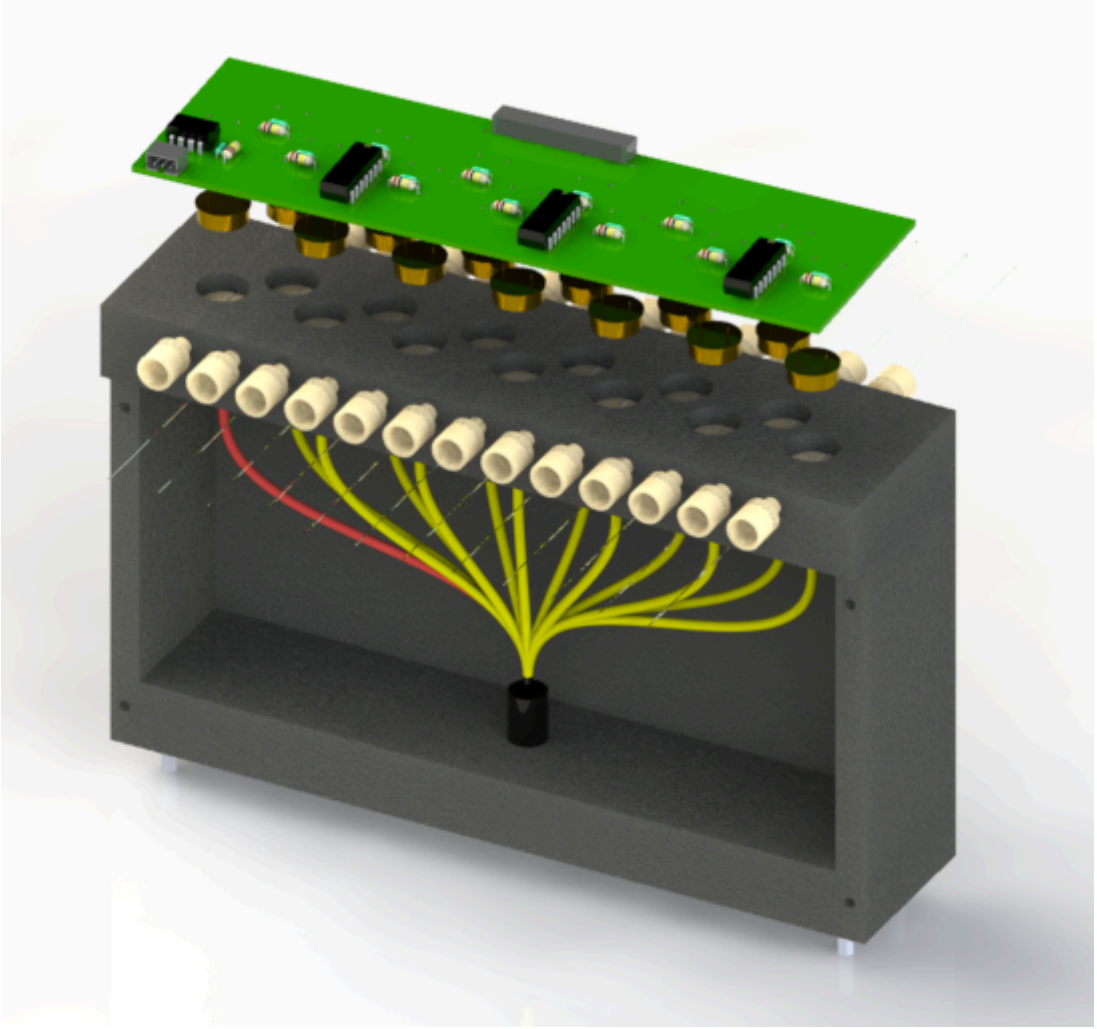

Figure 4-1 Three-dimensional rendering of the multiple-channel absorbance detector

Introduction

In recent years, comprehensive two-dimensional (2D) high performance liquid chromatography (HPLC) has become an emerging research topic because it can achieve a high peak capacity within a comparable separation time to that of one-dimensional liquid chromatography [127]. Two-dimensional separations may be performed either online or offline [128] depending on the desired result and time allocated for the total separation. The first online 2D-HPLC system was designed by Erni and Frei in 1978 [129] and utilized gel permeation chromatography (GPC) and reverse phase liquid chromatography (RPLC) in the first and second dimensions respectively. They separated Senna-glycoside with GPC over a course of 10 hours, collected and re-injected alternatively seven fractions using two sample loops in an eight-port valve for RPLC. This laid the groundwork for 2D-HPLC. If online 2D-HPLC is desired in a reduced total separation time, the 2^{nd}-D must include both the separation and re-equilibration steps in the fraction-collection time of the 1^{st}-D. In order to meet this requirement, setups have included two to four columns for use in the 2^{nd}-D separation. Bushey and Jorgenson [130] developed the first online 2D-HPLC system in 1990 to implement this strategy. They employed cation exchange and size exclusion columns for their two separation dimensions to separate a protein sample. By doing so, they created the foundation for the next generation of 2D-LC systems to come.

A good 2D-HPLC system should have two orthogonal separation dimensions. One can obtain improved orthogonality [131] by combining a variety of chromatographic modes of LC including ion-exchange chromatography (IEX) [132], size exclusion chromatography (SEC) [133], normal phase liquid chromatography

(NPLC) [134], reverse phase liquid chromatography [135], supercritical fluid chromatography (SFC) [136], hydrodynamic interaction liquid chromatography HILIC [137], etc. A first dimension (1^{st}-D) of IEX has been combined with a second dimension (2^{nd}-D) of RPLC in conventional 2D-HPLC schemes for peptide separation due to their relatively high orthogonality, fast re-equilibration time [138] and compatibility with mass spectrometry (MS) [139]. However, to this day, limited separation speed in the second separation dimension is still a major drawback for complex biological samples due to the current configuration of two-column/two-detector systems [140].

Current commercial systems utilize a series of valves in order to collect and store samples for future separation while still configured with only one column [141, 142]. This system, although robust and reproducible, does not address the issue of the limited separation speed in the 2^{nd}-D separation since these systems still run a single second dimension column at a time. One way to address this issue is to run the 2^{nd}-D columns in tandem in order to increase sample throughput, which in turn decreases the overall separation time. One such system has been recently developed in our research group. Zhu et al. [143] published this work showing continuous and comprehensive online analysis of intact proteins while obtaining over 500 protein peaks from an E. Coli lysate. This system re-equilibrated several 2^{nd}-dimensional columns while running separations on the rest. However, the major hurdle proved to be the detection aspect of the system due to no commercial systems available to detect the tandem columns.

Waters (Waters 2488) [144] offers a commercial multichannel UV/Vis detector, but there are only two channels. This system works in conjunction with common 2D-HPLC systems that store fractions and may have a maximum of two separation columns

but would not accommodate our needs. Other multichannel/multiplexed detection systems have been developed over the years including several capillary electrophoresis (CE) coupled to laser induced fluorescence detectors (LIF) [145-148] but due to cost and other system requirements, these were not an option. A literature search into multichannel absorbance detection, our preferred method of detection, showed very few multichannel absorbance detectors to have been constructed due to the limited demand of such a detector. Until now, a seven channel [149] absorbance detector was reported by our group and a 96-channel detector was commercialized by now a disbanded company CombiSep. Both of these absorbance systems were paired with CE similar to the LIF systems listed above.

In this work, we develop a 12-channel UV absorbance detector to meet this need. The detector consists of a deuterium lighthouse, a flow cell assembly (13 individual flow cell channel fitted with a 13-photodiode-detection system), and a data acquisition and monitoring terminal. A UV light beam from a deuterium lamp is monochromated and focused to the entrance of an optical fiber and then split into 13 beams (1 as reference and remaining 12 to the LC separation columns). Transmittance from each column is measured by a photodiode, converted to absorbance and acquired by the monitoring terminal. The detector has background noises at tens of μAU level and a linear range over three orders of magnitude. To demonstrate the feasibility and capabilities using this detector for 2D-HPLC, we construct an updated 2D-HPLC system using this detector and show the 2D separation results.

Experimental section

Reagents and materials

Fused-silica capillaries and the furcated-fiber optic cable were purchased from Polymicro Technologies Inc (Molex, Phoenix, AZ). Trifluoacetic acid, methanol and acetonitrile and other reagents used were obtained from EMD Chemicals, Inc. (Gibbstown, NJ). Water was purified by a NANO pure infinity ultrapure water system (Barnstead, Newton, WA). Ball lens and optical filters were purchased through Edmond Optics (Barrington, NJ). Printed circuit boards (PCB) were designed in house and manufactured by OSHPark (Portland, OR). The deuterium light source, an Apex Monochrometer Illuminator, was produced by Newport (Irvine, CA), while a comparative capillary-based absorbance detector (Linear UVis 200), was manufactured by Linear Instruments (Reno, NV).

UV absorbance detector design

The detector itself consists of a deuterium lighthouse, a flow cell assembly, a 13-channel flow cell fitted with a 13-photodiode detection system, and a data acquisition and monitoring terminal as depicted by the three dimensional rendering (Fig. 4-1). The machined optical fiber assembly is shown in Fig. 4-1 including the flow cell, furcated fiber optic cable, and printed circuit board with its electrical components. The optical fiber assembly consists of a custom 13-furcated fiber integrated into a machined and anodized aluminum box with the 13 individual flow cells (one for each of the 12 columns and the last for reference signal detection) integrated into a single piece, which bolts to the top of the housing for the furcated optical fiber. Each individual flow cell comprised of two PEEK fittings, a ball lens and a custom PEEK ball lens holder.

The total dimensions of the system including the lighthouse are 30 cm×17.5 cm×50 cm (l×w×h respectively) while the machined optical fiber assembly dimensions are 20 cm×5 cm×20 cm.

Fig. 4-2 depicts the optical path and includes Apex Monochrometer Illuminator that was used throughout this research as the lighthouse. The light originates from a deuterium lamp in the lighthouse where it is collimated, travels through a bandpass filter, and is focused on the fiber optic bundle housed within the flow cell assembly. The light then travels through the furcated fiber where it is split and subsequently focused on each capillary through a ball lens housed in each of the ball lens holders of the individual flow cells.

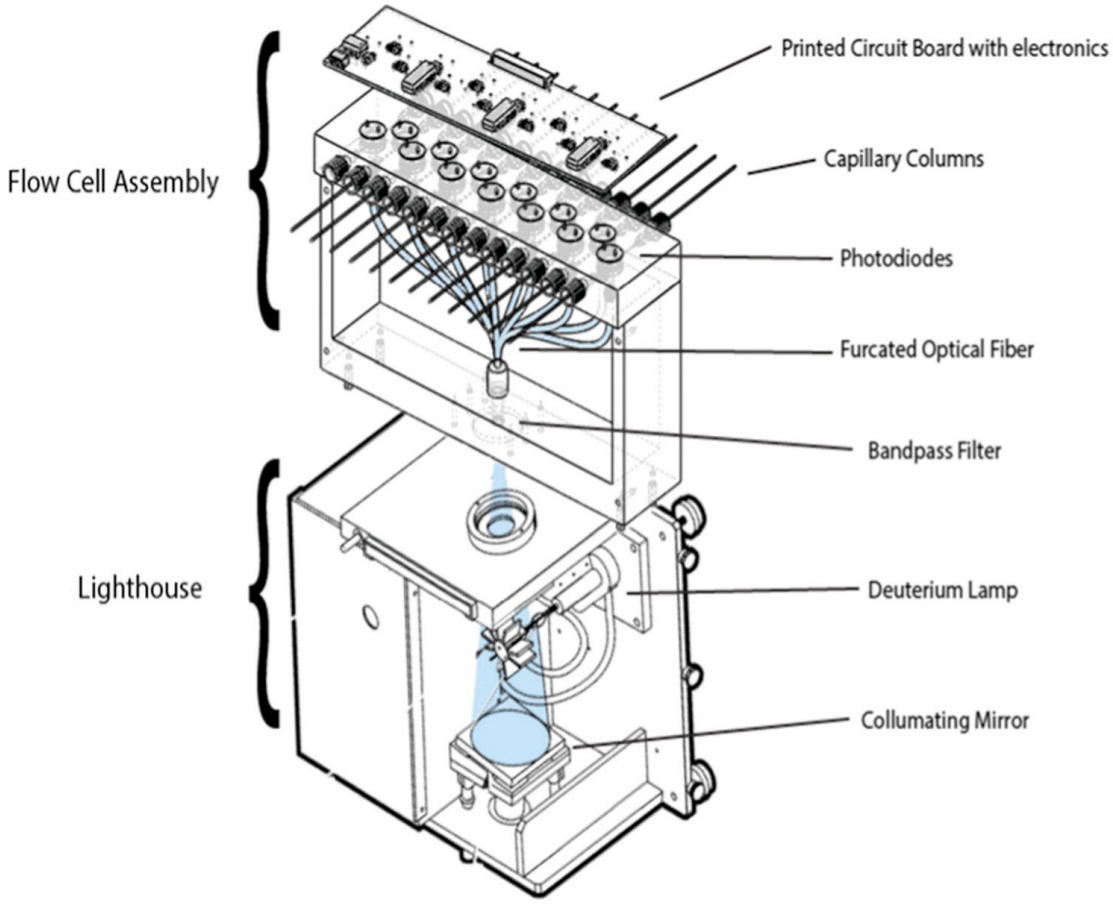

Figure 4-2 Light path and components of absorbance detector

The light path is shown from the Newport Apex Monochrometer Illuminator through the furcated fiber optic cable into each of the flow cells. The machined housing of the flow cell consisted of an aluminum shell that was powder coated black to eliminate light interference. (A) It housed a 13-furcated fiber optic cable and had a top flow cell piece comprising of 12 individual flow cells and a reference input. On top attached a printed circuit board integrating the photodiodes, amplification circuitry, and connections for source power and output signals.

Flow cell design

A series of 13 individual flow cells, the schematic for each was taken from previously developed designs, were combined in tandem and integrated into the top of the absorbance detector (Fig. 4-3A). A slice of the total flow cell reveals each individual flow cell design as depicted by the three-dimensional rendering in Fig. 4-3B. Each of these individual flow cells were composed of two compression fittings (Vici Valco, Houston, TX), a 1.58 diameter sapphire ball lens and an in-house machined PEEK ball lens holder that is used to align the capillary window with the input light from the optical fiber. A capillary window is created as previously described and then inserted into the flow cell. In brief, we remove ~3 mm of the polyacrylamide coating at the center of a 10 cm capillary, insert the capillary into the flow cell, align the window with the center of the ball lens holder and secure the capillary using the compression fittings. A detailed image of the light path through each flow cell can be seen in the slice-view of Fig. 4-4. As light enters the flow cell through a leg of the furcated optical fiber, it is focused through a sapphire ball lens on the capillary where absorption can take place. Light then can be seen passing through the capillary and being collected on the photodiode sensor at the top of the image.

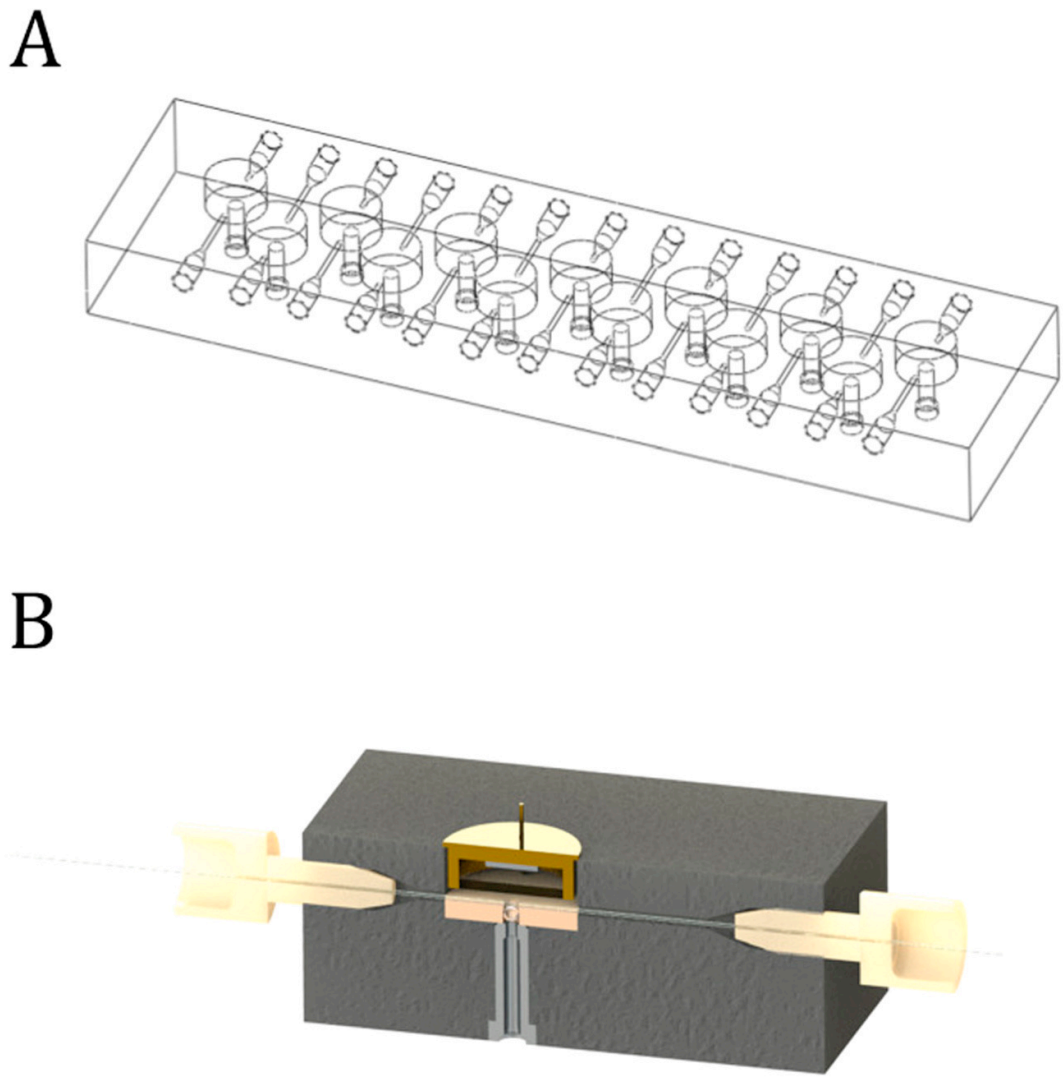

Figure 4-3 Flow cell design

(A) The flow cell in its entirety. It is comprised of 13 individual flow cells (center) for the 12 column channels and reference channel. (B) depicts a 3D rendering of each individual flow cell.

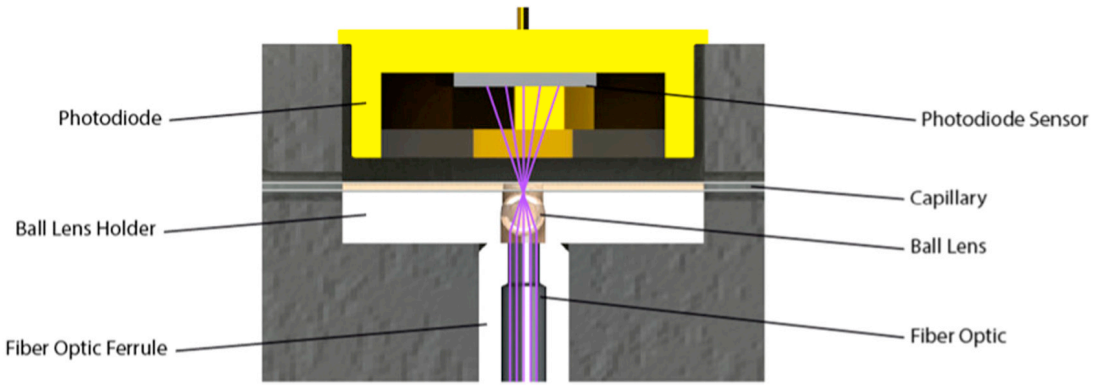

Figure 4-4 Flow cell components and light path

Each flow cell consists of the ball lens holder, a main component in each flow cell. Fabricated out of PEEK, the ball lens holder aligns a 1.58 mm diameter sapphire ball lens with a 360 µm OD (200 µm ID) capillary

Furcated-fiber

A custom 13-leg furcated-fiber was designed and then purchased through Polymicro Technologies Inc (Molex, Phoenix, AZ). The overall length of the fiber bundle was 15 cm to accommodate the machined housing. A 2:1 reference:sample ratio of light intensity was tested prior to designing the furcated fiber and this ratio proved to have the best signal to noise ratio. Also, the fiber size was tested extensively prior to the furcated bundle design to find the most appropriate diameter fiber for our application. A 300 μm fiber was chosen due to its S:N characteristics, flexibility, and overall fiber bundle size limitations. These tests can be seen in the supplementary data (Fig. 4-5). A total of 98 fibers were chosen for the fiber bundle to produce a splitting pattern. Each sample leg consisted of seven 300 μm deep UV silica core fibers while the reference leg comprised of 14 fibers to achieve the best packing density and 2:1 reference to signal light intensity. The overall splitting pattern for the common leg and each of the signal and reference legs can be seen in Fig. 4-6.

A

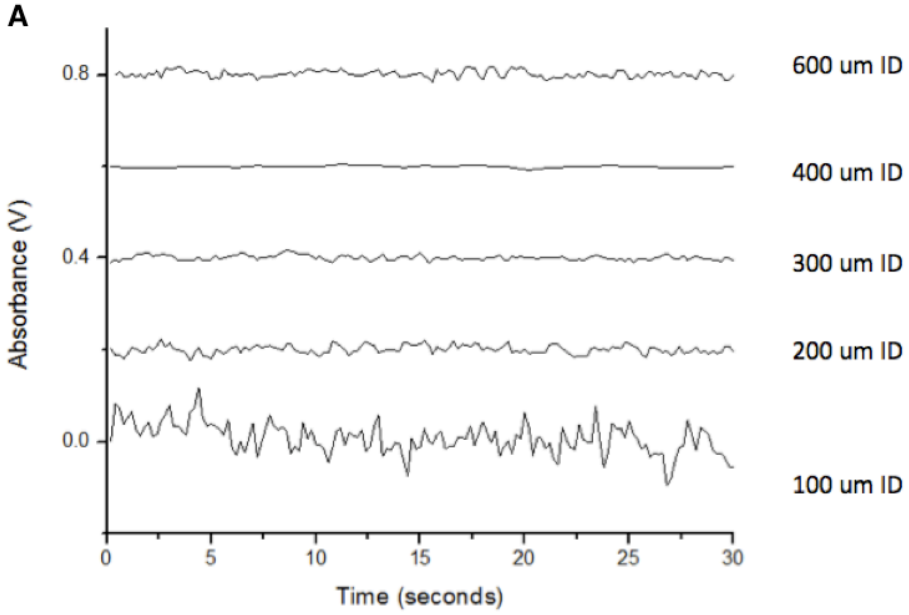

B

ID (μm)	Ref:Sig ratio	Noise	S/N
600	1.00	29.88	294.7
400	0.44	13.22	714.5
300	0.25	26.24	418.4
200	0.11	44.12	206.6
100	0.03	168.4	61.41

Figure 4-5 Fiber optic testing

Early tests of varying fiber optic size. A reference fiber of 600 μm was used for each test. Acetone was used as the sample analyte for each fiber and peak height was measured for each injection. Chromatograms of the signal can be seen (A) and S:N was calculated for each fiber (B).

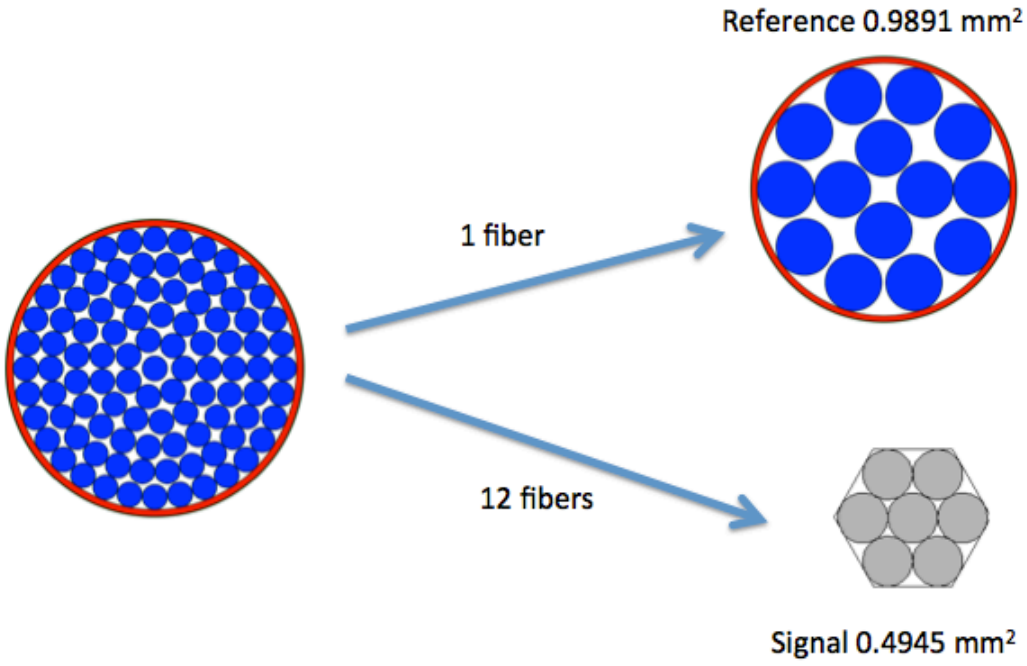

Figure 4-6 Furcated fiber design

Splitting and packing pattern of fibers in the custom furcated fiber. A 2:1 ratio of reference:signal strength yielded the best signal to noise ratio and the close hexagonal packing of 7 fibers dictated the fiber count for the column legs.

Electronic design

The current detector design integrated a 4-channel operational amplifier (opa404) for the sample channels while integrating a single channel amplifier (opa602) for the reference channel. Photodiodes (S1226, Hamamatsu Photonics, Bridgewater, NJ) were mounted to an opaque surface (black acrylic) to properly align the 13 photodiodes with the center of the flow cells. The holes for the photodiode legs were systematically laser cut using a 150 W Universal Laser System (Universal Laser Systems, Scottsdale, AZ). This acrylic/photodiode unit was then connected to a printed circuit board as shown in Fig. 4-8A. The output signals from the photodiodes were connected directly to the operational amplifiers through the circuit seen in Fig. 4-8B. Posts on the circuit board allow for selectable gains as well as to equilibrate the gains from each of the 13 channels through interchangeable resistors to assure equal gain for each channel. The output signal from each of the operational amplifiers is analog and is read through a data acquisition card (DAQ) (Measurement Computing, Norton, MA). The data is then processed and visualized using an in-house built LabView (National Instruments, Austin, TX) program. This program, visualized in Fig. 4-7, takes into consideration the dark current from each photodiode, converts signals to absorbance units using a sample to reference ratio, and can auto zero the channel outputs.

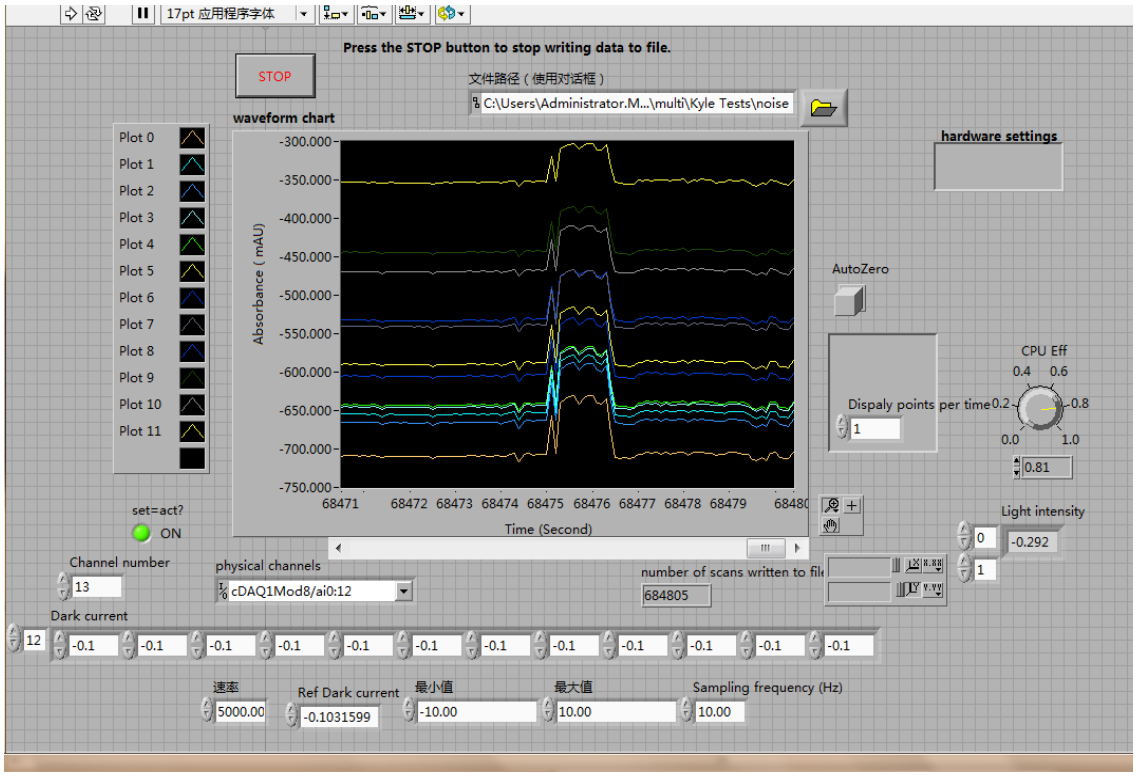

Figure 4-7 System's labview program

A sample image of the in-house Labview program to detect simultaneous 2nd-dimension separation channels. It takes the raw analog data from the output of each OPA and calculates absorbance in the units of mAU. There is an auto zero function as well as adjustment for individual dark currents.

A

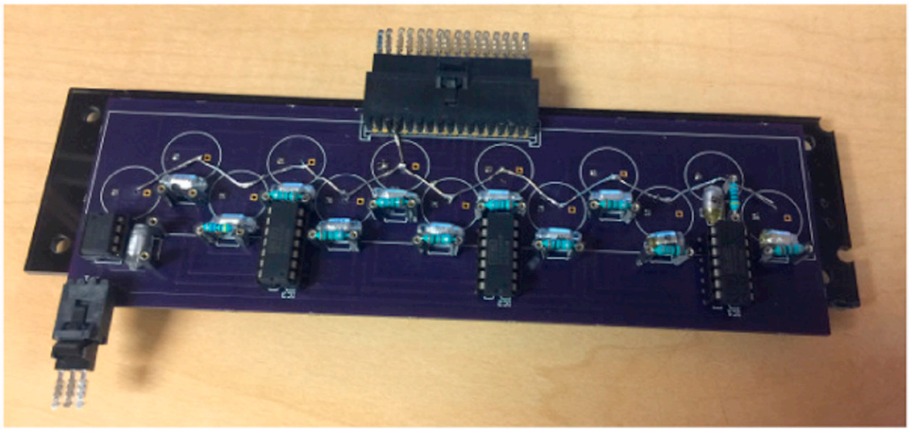

B

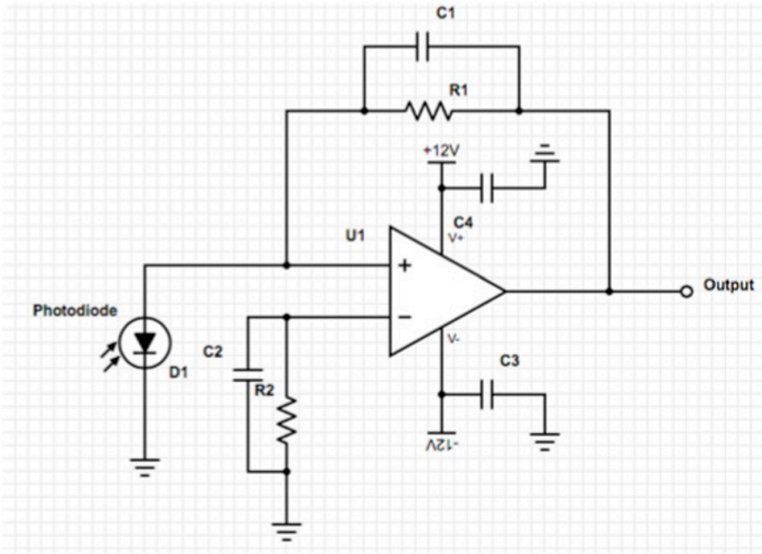

Figure 4-8 Printed circuit board design

(A) The circuit board contains the circuitry for the multichannel UV/Vis detector including the power inputs (bottom left), signal amplification (middle), photodiodes (underside), and data output (top-center). (B) The schematic for each of the photodiodes with their individual components.

Results and discussion

Noise and S/N characteristics

Table 4-1 shows the data for each of the channels for 100 μg/ml lysozyme at 220 nm. Each channels noise, signal, and S/N ratio as well as limit of detection and quantification can be seen. Channels p-p noise level was observed to range between 0-20 μAU. This is comparable to commercial based optical absorbance detectors. It is suggested that the variance in noise of the channels corresponds to the furcated-fiber legs not being symmetrically split. This phenomenon can be seen through the values associated with light intensity measured in volts for each specific channel. Note: these noise levels are raw signals with no data smoothing through averaging.

As observed in Fig. 4-9, the drift for the detector was tested and recorded to be in the range of 0.3-0.9 μAU/min. Detector baseline drift is commonly associated with temperature variations within the laboratory. External noise of the laboratory was mitigated through the printed circuit board circuitry. When the electronics were tested using a breadboard and prototype boards, the noise increased by orders of magnitude. A makeshift shield further decreased externally created noise. This noise could be completely mitigated with a custom machined metal cover that is grounded to the device.

Channel	Noise std (mAU)	Signal (mAU)	S/N	Light Intensity (V)	LOD (mAU)	LOQ (mAU)
Ch1	0.01050	11.9270	1135.90	1.698	0.0315	0.1050
Ch2	0.00900	12.7521	1416.90	1.165	0.0270	0.0900
Ch3	0.01050	10.4649	996.65	1.006	0.0315	0.1050
Ch4	0.00930	11.2115	1205.54	1.591	0.0279	0.0930
Ch5	0.00920	11.0836	1204.73	1.016	0.0276	0.0920
Ch6	0.00960	13.0808	1362.58	1.513	0.0288	0.0960
Ch7	0.01045	10.4822	1003.08	1.041	0.0314	0.1045
Ch8	0.00840	12.2327	1456.27	1.321	0.0252	0.0840
Ch9	0.00900	7.7345	859.39	1.381	0.0270	0.0900
Ch10	0.00960	10.8098	1126.02	1.131	0.0288	0.0960
Ch11	0.00920	11.5908	1259.87	1.465	0.0276	0.0920
Ch12	0.00850	13.8357	1627.73	1.629	0.0255	0.0850
ave.	0.00944	11.4338	1211.53	1.330	0.0283	0.0944

Table 4-1 Raw individual channel data

Data for each of the channels tested with a sample of 100 µg/ml lysozyme at 220 nm. Each channels noise, signal, and S/N ratio as well as limit of detection and quantification can be seen. Also recorded was the light intensity measured in volts for the specific channel.

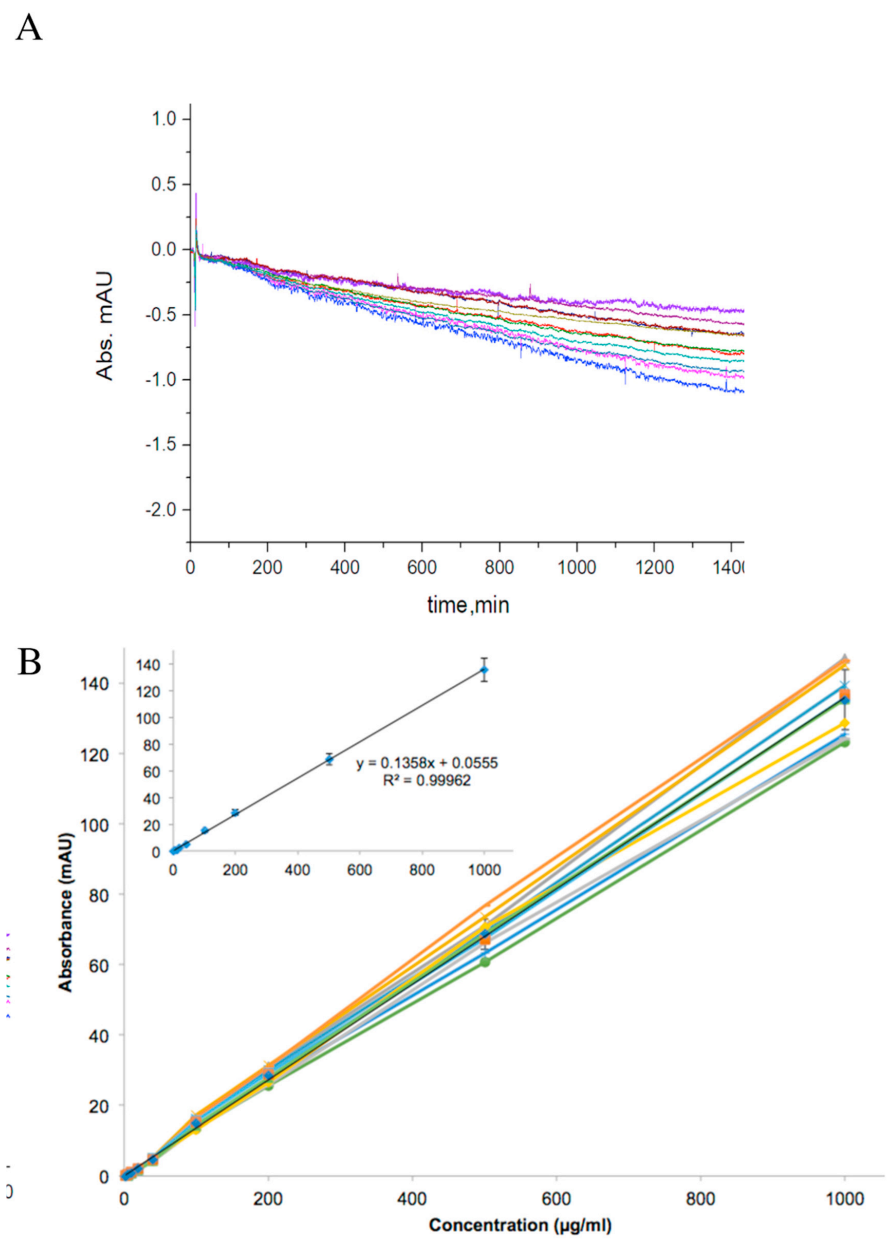

Figure 4-9 Drift and linear dynamic range measurements

(A) drift ranges from −0.019 mAU/h to −0.052 mAU/h. A calibration plot (B) showing the linear dynamic range of lysozyme concentration at 220 nm. Absorbance was measured from 150 µAU to 135 mAU for lysozyme concentrations ranging from 3 µg/ml to 1000 µg/ml respectively. The individual channels are shown above as well as the averaged values with their standard deviations shown in the inset.

Linearity studies

Linearity over a range of several orders of magnitudes is a required characteristic for any analytical detector. As shown previously, capillary-based absorbance detectors show a linear relationship between concentration and transmittance due to their low absorbance values. A calibration plot (Fig. 4-9B) showing the log of the averaged measured lysozyme concentration against the theoretical concentration was performed giving a linearity from 150 μAU to 135 mAU or 3 μg/ml to 1000 μg/ml of lysozyme respectively. Consistency between channels can be seen in Fig. 4-10 with all twelve channels absorbance tested with a sample of concentrations varying from 2-2000 μg/ml of lysozyme at 220 nm.

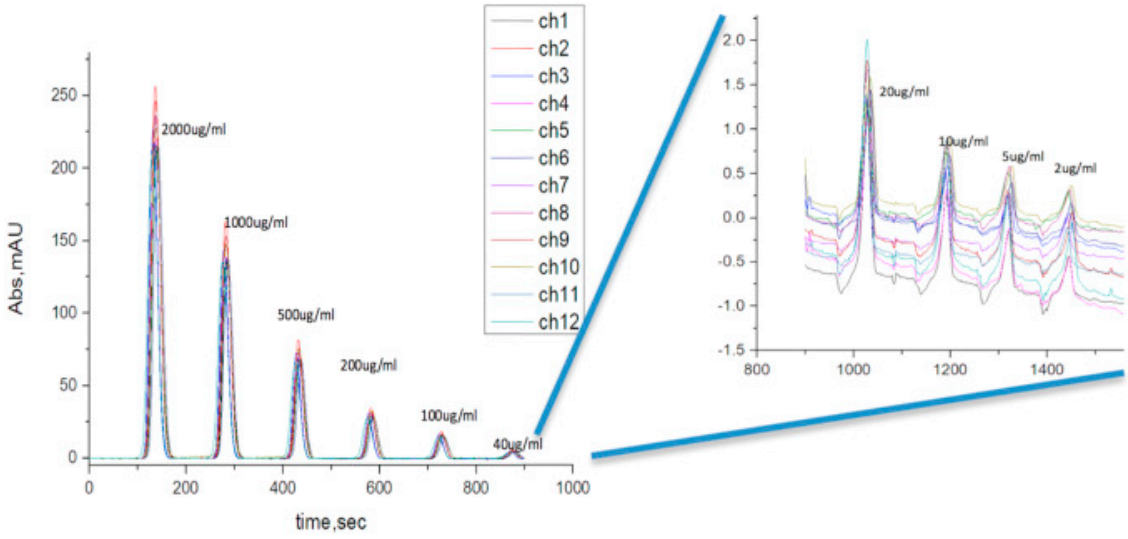

Figure 4-10 Channel reproducibility

Consistency between channels can be seen above with all twelve channels absorbance tested with a sample of varying concentrations of lysozyme at 220 nm.

Two-dimensional LC application

As described in the introduction, the purpose of this absorbance detector was to provide detection of our 12 2^{nd}-D columns in order to allow for both fast fractionation of the 1^{st}-D and an overall shortened separation time. New multi-position valves (V1 and V2 in Fig. 4-11) were designed (Vici Valco) and implemented in our system. Six 2^{nd}-D columns are attached to each of these two valves and may be selected individually (see V1) or concurrently (see V2). In addition to valves V1 and V2 as well as the 12 2^{nd}-D columns, a four-port two-position switching valve (Vs) is utilized. This allows the first dimension (IEX) and second dimension (RP) to operate simultaneously, leading to six consecutive RP separations while six fractions are being loaded.

A brief description of the protocol used is as followed. Once the gradient is started in the first dimension (t = 0 min), fractions from IEX column are loaded onto the six RP columns of V1 every 3.5 min. After 21 min, Vs is switched allowing the IEX fractions to be loaded onto the RP columns of V2 alternatively. At the same time, V1 is switched positions to elute all-ports. When this occurs, the first six fraction separations are performed from t = 21 min to t = 42 min (while fractions seven to twelve are loaded on V2). At 42 min, the three valves (V1, V2 and Vs) are switched. Fractions are now loaded onto V1 again while the separations from V2 are performed. Comprehensive 2D-LC data of protein samples was obtained via the multichannel UV/Vis absorbance detector. The total analysis time was 4.2 hours. Within this time, E. Coli lysate was separated. Fig. 7 shows over 900 peaks that were able through the novel 2D-LC system in both raw chromatograms for all fractions (Fig. 4-12) and a 3D representation for the 2^{nd}-D separations (Fig. 4-13). A more in-depth look at this new multidimensional 2D-

HPLC system will be published elsewhere.

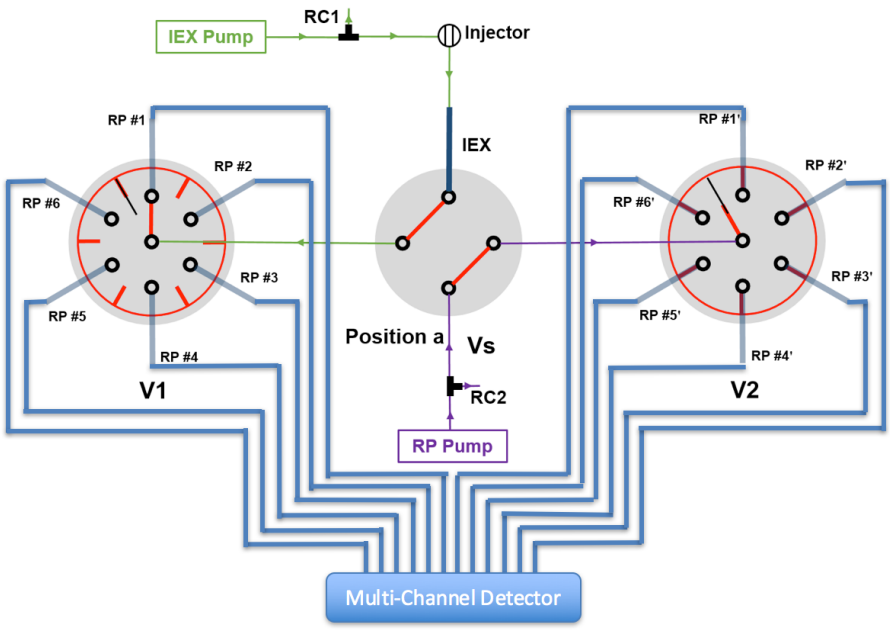

Figure 4-11 2D-LC valve schematic

The two-dimensional-HPLC system configuration can be seen above. It consists of one 1st-D IEX column (250 µm I.D) and 12 2nd-D RP columns (250 µm I.D). These columns are connected through a series of four valves; two new custom-designed multi-position valves (V1 and V2), a two-way four-port valve for switching between V1 and V2, and a 20-µL injection valve. All 2nd-D RP columns pass through the multichannel UV absorbance detector where data is collected using a Measurement Computing data acquisition card and analyzed within a custom LabView program.

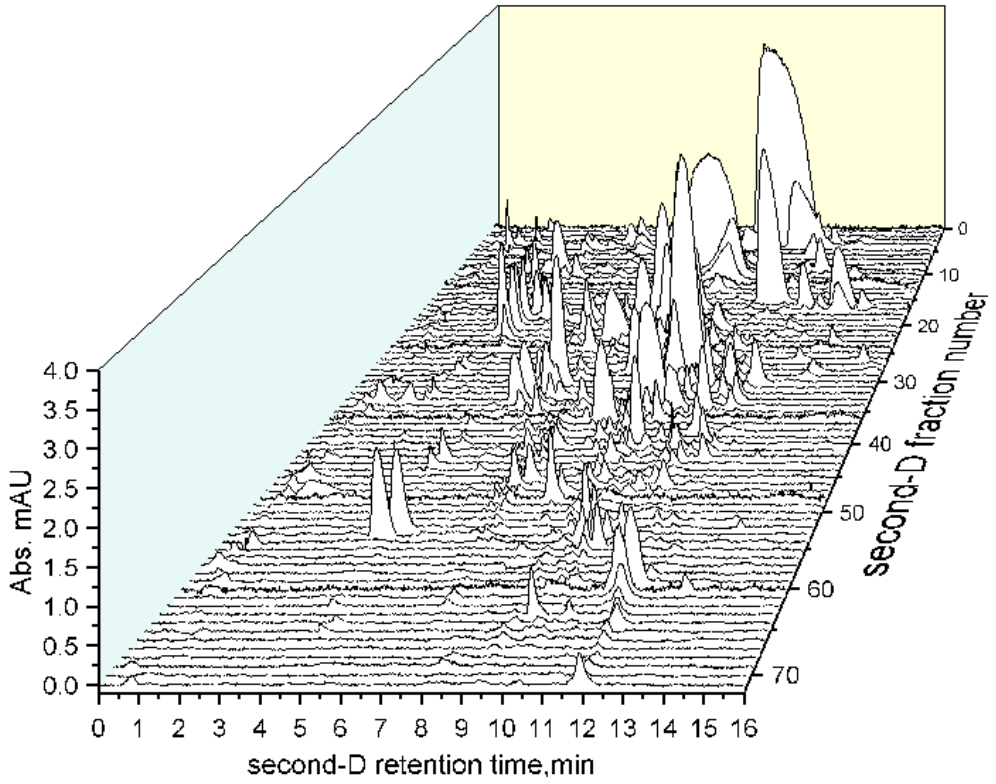

Figure 4-12 2D-HPLC Separation Chromatogram. Sample-E. Coli lysate

A visual representation of the individual raw chromatograms from the second-dimension RP separations. A total of 72 fractions took place over a four-hour period with a 220-nm wavelength to monitor the protein separation.

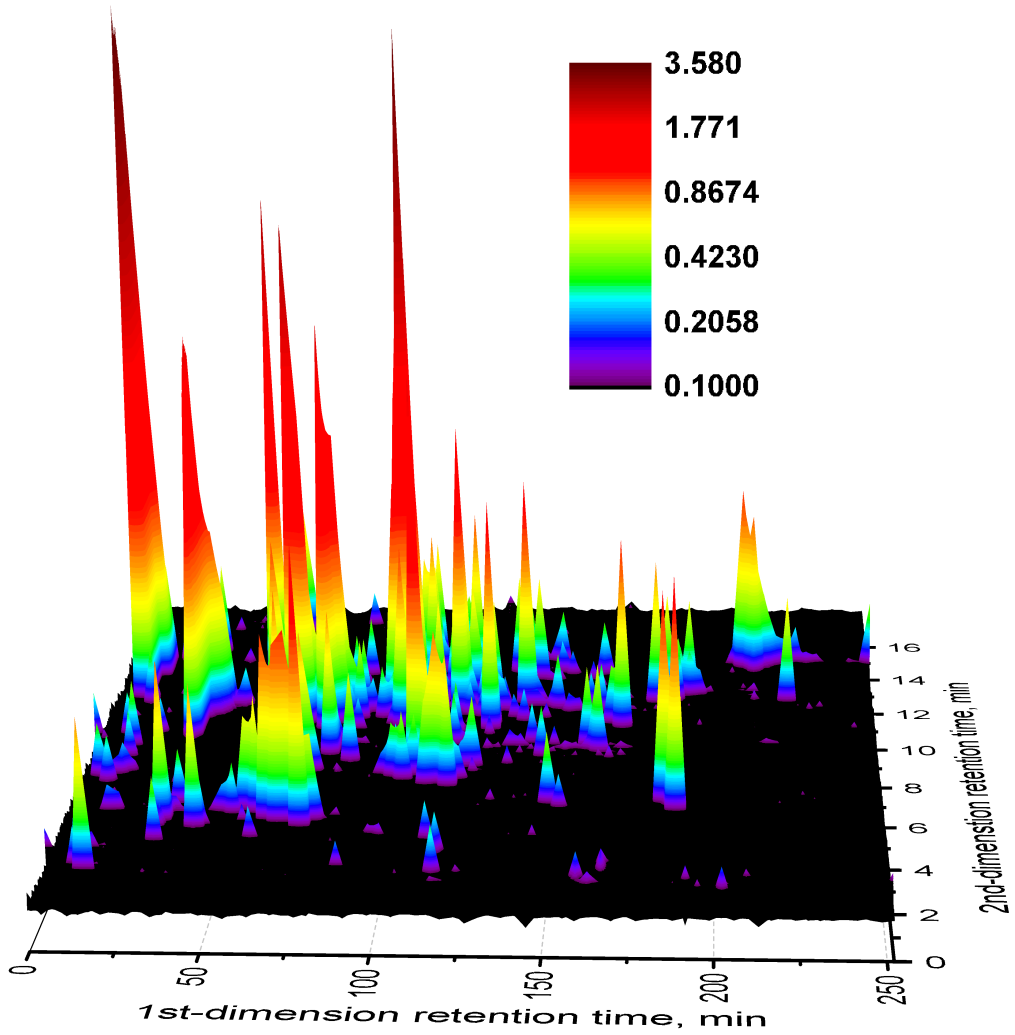

Figure 4-13 3D-representation of 2nd-D separation

A three dimensional representation for the second dimension E. Coli lysate separation based on the separation time.

Concluding remarks

This detector, in conjunction with a novel online 2D separation configuration developed within our lab, allowed for the simultaneous detection of a complex real world protein sample. Compared to a commercialized multichannel UV/Vis detector like Waters 2488 UV/Vis, our device is smaller, has fewer parts, and provides up to a 6 times increase in channel detection while residing within the same noise region and linear dynamic range. Through the use of a custom high quality furcated optical fiber, the precise machining of a flow cell, accurate capillary alignment to the source light, and high-performance operational amplifier; a versatile multi-absorbance detector was constructed for the application of a novel 2D-HPLC system. The background noise level drops down into tens of μAU and a linear range up to ~1.5 AU. This multichannel detector bears the features of high throughput sampling rate simultaneously, even though we currently are not at its current detection limit. The detector may be scaled up to further increase the throughput. Future improvements to the detector include the integration of a smaller lighthouse to decrease the overall detector size. Also, a change in the configuration of the 2D-HPLC system would allow for all 12 ports of the detector to be used simultaneously further either decreasing the overall separation time or increasing the resolving power by allowing for smaller fraction sizes to be taken.

The materials in Chapter 4 are adapted from Lynch et al., Talanta 181 (2018) 416-421. The copyright was obtained from Elsevier and the license number is 4315040872562. For more details, please see Appendix F.

Chapter 5: Overall Summary And Future Directions

Overall summary

The work covered within this dissertation was devoted to making miniaturized chemistry systems for chromatographic separations and detection. The need for these systems arises from the recent trend in analytical systems for point-of-care analysis. For quick detection of diseases and contaminants in the field, more portable diagnostic tools are required. The most common system for doing detection of complex samples such as blood or saliva is HPLC. These systems combine a separation platform with a detection method. Commercial systems are generally large in size, have large power requirements, and lack the ability to provide onsite analysis. The work in this thesis addresses these issues within the previous three chapters.

Through previous work on gradient generation techniques within our lab along with creating EOPs capable of producing high pressure and adequate flow rates for HPLC separations, a prototype HPLC cartridge was designed and constructed as shown in Chapter 2. This system utilized a novel EOP manifold that combined four negatively charged EOP monoliths in parallel allowing for a separation pressure and flow rate of ~2500 psi and ~200 nL/min (separation column flow rate) respectively. One of these pumps was used for the uptake a series of nine solutions of varying acetonitrile concentrations to generate the gradient profile required for the separation while a secondary pump system drove the eluent out and provided the separation. These two pumps were controlled using a dual 8-kV HVPS created in-house. The ability to change the concentration of the nine solutions and the volume of uptake for each one, it was

possible to configure the gradient profile according to the sample separation of interest. Trypsic BSA and myoglobin digests provided the complex samples required for proof of concept of the cartridge system and an absorbance detector as well as mass spectrometer was utilized to monitor the separations.

The next capillary-based prototype system developed was a bench top LIF system. LIF systems are notorious for their high level of sensitivity compared to that of absorbance detectors. Commercial systems as of right now have not been developed for capillary diameters in the low to sub-micron level. We addressed this deficiency in Chapter 3 through the presented narrow-capillary LIF prototype. The confocal laser system utilized a previously published method known as BaNC-HDC and was tested using a 2 μm-i.d. capillary and provided validation tests in the form of fluorescein and a DNA ladder. The detector had a LOD of 0.8 nM of fluorescein that corresponds to a yoctomole detection limit. The system had three orders of magnitude linear dynamic range. Lastly, a 1 kb DNA ladder was separated using BaNC-HDC and both qualitative and quantitative measurements were able to be made.

The third and last prototype discussed was a multiple-channel UV/Vis detector for high throughput chromatographic screening. A novel 2D-LC system developed within our lab increased the total number of simultaneous second dimension separation columns from the traditional one or two up to twelve. By doing so, separation times of complex samples could be greatly reduced. Since no commercial spectroscopic detector existed for this many columns, the

reduction of separation time could only be realized through the creation of the 12-channel absorbance detector presented in Chapter 4. This detector consists of a deuterium lighthouse, a flow cell assembly (a 13-channel flow cell fitted with a 13-photodiode-detection system), and a data acquisition and monitoring terminal. The flow cell assembly is further divided into the circuitry, 12 individual flow cells and a reference position, as well as a 13-furcated fiber optic cable all enclosed within a custom machined aluminum housing. A Labview program provided the platform for data collection and visualization. This detection system allowed for the completion of the 2D-HPLC that was being designed in tandem. The system allowed for three orders of magnitude linear dynamic range with noise in the tens of μAU. When combined with a novel 2D-LC system within our lab to perform detection for a complex separation, over 900 peaks were able to be distinguished using E. Coli lysate as the sample. This detector allowed for an overall increase in channel detection compared to commercial systems while still retaining comparable performance.

Future directions

Both the prototype of the HPLC cartridge and LIF detector represented the culmination of their respective projects. However, the possibility of optimizing the HPLC cartridge for its size and weight still exists. The current design was a proof-of-concept and thus a form of acrylic known as lexan made the enclosure. This contributed significantly to the overall weight of the system and if constructed out of metal such as aluminum could greatly reduce the overall weight. As chip-based monolithic systems

are further optimized, integrating the pump system into a microfluidic platform would further reduce the overall size and weight. Also, the portable system as currently presented is fully powered by a USB port and has many unused ports on the DAQ card. That being said, building compatible detectors to the system such as a LED-based absorbance detector or a microLIF-detector for on-site analysis may not be out of the realm of possibilities. This system could also be adapted to work in conjunction with current miniature mass spectrometry systems that are being developed to provide additional information than the other spectroscopic techniques mentioned previously. The LIF prototypes produced are all perfectly working systems that continue to be utilized within our laboratory. An improvement to be made to future systems would include black anodizing the internal components of the system in order to reduce stray light.

The future of the multiple-channel UV/Vis detector is the most promising. A redesign of the valve system allows for the total number of columns to be doubled while still utilizing the same detector. This is because at any given moment, only six channels were collecting column separation data while the other six columns were being reconditioned. Improvements to the detector may include a better electronic shield to reduce environmental noise, a dedicated tunable wavelength light source, and an improved furcated-fiber that allows for a better randomization of the improved light source. Also, it is our hopes that as higher throughput, multiple-channel 2D-HPLC systems become more popular; direct integration into a mass spectrometer could be possible. For example, if each column terminated with an ESI probe, and all of the twelve probes were positioned in a conical shape focused on the inlet of the mass

spectrometer, each channel could be systematically switched on and off sequentially allowing for the sprays of each column to be connected by the mass spectrometer. The resulting singular data would then need to be separated out into the intervals and reconfigured into twelve different chromatograms representing the twelve ESI probes respective sprays.

References

1. V. Gubala, L.F. Harris, A.J. Ricco, M.X. Tan, D.E. Williams, Point of care diagnostics: status and future, Analytical chemistry 84(2) (2011) 487-515.

2. P. Vandenabeele, H.G.M. Edwards, J. Jehlicka, The role of mobile instrumentation in novel applications of Raman spectroscopy: archaeometry, geosciences, and forensics, Chemical Society Reviews 43(8) (2014) 2628-2649.

3. G. Mogilevsky, L. Borland, M. Brickhouse, A.W. Fountain III, Raman Spectroscopy for Homeland Security Applications, 2012.

4. A. Kaushik, A. Vasudev, S.K. Arya, S.K. Pasha, S. Bhansali, Recent advances in cortisol sensing technologies for point-of-care application, Biosensors and Bioelectronics 53 (2014) 499-512.

5. P.K. Dasgupta, S. Liu, Electroosmosis: A Reliable Fluid Propulsion System for Flow Injection Analysis, Analytical Chemistry 66(11) (1994) 1792-1798.

6. P.H. Paul, D.W. Arnold, D.J. Rakestraw, Electrokinetic Generation of High Pressures using Porous Microstructures, in: D.J. Harrison, A. van den Berg (Eds.), Micro Total Analysis Systems '98: Proceedings of the uTAS '98 Workshop, held in Banff, Canada, 13–16 October 1998, Springer Netherlands, Dordrecht, 1998, pp. 49-52.

7. I.M. Lazar, B.L. Karger, Multiple Open-Channel Electroosmotic Pumping System for Microfluidic Sample Handling, Analytical Chemistry 74(24) (2002) 6259-6268.

8. X. Wang, C. Cheng, S. Wang, S. Liu, Electroosmotic pumps and their applications in microfluidic systems, Microfluidics and Nanofluidics 6(2) (2009) 145-162.

9. C. He, Z. Zhu, C. Gu, J. Lu, S. Liu, Stacking open-capillary electroosmotic pumps in series to boost the pumping pressure to drive high-performance liquid chromatographic separations, Journal of Chromatography A 1227 (2012) 253-258.

10. A. Chen, K.B. Lynch, X. Wang, J.J. Lu, C. Gu, S. Liu, Incorporating high-pressure electroosmotic pump and a nano-flow gradient generator into a miniaturized liquid chromatographic system for peptide analysis, Analytica Chimica Acta 844 (2014) 90-98.

11. K.B. Lynch, A. Chen, Y. Yang, J.J. Lu, S. Liu, High-performance liquid chromatographic cartridge with gradient elution capability coupled with UV absorbance detector and mass spectrometer for peptide and protein analysis, Journal of Separation Science n/a-n/a.

12. A. Chen, J.J. Lu, C. Gu, M. Zhang, K.B. Lynch, S. Liu, Combining selection valve and mixing chamber for nanoflow gradient generation: Toward developing a liquid chromatography cartridge coupled with mass spectrometer for protein and peptide analysis, Analytica Chimica Acta 887 (2015) 230-236.

13. L. Zhou, J.J. Lu, C. Gu, S. Liu, Binary Electroosmotic-Pump Nanoflow Gradient Generator for Miniaturized High-Performance Liquid Chromatography, Analytical Chemistry 86(24) (2014) 12214-12219.

14. D.S. Hage, J.A. Anguizola, C. Bi, R. Li, R. Matsuda, E. Papastavros, E. Pfaunmiller, J. Vargas, X. Zheng, Pharmaceutical and biomedical applications of affinity chromatography: recent trends and developments, Journal of pharmaceutical and biomedical analysis 69 (2012) 93-105.

15. T. Tsuda, M. Novotny, Packed microcapillary columns in high performance liquid chromatography, Analytical Chemistry 50(2) (1978) 271-275.

16. T. Tsuda, G. Nakagawa, Open-tubular liquid chromatography with 5–10-μm ID Columns, Journal of Chromatography A 268 (1983) 369-374.

17. R.T. Kennedy, J.W. Jorgenson, Preparation and evaluation of packed capillary liquid chromatography columns with inner diameters from 20 to 50 micrometers, Analytical Chemistry 61(10) (1989) 1128-1135.

18. S. Hsieh, J.W. Jorgenson, Preparation and Evaluation of Slurry-Packed Liquid Chromatography Microcolumns with Inner Diameters from 12 to 33 μm, Analytical Chemistry 68(7) (1996) 1212-1217.

19. T. Takeuchi, D. Ishii, High-performance micro packed flexible columns in liquid chromatography, Journal of Chromatography A 213(1) (1981) 25-32.

20. T. Takeuchi, D. Ishii, Micro-high-performance liquid chromatography with long micro-packed flexible fused-silica columns, Journal of Chromatography A 238(2) (1982) 409-418.

21. F.J. Yang, Fused-silica narrow-bore microparticle-packed-column high-performance liquid chromatography, Journal of Chromatography A 236(2) (1982) 265-277.

22. K.E. Karlsson, M. Novotny, A miniature gradient elution system for liquid chromatography with packed capillary columns, Journal of High Resolution Chromatography 7(7) (1984) 411-413.

23. F. Andreolini, C. Borra, M. Novotny, Preparation and evaluation of slurry-packed capillary columns for normal-phase liquid chromatography, Analytical Chemistry 59(19) (1987) 2428-2432.

24. C. Borra, S.M. Han, M. Novotny, Quantitative analytical aspects of reversed-phase liquid chromatography with slurry-packed capillary columns, Journal of Chromatography A 385 (1987) 75-85.

25. K.E. Karlsson, M. Novotny, Separation efficiency of slurry-packed liquid chromatography microcolumns with very small inner diameters, Analytical Chemistry 60(17) (1988) 1662-1665.

26. J.E. MacNair, K.D. Patel, J.W. Jorgenson, Ultrahigh-Pressure Reversed-Phase Capillary Liquid Chromatography: Isocratic and Gradient Elution Using Columns Packed with 1.0-μm Particles, Analytical Chemistry 71(3) (1999) 700-708.

27. J.E. MacNair, K.C. Lewis, J.W. Jorgenson, Ultrahigh-Pressure Reversed-Phase Liquid Chromatography in Packed Capillary Columns, Analytical Chemistry 69(6) (1997) 983-989.

28. B.J. Rogers, R.E. Birdsall, Z. Wu, M.J. Wirth, RPLC of Intact Proteins Using Sub-0.5 μm Particles and Commercial Instrumentation, Analytical Chemistry 85(14) (2013) 6820-6825.

29. B. He, N. Tait, F. Regnier, Fabrication of Nanocolumns for Liquid Chromatography, Analytical Chemistry 70(18) (1998) 3790-3797.

30. X. Huang, F. Qin, X. Chen, Y. Liu, H. Zou, Short columns with molecularly imprinted monolithic stationary phases for rapid separation of diastereomers and enantiomers, Journal of Chromatography B 804(1) (2004) 13-18.

31. Y. Li, H.D. Tolley, M.L. Lee, Preparation of monoliths from single crosslinking monomers for reversed-phase capillary chromatography of small molecules, Journal of Chromatography A 1218(10) (2011) 1399-1408.

32. T. Hara, H. Kobayashi, T. Ikegami, K. Nakanishi, N. Tanaka, Performance of Monolithic Silica Capillary Columns with Increased Phase Ratios and Small-Sized Domains, Analytical Chemistry 78(22) (2006) 7632-7642.

33. S.D. Chambers, T.W. Holcombe, F. Svec, J.M.J. Fréchet, Porous Polymer Monoliths Functionalized through Copolymerization of a C60 Fullerene-Containing Methacrylate Monomer for Highly Efficient Separations of Small Molecules, Analytical Chemistry 83(24) (2011) 9478-9484.

34. P. Aggarwal, J.S. Lawson, H.D. Tolley, M.L. Lee, High efficiency polyethylene glycol diacrylate monoliths for reversed-phase capillary liquid chromatography of small molecules, Journal of Chromatography A 1364 (2014) 96-106.

35. S. Eeltink, S. Wouters, J.L. Dores-Sousa, F. Svec, Advances in organic polymer-based monolithic column technology for high-resolution liquid chromatography-mass spectrometry profiling of antibodies, intact proteins, oligonucleotides, and peptides, J Chromatogr A 1498 (2017) 8-21.

36. R. Rathnasekara, S. Khadka, M. Jonnada, Z. El Rassi, Polar and nonpolar organic polymer-based monolithic columns for capillary electrochromatography and high-performance liquid chromatography, Electrophoresis 38(1) (2017) 60-79.

37. Q. Luo, Y. Gu, S.-L. Wu, T. Rejtar, B.L. Karger, Two-dimensional strong cation exchange/porous layer open tubular/mass spectrometry for ultratrace proteomic analysis using a 10 μm id poly(styrene- divinylbenzene) porous layer open tubular column with an on-line triphasic trapping column, ELECTROPHORESIS 29(8) (2008) 1604-1611.

38. M. Rogeberg, S.R. Wilson, T. Greibrokk, E. Lundanes, Separation of intact proteins on porous layer open tubular (PLOT) columns, Journal of Chromatography A 1217(17) (2010) 2782-2786.

39. D. Thakur, T. Rejtar, D. Wang, J. Bones, S. Cha, B. Clodfelder-Miller, E. Richardson, S. Binns, S. Dahiya, D. Sgroi, B.L. Karger, Microproteomic analysis of 10,000 laser captured microdissected breast tumor cells using short-range sodium dodecyl sulfate-polyacrylamide gel electrophoresis and porous layer open tubular liquid chromatography tandem mass spectrometry, Journal of Chromatography A 1218(45) (2011) 8168-8174.

40. M. Rogeberg, T. Vehus, L. Grutle, T. Greibrokk, S.R. Wilson, E. Lundanes, Separation optimization of long porous-layer open-tubular columns for nano-LC–MS of limited proteomic samples, Journal of Separation Science 36(17) (2013) 2838-2847.

41. H.K. Hustoft, T. Vehus, O.K. Brandtzaeg, S. Krauss, T. Greibrokk, S.R. Wilson, E. Lundanes, Open Tubular Lab-On-Column/Mass Spectrometry for Targeted Proteomics of Nanogram Sample Amounts, PLOS ONE 9(9) (2014) e106881.

42. C.P. Kapnissi-Christodoulou, X. Zhu, I.M. Warner, Analytical separations in open-tubular capillary electrochromatography, Electrophoresis 24(22-23) (2003) 3917-34.

43. E. Guihen, J.D. Glennon, Recent highlights in stationary phase design for open-tubular capillary electrochromatography, J Chromatogr A 1044(1-2) (2004) 67-81.

44. W.J. Cheong, F. Ali, Y.S. Kim, J.W. Lee, Comprehensive overview of recent preparation and application trends of various open tubular capillary columns in separation science, J Chromatogr A 1308 (2013) 1-24.

45. [45] M.D. Hargreaves, R.L. Green, W. Jalenak, C.D. Brown, C. Gardner, Handheld Raman and FT-IR Spectrometers, Infrared and Raman Spectroscopy in Forensic Science, John Wiley & Sons, Ltd2012, pp. 275-287.

46. I. Miralles, S.E. Jorge-Villar, Y. Cantón, F. Domingo, Using a Mini-Raman Spectrometer to Monitor the Adaptive Strategies of Extremophile Colonizers in Arid Deserts: Relationships Between Signal Strength, Adaptive Strategies, Solar Radiation, and Humidity, Astrobiology 12(8) (2012) 743-753.

47. J.A. Cayuela, C. Weiland, Intact orange quality prediction with two portable NIR spectrometers, Postharvest Biology and Technology 58(2) (2010) 113-120.

48. Y.-d. Liu, R.-j. Gao, X.-d. Sun, Review of Portable NIR Instruments for Detecting Fruit Interior Quality, Spectroscopy and Spectral Analysis 30(10) (2010) 2874-2878.

49. C.A.T. dos Santos, M. Lopo, R.N.M.J. Páscoa, J.A. Lopes, A Review on the Applications of Portable Near-Infrared Spectrometers in the Agro-Food Industry, Applied Spectroscopy 67(11) (2013) 1215-1233.

50. M. Ecarnot, P. Bączyk, L. Tessarotto, C. Chervin, Rapid phenotyping of the tomato fruit model, Micro-Tom, with a portable VIS–NIR spectrometer, Plant Physiology and Biochemistry 70 (2013) 159-163.

51. Y. Hoshi, Functional near-infrared spectroscopy: current status and future prospects, Journal of Biomedical Optics 12(6) (2007) 062106-062106-9.

52. M.-T. Sánchez, M.-J. De la Haba, D. Pérez-Marín, Internal and external quality assessment of mandarins on-tree and at harvest using a portable NIR spectrophotometer, Computers and Electronics in Agriculture 92 (2013) 66-74.

53. X.-X. Fang, H.-Y. Li, P. Fang, J.-Z. Pan, Q. Fang, A handheld laser-induced fluorescence detector for multiple applications, Talanta 150 (2016) 135-141.

54. M.T. Weaver, K.B. Lynch, Z. Zhu, H. Chen, J.J. Lu, Q. Pu, S. Liu, Confocal laser-induced fluorescence detector for narrow capillary system with yoctomole limit of detection, Talanta 165 (2017) 240-244.

55. F.-B. Yang, J.-Z. Pan, T. Zhang, Q. Fang, A low-cost light-emitting diode induced fluorescence detector for capillary electrophoresis based on an orthogonal optical arrangement, Talanta 78(3) (2009) 1155-1158.

56. A.J. Das, A. Wahi, I. Kothari, R. Raskar, Ultra-portable, wireless smartphone spectrometer for rapid, non-destructive testing of fruit ripeness, Scientific Reports 6 (2016) 32504.

57. A. Gałuszka, Z.M. Migaszewski, J. Namieśnik, Moving your laboratories to the field – Advantages and limitations of the use of field portable instruments in environmental sample analysis, Environmental Research 140 (2015) 593-603.

58. Y. Xiong, J. Tan, S. Fang, C. Wang, Q. Wang, J. Wu, J. Chen, M. Duan, A

LED-based fiber-optic sensor integrated with lab-on-valve manifold for colorimetric determination of free chlorine in water, Talanta 167 (2017) 103-110.

59. C.C. Hong, C.Y. Wang, K.T. Peng, I.M. Chu, A microfluidic chip platform with electrochemical carbon nanotube electrodes for pre-clinical evaluation of antibiotics nanocapsules, Biosens Bioelectron 26(8) (2011) 3620-6.

60. Y. Sameenoi, M.M. Mensack, K. Boonsong, R. Ewing, W. Dungchai, O. Chailapakul, D.M. Cropek, C.S. Henry, Poly(dimethylsiloxane) cross-linked carbon paste electrodes for microfluidic electrochemical sensing, Analyst 136(15) (2011) 3177-84.

61. W. Liang, Y. Li, B. Zhang, Z. Zhang, A. Chen, D. Qi, W. Yi, C. Hu, A novel microfluidic immunoassay system based on electrochemical immunosensors: an application for the detection of NT-proBNP in whole blood, Biosens Bioelectron 31(1) (2012) 480-5.

62. J. Yang, J.H. Yu, J. Rudi Strickler, W.J. Chang, S. Gunasekaran, Nickel nanoparticle-chitosan-reduced graphene oxide-modified screen-printed electrodes for enzyme-free glucose sensing in portable microfluidic devices, Biosens Bioelectron 47 (2013) 530-8.

63. [63] T. Pluangklang, J.B. Wydallis, D.M. Cate, D. Nacapricha, C.S. Henry, A simple microfluidic electrochemical HPLC detector for quantifying Fenton reactivity from welding fumes, Analytical Methods 6(20) (2014) 8180-8186.

64. M.L. Yola, T. Eren, N. Atar, A sensitive molecular imprinted electrochemical sensor based on gold nanoparticles decorated graphene oxide: Application to selective determination of tyrosine in milk, Sensors and Actuators B: Chemical 210 (2015) 149-157.

65. G.L. Bosco, Development and application of portable, hand-held X-ray fluorescence spectrometers, TrAC Trends in Analytical Chemistry 45 (2013) 121-134.

66. D.C. Weindorf, N. Bakr, Y. Zhu, Advances in Portable X-ray Fluorescence (PXRF) for Environmental, Pedological, and Agronomic Applications, Advances in Agronomy 128 (2014) 1-45.

67. K.E. Young, C.A. Evans, K.V. Hodges, J.E. Bleacher, T.G. Graff, A review of the handheld X-ray fluorescence spectrometer as a tool for field geologic investigations on Earth and in planetary surface exploration, Applied Geochemistry 72 (2016) 77-87.

68. D.T. Snyder, C.J. Pulliam, Z. Ouyang, R.G. Cooks, Miniature and Fieldable Mass Spectrometers: Recent Advances, Analytical Chemistry 88(1) (2016) 2-29.

69. L. Novak, P. Neuzil, J. Pipper, Y. Zhang, S. Lee, An integrated fluorescence detection system for lab-on-a-chip applications, Lab on a Chip 7(1) (2007) 27-29.

70. LABORATORY DATA CONTROL, Analytical Chemistry 50(3) (1978) 397A-397A.

71. B. Bomastyk, I. Petrovic, P.C. Hauser, Absorbance detector for high-performance liquid chromatography based on light-emitting diodes for the deep-ultraviolet range, Journal of Chromatography A 1218(24) (2011) 3750-3756.

72. D.A. Bui, P.C. Hauser, Absorbance detector for capillary electrophoresis based on light-emitting diodes and photodiodes for the deep-ultraviolet range, Journal of Chromatography A 1421 (2015) 203-208.

73. D.A. Bui, P.C. Hauser, A deep-UV light-emitting diode-based absorption detector for benzene, toluene, ethylbenzene, and the xylene compounds, Sensors and Actuators B: Chemical 235 (2016) 622-626.

74. F. Cecil, M. Zhang, R.M. Guijt, A. Henderson, P.N. Nesterenko, B. Paull, M.C. Breadmore, M. Macka, 3D printed LED based on-capillary detector housing with integrated slit, Analytica Chimica Acta 965 (2017) 131-136.

75. Z. Ding, D. Zhang, G. Wang, M. Tang, Y. Dong, Y. Zhang, H.-p. Ho, X. Zhang, An in-line spectrophotometer on a centrifugal microfluidic platform for real-time protein determination and calibration, Lab on a Chip 16(18) (2016) 3604-3614.

76. S. Schmid, M. Macka, P.C. Hauser, UV-absorbance detector for HPLC based on a light-emitting diode, Analyst 133(4) (2008) 465-469.

77. S. Sharma, H.D. Tolley, P.B. Farnsworth, M.L. Lee, LED-Based UV Absorption Detector with Low Detection Limits for Capillary Liquid Chromatography, Anal. Chem. 87(2) (2015) 1381-1386.

78. A.J.P. Martin, R.L.M. Synge, A new form of chromatogram employing two liquid phases, Biochemical Journal 35(12) (1941) 1358.

79. J.M. Miller, Dynamics of Chromatography, Science 152(3725) (1966) 1051.

80. C.G. Horvath, S.R. Lipsky, Peak capacity in chromatography, Analytical chemistry 39(14) (1967) 1893-1893.

81. I. Halasz, I. Sebestian, New stationary phase for chromatography, Angewandte Chemie International Edition in English 8(6) (1969) 453-454.

82. J.F.K. Huber, High efficiency, high speed liquid chromatography in columns, Oxford University Press, 1969.

83. L. Snyder, Column efficiencies in liquid adsorption chromatography: Past, present and future, Oxford University Press, 1969.

84. G. Baram, M. Grachev, N.e.a. Komarova, M. Perelroyzen, Y.A. Bolvanov, S. Kuzmin, V. Kargaltsev, E. Kuper, Micro-column liquid chromatography with multi-wave-length photometric detection: I. The OB-4 micro-column liquid chromatograph, Journal of Chromatography A 264 (1983) 69-90.

85. T. Otagawa, J.R. Stetter, S. Zaromb, Portable liquid chromatograph for analysis of primary aromatic amines in coal-derived materials, Journal of Chromatography A 360 (1986) 252-259.

86. G.I. Baram, Portable liquid chromatograph for mobile laboratories, Journal of Chromatography A 728(1) (1996) 387-399.

87. V.M. Tulchinsky, D.E. St. Angelo, A practical portable HPLC system—MINICHROM, a new generation for field HPLC, Field Analytical Chemistry & Technology 2(5) (1998) 281-285.

88. http://www.iconsci.com/worldssmallesthplc.html.

89. J.W. Dolan, Dwell Volume Revisited, LCGC North America 25(5) (2006) 458-466.

90. J.V. Hinshaw, What Is "Dead" Volume and Why Should Chromatographers Worry About It?, LCGC North America 33(11) (2015) 850-855.

91. A. Ishida, M. Fujii, T. Fujimoto, S. Sasaki, I. Yanagisawa, H. Tani, M. Tokeshi, A Portable Liquid Chromatograph with a Battery-operated Compact Electroosmotic Pump and a Microfluidic Chip Device with a Reversed Phase Packed Column, Analytical Sciences 31(11) (2015) 1163-1169.

92. S. Sharma, A. Plistil, H.E. Barnett, H.D. Tolley, P.B. Farnsworth, S.D. Stearns, M.L. Lee, Hand-Portable Gradient Capillary Liquid Chromatography Pumping System, Analytical Chemistry 87(20) (2015) 10457-10461.

93. S. Sharma, A. Plistil, R.S. Simpson, K. Liu, P.B. Farnsworth, S.D. Stearns, M.L. Lee, Instrumentation for hand-portable liquid chromatography, Journal of Chromatography A 1327 (2014) 80-89.

94. C.B. Boring, P.K. Dasgupta, A. Sjögren, Compact, field-portable capillary ion chromatograph, Journal of Chromatography A 804(1) (1998) 45-54.

95. http://www.srigc.com/2005catalog/cat92-95.htm.

96. C. Albrecht, Joseph R. Lakowicz: Principles of fluorescence spectroscopy, Analytical and Bioanalytical chemistry 390(5) (2008) 1223-1224.

97. J. Stephan, K. Dörre, S. Brakmann, T. Winkler, T. Wetzel, M. Lapczyna, M. Stuke, B. Angerer, W. Ankenbauer, Z. Földes-Papp, Towards a general procedure for sequencing single DNA molecules, Journal of biotechnology 86(3) (2001) 255-267.

98. N. Billinton, A.W. Knight, Seeing the wood through the trees: a review of techniques for distinguishing green fluorescent protein from endogenous autofluorescence, Analytical biochemistry 291(2) (2001) 175-197.

99. B. Valeur, M.N. Berberan-Santos, Molecular fluorescence: principles and applications, John Wiley & Sons2012.

100. T. Huang, J. Pawliszyn, Axially illuminated fluorescence imaging detection for capillary isoelectric focusing on Teflon capillary, Analyst 125(7) (2000) 1231-1233.

101. D.B. Craig, J.C.Y. Wong, N.J. Dovichi, Detection of Attomolar Concentrations of Alkaline Phosphatase by Capillary Electrophoresis Using Laser-Induced Fluorescence Detection, Analytical Chemistry 68(4) (1996) 697-700.

102. N.I. Davis, M. Mamunooru, C.A. Vyas, J.G. Shackman, Capillary and Microfluidic Gradient Elution Isotachophoresis Coupled to Capillary Zone Electrophoresis for Femtomolar Amino Acid Detection Limits, Analytical Chemistry 81(13) (2009) 5452-5459.

103. X. Wang, C. Cheng, S. Wang, M. Zhao, P.K. Dasgupta, S. Liu, Nanocapillaries for Open Tubular Chromatographic Separations of Proteins in Femtoliter to Picoliter Samples, Analytical Chemistry 81(17) (2009) 7428-7435.

104. L. Zeng, D.B. Kassel, Developments of a Fully Automated Parallel HPLC/Mass Spectrometry System for the Analytical Characterization and Preparative Purification of Combinatorial Libraries, Analytical Chemistry 70(20) (1998) 4380-4388.

105. J.F. Cargill, M. Lebl, New methods in combinatorial chemistry — robotics and parallel synthesis, Current Opinion in Chemical Biology 1(1) (1997) 67-71.

106. P.A. Cremin, L. Zeng, High-Throughput Analysis of Natural Product Compound Libraries by Parallel LC−MS Evaporative Light Scattering Detection, Analytical Chemistry 74(21) (2002) 5492-5500.

107. A.B. Darcy Shave, Warren Potts, Ronan Cleary, Paul Lefebvre, Cozette Cuppett, HIGH THROUGHPUT MASS-DIRECTED PURIFICATION OF DRUG DISCOVERY COMPOUNDS, 200. http://www.waters.com/webassets/cms/library/docs/720001011en.pdf.

108. Sepiatec, 8x Screening HPLC system (2012).

109. C. Jing, X. Qun, J. Rohrer, Sensitive Determination of Explosive Compounds in Water.

110. T. Otagawa, J.R. Stetter, S. Zaromb, Portable Liquid Chromatograph for Analysis of Primary Aromatic-Amines in Coal-Derived Materials, J. Chromatogr. 360(1) (1986) 252-259.

111. C.E.D. Nazario, M.R. Silva, M.S. Franco, F.M. Lancas, Evolution in miniaturized column liquid chromatography instrumentation and applications: An overview, J. Chromatogr. A 1421 (2015) 18-37.

112. J. Sestak, D. Moravcova, V. Kahle, Instrument platforms for nano liquid chromatography, J. Chromatogr. A 1421 (2015) 2-17.

113. S. Sharma, L.T. Tolley, H.D. Tolley, A. Plistil, S.D. Stearns, M.L. Lee, Hand-portable liquid chromatographic instrumentation, J. Chromatogr. A 1421 (2015) 38-47.

114. C. Gu, Z. Jia, Z. Zhu, C. He, W. Wang, A. Morgan, J.J. Lu, S. Liu, Miniaturized Electroosmotic Pump Capable of Generating Pressures of More than 1200 Bar, Anal. Chem. 84(21) (2012) 9609-9614.

115. C. He, Z. Zhu, C. Gu, J. Lu, S. Liu, Stacking open-capillary electroosmotic pumps in series to boost the pumping pressure to drive high-performance liquid chromatographic separations, J. Chromatogr. A 1227(0) (2012) 253-258.

116. X.X. Fang, H.Y. Li, P. Fang, J.Z. Pan, Q. Fang, A handheld laser-induced fluorescence detector for multiple applications, Talanta 150 (2016) 135-141.

117. J.R. Scherer, P. Liu, R.A. Mathies, Design and operation of a portable scanner for high performance microchip capillary array electrophoresis, Rev. Sci. Instrum. 81(11) (2010).

118. R.V. Chimenti, R.J. Thomas, Miniature spectrometer designs open new applications potential, Laser Focus World 49(5) (2013) 34-+.

119. A. Chen, K.B. Lynch, X.C. Wang, J.J. Lu, C.Y. Gu, S.R. Liu, Incorporating high-pressure electroosmotic pump and a nano-flow gradient generator into a miniaturized liquid chromatographic system for peptide analysis, Anal. Chim. Acta 844 (2014) 90-98.

120. J. Yi, J. Heinecke, H. Tan, P.C. Ford, G.B. Richter-Addo, The distal pocket

histidine residue in horse heart myoglobin directs the O-binding mode of nitrite to the heme iron, J. Am. Chem. Soc. 131(50) (2009) 18119-28.

121. A. Chen, J.J. Lu, C. Gu, M. Zhang, K.B. Lynch, S. Liu, Combining selection valve and mixing chamber for nanoflow gradient generation: Toward developing a liquid chromatography cartridge coupled with mass spectrometer for protein and peptide analysis, Anal. Chim. Acta 887 (2015) 230-6.

122. L. Zhou, J.J. Lu, C. Gu, S. Liu, Binary electroosmotic-pump nanoflow gradient generator for miniaturized high-performance liquid chromatography, Analytical chemistry 86(24) (2014) 12214-9.

123. P. Yue, Z.L. Li, J. Moult, Loss of protein structure stability as a major causative factor in monogenic disease, J. Mol. Biol. 353(2) (2005) 459-473.

124. U.B. Hendgen-Cotta, U. Flogel, M. Kelm, T. Rassaf, Unmasking the Janus face of myoglobin in health and disease, J. Exp. Biol. 213(Pt 16) (2010) 2734-40.

125. S. Shiva, Nitrite: A Physiological Store of Nitric Oxide and Modulator of Mitochondrial Function, Redox Biol 1(1) (2013) 40-44.

126. J.G. Guillemette, Y. Matsushimahibiya, T. Atkinson, M. Smith, Expression in Escherichia-Coli of a Synthetic Gene Coding for Horse Heart Myoglobin, Protein Eng. 4(5) (1991) 585-592.

127. D. Li, C. Jakob, O. Schmitz, Practical considerations in comprehensive two-dimensional liquid chromatography systems (LCxLC) with reversed-phases in both dimensions, Analytical and Bioanalytical Chemistry 407(1) (2015) 153-167.

128. F. Cacciola, S. Farnetti, P. Dugo, P.J. Marriott, L. Mondello, Comprehensive two-dimensional liquid chromatography for polyphenol analysis in foodstuffs, Journal of Separation Science 40(1) (2017) 7-24.

129. F. Erni, R. Frei, Two-dimensional column liquid chromatographic technique for resolution of complex mixtures, Journal of Chromatography A 149 (1978) 561-569.

130. M.M. Bushey, J.W. Jorgenson, Automated instrumentation for comprehensive

two-dimensional high-performance liquid chromatography of proteins, Analytical chemistry 62(2) (1990) 161-167.

131. M. Gilar, P. Olivova, A.E. Daly, J.C. Gebler, Orthogonality of separation in two-dimensional liquid chromatography, Analytical chemistry 77(19) (2005) 6426-6434.

132. K. Kabytaev, A. Durairaj, D. Shin, C.L. Rohlfing, S. Connolly, R.R. Little, A.V. Stoyanov, Two‐step ion‐exchange chromatographic purification combined with reversed‐phase chromatography to isolate C‐peptide for mass spectrometric analysis, Journal of separation science 39(4) (2016) 676-681.

133. X. Gjoka, M. Schofield, A. Cvetkovic, R. Gantier, Combined Protein A and size exclusion high performance liquid chromatography for the single-step measurement of mAb, aggregates and host cell proteins, Journal of Chromatography B 972(Supplement C) (2014) 48-52.

134. Y. Wei, T. Lan, T. Tang, L. Zhang, F. Wang, T. Li, Y. Du, W. Zhang, A comprehensive two-dimensional normal-phase x reversed-phase liquid chromatography based on the modification of mobile phases, Journal of chromatography. A 1216(44) (2009) 7466-71.

135. J.-F. Li, H. Fang, X. Yan, F.-R. Chang, Z. Wu, Y.-L. Wu, Y.-K. Qiu, On-line comprehensive two-dimensional normal-phase liquid chromatography× reversed-phase liquid chromatography for preparative isolation of toad venom, Journal of Chromatography A 1456 (2016) 169-175.

136. C. Venkatramani, M. Al-Sayah, G. Li, M. Goel, J. Girotti, L. Zang, L. Wigman, P. Yehl, N. Chetwyn, Simultaneous achiral-chiral analysis of pharmaceutical compounds using two-dimensional reversed phase liquid chromatography-supercritical fluid chromatography, Talanta 148 (2016) 548-555.

137. P. Hemström, K. Irgum, Hydrophilic interaction chromatography, Journal of separation science 29(12) (2006) 1784-1821.

138. D.R. Stoll, J.D. Cohen, P.W. Carr, Fast, comprehensive online two-dimensional high performance liquid chromatography through the use of high temperature ultra-fast gradient elution reversed-phase liquid chromatography, Journal of Chromatography a 1122(1) (2006) 123-137.

139. G. Guiochon, N. Marchetti, K. Mriziq, R.A. Shalliker, Implementations of two-dimensional liquid chromatography, Journal of Chromatography A 1189(1) (2008) 109-168.

140. D.R. Stoll, Recent advances in 2D-LC for bioanalysis, Bioanalysis 7(24) (2015) 3125-42.

141. P.W. Carr, D.R. Stoll, Two-Dimensional Liquid Chromatography Principles, Practical Implementation and Applications, Agilent Technologies, Inc., 2015.

142. Z. Li, P. Hong, P. McConville, Effective Determination of Pharmaceutical Impurities by Two Dimensional Liquid Chromatography (2DLC), Waters Corporation, 2017.

143. Z. Zhu, H. Chen, J. Ren, J.J. Lu, C. Gu, K.B. Lynch, S. Wu, Z. Wang, C. Cao, S. Liu, Two-dimensional chromatographic analysis using three second-dimension columns for continuous comprehensive analysis of intact proteins, Talanta (2017).

144. Waters, Waters 2488 Multichannel Absorbance Detector with MassLynx Control, http://www.waters.com/webassets/cms/support/docs/71500248802ra.pdf, 2001.

145. Q. Gao, Y. Shi, S. Liu, Multiple-channel microchips for high-throughput DNA analysis by capillary electrophoresis, Fresenius' journal of analytical chemistry 371(2) (2001) 137-145.

146. J. Tu, L.N. Anderson, J. Dai, K. Peters, A. Carr, P. Loos, D. Buchanan, J.J. Bao, C. Liu, K.R. Wehmeyer, Application of multiplexed capillary electrophoresis with laser-induced fluorescence (MCE–LIF) detection for the rapid measurement of endogenous extracellular signal-regulated protein kinase (ERK) levels in cell extracts, Journal of Chromatography B 789(2) (2003) 323-335.

147. M. Benhabib, T.N. Chiesl, A.M. Stockton, J.R. Scherer, R.A. Mathies, Multichannel Capillary Electrophoresis Microdevice and Instrumentation for in Situ Planetary Analysis of Organic Molecules and Biomarkers, Analytical Chemistry 82(6) (2010) 2372-2379.

148. T. Anazawa, Y. Uchiho, T. Yokoi, G. Chalkidis, M. Yamazaki, A simple and highly sensitive spectroscopic fluorescence-detection system for multi-channel

plastic-microchip electrophoresis based on side-entry laser-beam zigzag irradiation, Lab on a Chip (2017).

149. S. Liu, Q. Pu, L. Gao, J. Lu, An economic approach for construction of a multiplexed capillary electrophoresis system, Talanta 70(3) (2006) 644-650.

Appendix A

Thank you for your order!

Dear Kyle Lynch,

Thank you for placing your order through Copyright Clearance Center's RightsLink® service.

Order Summary

Licensee:	Kyle B Lynch
Order Date:	Mar 23, 2018
Order Number:	4315050158423
Publication:	Talanta
Title:	Miniaturized high-performance liquid chromatography instrumentation
Type of Use:	reuse in a thesis/dissertation
Order Ref:	5241988
Order Total:	0.00 USD

View or print complete details of your order and the publisher's terms and conditions.

Sincerely,

Copyright Clearance Center

How was your experience? Fill out this survey to let us know.

Tel: +1-855-239-3415 / +1-978-646-2777
customercare@copyright.com
https://myaccount.copyright.com

Copyright Clearance Center RightsLink®

Appendix B

Thank you for your order!

Dear Kyle Lynch,

Thank you for placing your order through Copyright Clearance Center's RightsLink® service.

Order Summary

Licensee:	Kyle B Lynch
Order Date:	Mar 23, 2018
Order Number:	4315041474845
Publication:	Journal of Separation Science
Title:	High–performance liquid chromatographic cartridge with gradient elution capability coupled with UV absorbance detector and mass spectrometer for peptide and protein analysis
Type of Use:	Dissertation/Thesis
Order Ref:	5241988
Order Total:	0.00 USD

View or print complete details of your order and the publisher's terms and conditions.

Sincerely,

Copyright Clearance Center

How was your experience? Fill out this survey to let us know.

Tel: +1-855-239-3415 / +1-978-646-2777
customercare@copyright.com
https://myaccount.copyright.com

Copyright Clearance Center RightsLink®

Appendix C

Thank you for your order!

Dear Kyle Lynch,

Thank you for placing your order through Copyright Clearance Center's RightsLink® service.

Order Summary

Licensee:	Kyle B Lynch
Order Date:	Mar 26, 2018
Order Number:	4316591286765
Publication:	Analytica Chimica Acta
Title:	Incorporating high-pressure electroosmotic pump and a nano-flow gradient generator into a miniaturized liquid chromatographic system for peptide analysis
Type of Use:	reuse in a thesis/dissertation
Order Ref:	5241988
Order Total:	0.00 USD

View or print complete details of your order and the publisher's terms and conditions.

Sincerely,

Copyright Clearance Center

How was your experience? Fill out this survey to let us know.

Tel: +1-855-239-3415 / +1-978-646-2777
customercare@copyright.com
https://myaccount.copyright.com

Copyright Clearance Center RightsLink®

Appendix D

Thank you for your order!

Dear Kyle Lynch,

Thank you for placing your order through Copyright Clearance Center's RightsLink® service.

Order Summary

Licensee:	Kyle B Lynch
Order Date:	Mar 26, 2018
Order Number:	4316600057156
Publication:	Analytica Chimica Acta
Title:	Combining selection valve and mixing chamber for nanoflow gradient generation: Toward developing a liquid chromatography cartridge coupled with mass spectrometer for protein and peptide analysis
Type of Use:	reuse in a thesis/dissertation
Order Ref:	5241988
Order Total:	0.00 USD

View or print complete details of your order and the publisher's terms and conditions.

Sincerely,

Copyright Clearance Center

How was your experience? Fill out this survey to let us know.

Tel: +1-855-239-3415 / +1-978-646-2777
customercare@copyright.com
https://myaccount.copyright.com

Copyright Clearance Center RightsLink®

Appendix E

Thank you for your order!

Dear Kyle Lynch,

Thank you for placing your order through Copyright Clearance Center's RightsLink® service.

Order Summary

Licensee:	Kyle B Lynch
Order Date:	Mar 23, 2018
Order Number:	4315041314106
Publication:	Talanta
Title:	Confocal laser-induced fluorescence detector for narrow capillary system with yoctomole limit of detection
Type of Use:	reuse in a thesis/dissertation
Order Ref:	05241988
Order Total:	0.00 USD

View or print complete details of your order and the publisher's terms and conditions.

Sincerely,

Copyright Clearance Center

How was your experience? Fill out this survey to let us know.

Tel: +1-855-239-3415 / +1-978-646-2777
customercare@copyright.com
https://myaccount.copyright.com

Copyright Clearance Center RightsLink®

Appendix F

Thank you for your order!

Dear Kyle Lynch,

Thank you for placing your order through Copyright Clearance Center's RightsLink® service.

Order Summary

Licensee:	Kyle B Lynch
Order Date:	Mar 23, 2018
Order Number:	4315040872562
Publication:	Talanta
Title:	Multiple-channel ultra-violet absorbance detector for two-dimensional chromatographic separations
Type of Use:	reuse in a thesis/dissertation
Order Ref:	5241988
Order Total:	0.00 USD

View or print complete details of your order and the publisher's terms and conditions.

Sincerely,

Copyright Clearance Center

How was your experience? Fill out this survey to let us know.

Tel: +1-855-239-3415 / +1-978-646-2777
customercare@copyright.com
https://myaccount.copyright.com

Copyright Clearance Center RightsLink®